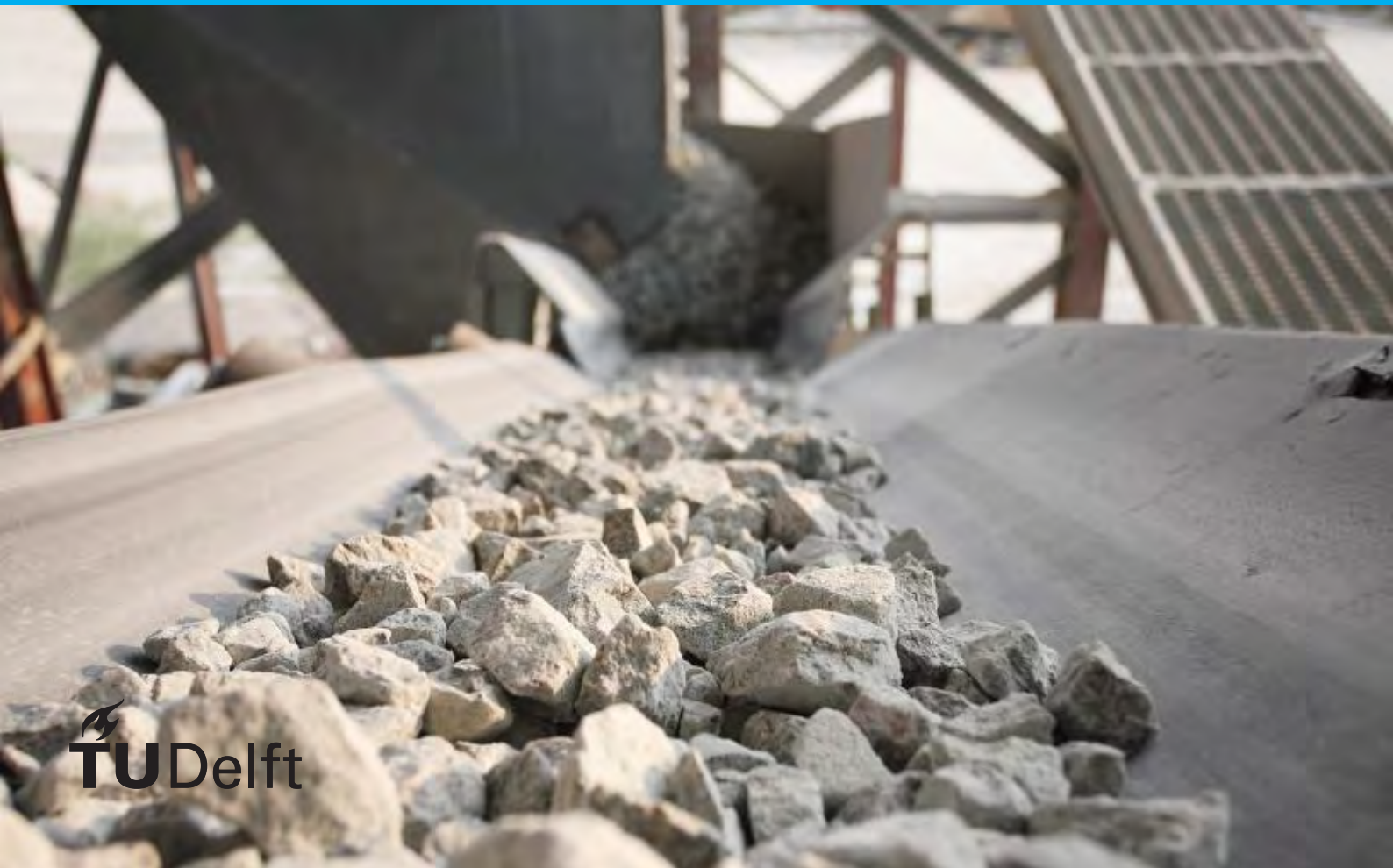


MSc Thesis

Experimental investigation
of concrete mixtures
incorporating recycled
concrete aggregates

A.I. Mylonas



MSc Thesis

Experimental investigation of concrete mixtures
incorporating recycled concrete aggregates

by

Antonios Ioannis Mylonas

to obtain the degree of Master of Science at the Delft University of Technology,
to be defended publicly on Tuesday 13th of July, 2021 at 15:30

Student number: 5160766
Project duration: September 1, 2020 – July 1, 2021
Scientific committee: Dr. Marija Nedeljkovic, TU Delft, CiTG, Materials & Environment
Prof.dr.ir. Erik Schlangen, TU Delft, CiTG, Materials & Environment
Dr. Jeanette Visser, TNO, Structural Reliability
Mrs. dr. ir. Mladena Lukovic, TU Delft, CiTG, Engineering Structures



An electronic version of this dissertation is available at <http://repository.tudelft.nl/>.

Contents

List of Figures	ix
List of Tables	xv
Preface	xvii
Summary	xix
1 Introduction	1
1.1 Research background	2
1.1.1 Circular Economy	2
1.1.2 Construction and Demolition Waste (CDW)	3
1.2 Problem statement	4
1.3 Significance of the research.	5
1.4 Description of the project	8
1.5 Aim of the research	8
1.6 Research objectives	8
1.7 Research questions	9
1.8 Hypothesis.	9
1.9 Assumptions and Scope.	9
1.10 Outline of the thesis	10

2	Literature review	13
2.1	Fresh properties of concrete with RCA	13
2.1.1	Workability	13
2.1.2	Air content.	17
2.2	Mechanical properties of concrete with RCA.	19
2.2.1	Compressive strength	19
2.2.2	Tensile splitting strength	21
2.2.3	Elastic modulus	22
2.3	Time-dependent properties of concrete with RCA	24
2.3.1	Shrinkage	24
2.4	Synopsis	25
3	Experimental program	27
3.1	Characterization of fine Recycled Concrete Aggregates (fRCA)	28
3.1.1	Moisture content and water absorption.	30
3.1.2	SSD density	31
3.1.3	Particle size distribution.	31
3.2	Characterization of Coarse Recycled Concrete Aggregates (CRCA) 33	
3.2.1	Moisture content and water absorption.	33
3.2.2	SSD density	34
3.2.3	Particle size distribution.	34
3.3	Mortars.	36
3.3.1	Mortar series	36
3.3.2	Flow measurement.	37
3.3.3	Air content.	37

3.3.4	Flexural and compressive strength	37
3.3.5	Porosity tests	37
3.3.6	Mercury Intrusion Porosimetry (MIP)	38
3.3.7	Optical microscopy	38
3.4	Concrete	39
3.4.1	Workability	41
3.4.2	Air content.	42
3.4.3	Compressive strength	43
3.4.4	Elastic modulus & Poisson's Ratio	43
3.4.5	Shrinkage & Mass loss	44
4	Results	47
4.1	Recycled materials	48
4.2	Mortar level	55
4.2.1	Fresh density	55
4.2.2	Flow.	55
4.2.3	Air content.	56
4.2.4	Compressive strength and flexural strength	57
4.2.5	Porosity	62
4.2.6	Microscopic analysis	63
4.3	Concrete level	66
4.3.1	Slump	66
4.3.2	Air content.	69
4.3.3	Fresh and hardened density	72
4.3.4	Compressive strength	73
4.3.5	Elastic modulus and Poisson's ratio ν	79

4.3.6	Shrinkage and mass loss	81
5	Discussion	87
5.1	Slump	87
5.2	Air content.	89
5.3	Compressive strength	90
5.4	Shrinkage	94
6	Conclusions and future recommendations	97
7	Bibliography	101
	References.	101
8	Appendix	107
8.1	Mortar mix designs of Series 1	107
8.2	Grading curves for aggregates 0-16 mm used in concrete mix- tures	109
8.3	Concrete mix designs	111

List of Figures

1.1	Circular building economy - “Cradle to cradle” process [3].	3
1.2	Recycling, backfilling, energy recovery, incineration and landfilling as a percentage of total mineral CDW [5].	4
1.3	Embodied carbon in various activities in construction building process [10].	6
1.4	Landscape alteration due to excessive sand mining in Poyang Lake, China [11].	7
1.5	Waste generation by economic activities and households in EU members in 2018 [5].	7
1.6	Thesis outline	12
2.1	Water absorption kinetics in recycled aggregates (RA) for(a) 24h and (b) 144h [26].	15
2.2	Water reduction in relation to fRCA replacement ratios and type of SP [27].	16
2.3	Air content in relation to fRCA replacement ratio for both Recycled Fine Aggregates (RFA) and carbonated Recycled Fine Aggregates (CRFA) [32].	18
2.4	Relationship between compressive strength loss and fRCA replacement ratio found in literature [18],[19],[20],[21],[24],[34],[35],[37].	21
2.5	Relationship between tensile splitting strength loss and fRCA replacement ratio [27],[34],[37],[42],[43],[44].	22
2.6	BSE images of (a) saturated fRCA mortars and (b) dried fRCA mortars [24].	22
2.7	Elastic modulus of fRCA concrete in relation to fRCA incorporation ratio [8],[32],[47].	23

2.8 Shrinkage deformation of concrete mixtures with fRCA and CRCA originating from laboratory crushed concrete [21].	25
3.1 First and second delivery of fRCA B	28
3.2 First and second delivery of fRCA C	29
3.3 First and second delivery of fRCA D	29
3.4 Drying and preparing fRCA sample for water absorption determination.	30
3.5 Shape of aggregate sample after cone testing. SSD state is reached in the last picture.	31
3.6 Sieve tower for particle size distribution of fRCA.	32
3.7 Various fractions of fRCA NB - From left to right : >4 mm, 2-4 mm, 1-2 mm, 0.5-1 mm, 0.25-0.5 mm, 0.125-0.25 mm, <0.125 mm.	32
3.8 Various fractions of fRCA NC - From left to right : >4 mm, 1-4 mm, 0.5-1 mm, 0.25-0.5 mm, 0.125-0.25 mm, <0.125 mm.	32
3.9 Various fractions of fRCA ND - From left to right : >4 mm, 1-4 mm, 0.5-1 mm, 0.25-0.5 mm, 0.125-0.25 mm, <0.125 mm.	33
3.10 Coarse Recycled Concrete Aggregates (CRCA)	33
3.11 Preparation of test portion of CRCA for water absorption measurement	34
3.12 Various fractions of CRCA	35
3.13 Polished section of a mortar mixture of Series 1	39
3.14 Modified mixing sequence applied for concrete mixtures	41
3.15 Slump test set up for fresh concrete mixtures	41
3.16 Air content experiment of fresh concrete mixtures.	42
3.17 Casting concrete cubes for compression tests	43
3.18 Experimental setup for elastic modulus tests of concrete	44
3.19 Dimensions of molds and hardened shrinkage concrete specimens	45
3.20 Measuring gauge device for shrinkage of concrete	45

4.1	Microphotographs of 0.063-2 mm and 2-4 mm fractions of river sand A and fRCA B, C, D [15]	49
4.2	Moisture content of natural and recycled aggregates	51
4.3	Water absorption of natural and recycled aggregates	51
4.4	SSD density of natural and recycled aggregates	52
4.5	Particle size distribution of fine and coarse aggregates	53
4.6	Fine content 0-0.25 mm for fine aggregates	54
4.7	Fresh density of mortar mixtures of Series 1	55
4.8	Flow of mortar mixtures of Series 1	56
4.9	Air content of mortar mixtures of Series 1	57
4.10	Compressive strength of mortar mixtures	58
4.11	Compressive strength time development	59
4.12	Flexural strength of mortar mixtures of Series 1	60
4.13	Flexural strength time development of mortar mixtures of Series 1	61
4.14	Relationship between compressive and flexural strength of mortar mixtures of Series 1 at 28 days	61
4.15	Porosity of mortar mixtures of Series 1	62
4.16	Carbonated paste in mortar mixtures (a) NBFA and (b) NDFA	64
4.17	Old adhered paste on fRCA and presence of ITZs in mortar mixtures (a) NDFA and (b) NFFA	65
4.18	Presence of entrapped air in mortar mixtures (a) NB and (b) NC	65
4.19	Stable concrete mixture after slump testing	67
4.20	Slump of concrete mixtures	68
4.21	Surface of concrete mixtures (i) A100 and (ii) C25 after compaction	69
4.22	(i) As received fRCA D in water and appearance of air bubble, (ii) Appearance of dirty water and foam when water is mixed with fRCA D, (iii) Visual observations of air bubbles on the top of the mortar container after compaction	70

4.23 Air content in % of concrete mixtures	71
4.24 (i) Air content in concrete mixtures with as received and dry fRCA, (ii) Effect of SP on air content of concrete mixtures with 25 % fRCA and 30 % CRCA	72
4.25 Fresh density and hardened density of concrete mixtures after 28 days of curing	73
4.26 Compressive strength results	74
4.27 7 days compressive strength	76
4.28 28 days compressive strength	76
4.29 56 days compressive strength	77
4.30 Compressive strength time development. Maximum strength is mea- sured for B25 at 56 days, whereas minimum strength is obtained for D25. C25 and D25 show large standard deviations at 28 days.	78
4.31 Elastic modulus E_{cm} of concrete mixtures at 28 days	80
4.32 Poisson's ratio ν of concrete mixtures at 28 days	80
4.33 Shrinkage for concrete mixtures with fRCA B and CRCA. Comparison with A100 and A70.	82
4.34 Shrinkage for concrete mixtures with fRCA C and CRCA. Comparison with A100 and A70.	82
4.35 Shrinkage for concrete mixtures with fRCA D and CRCA. Comparison with A100 and A70.	83
4.36 Mass loss for concrete mixtures with fRCA B and CRCA. Comparison with A100 and A70.	84
4.37 Mass loss for concrete mixtures with fRCA C and CRCA. Comparison with A100 and A70.	85
4.38 Mass loss for concrete mixtures with fRCA D and CRCA. Comparison with A100 and A70.	85
5.1 (i) Storage of material causes particle agglomeration and entrap- ment of air in empty spaces, (ii) Presence of impurities on the surface of fRCA particles	90

5.2	Air content effect on compressive strength of concrete mixtures with 1st and 2nd delivery of fRCA	91
5.3	Microphotographs under UV light for (i) fRCA aggregate in mortar NC and (ii) fRCA aggregate in mortar ND	92
5.4	Pore size distribution of mortars derived from concrete mixtures A100, B25, C25, D25	93
5.5	Total capillary pore volume of mortars derived from concrete mixtures A100, B25, C25, D25	94
8.1	Mortar mix design NB	107
8.2	Mortar mix design NC	107
8.3	Mortar mix design ND	108
8.4	Mortar mix design NF	108
8.5	Mortar mix design NBFA	108
8.6	Mortar mix design NCFA	108
8.7	Mortar mix design NDFA	109
8.8	Mortar mix design NFFA	109
8.9	Final grading curves of A100, B25, C25 and D25	110
8.10	Final grading curves of A100, NB25, NC25 and ND25	110
8.11	Final grading curves of A100, A70, NB25/30, NC25/30 and ND25/30	111
8.12	Concrete mix design A100	111
8.13	Concrete mix design A70	112
8.14	Concrete mix design B25	112
8.15	Concrete mix design NB25	113
8.16	Concrete mix design NB25/30	113
8.17	Concrete mix design C25	114
8.18	Concrete mix design NC25	114

8.19 Concrete mix design NC25/30	115
8.20 Concrete mix design D25	115
8.21 Concrete mix design ND25	116
8.22 Concrete mix design ND25/30	116

List of Tables

- 4.1 Physical and chemical characterization of studied sands [15] 52
- 4.2 Comparison of wcr calculated from mix designs and from optical microscopic analysis 63
- 4.3 Comparison of air content measured experimentally and derived from optical microscopic analysis 64

- 5.1 Correlation between air content and compressive strength of concrete mixtures 91

Preface

I would like to start by saying what a great time has been at TU Delft. The moments that I experienced during this amazing journey will accompany me forever in the future, showing me the way to personal and professional excellence.

This master thesis is the result of the work performed during the past year, in order to obtain the Master of Science degree in Civil Engineering at the Technical University of Delft. The work contained herein was carried out as a collaboration between the Microlab at the section of Materials and Environment, Faculty of Civil Engineering and Geosciences at Delft University of Technology and TNO.

This basis for this research originally stemmed from my passion for a sustainable building industry. I feel that we, as the young scientists generation, ought to promote environmental awareness and apply our humble knowledge towards the prosperity of society. We must act and we must act now!

The author acknowledges funding provided by the Materials innovation institute M2i (www.m2i.nl), Rijkswaterstaat, TweeR Recycling, AVG, Caron Recycling (CRH). Furthermore, I would like to thank for the material contribution (sample of fRCA) made by the recycling plants TweeR Recycling, AVG and Caron Recycling (CRH). I would also like to thank Henriëtte Dikmans, Virginie Wiktor, Hans Huppertz and R&D Cugla for their precious help with the superplasticizers part in this study and for supplying the superplasticizer.

First of all, an immense thank goes to my parents for their infinite support and never-ending love. They were always on my side, showing me the way to become a better person and equipping me with virtues and values, that will accompany me throughout my life. To my brother, Spiros, who always knew how to make me feel better and always believed in me. I thank you and always love you.

A sincere thank you goes to all the committee members of this thesis. Thank to Dr. Marija Nedeljkovic, without whom this research would not be possible. She was not only my daily supervisor, but more a mentor and a friend. Her passion about the topic stimulated my interest since the very first days. She taught me how to think and always challenged me to go one step further. I will always be grateful to her for that. I want also to thank Prof.dr.ir. E. Schlangen for his interest in the research topic, his criticism and guidance throughout the project. I want to thank Dr. Jeanette Visser, my supervisor at TNO, that gave me the opportunity to do my internship in this amazing working environment. Her guidance and expertise taught

me to look things from a different perspective and that is a lesson that I will always carry with me in the future. Finally, I want to thank Mrs. dr. ir. M. Lukovic for her professional view on the topic.

An immense thank you goes to people from the Microlab and Stevin laboratory: Maiko van Leeuwen for his professionalism and making concrete experiments an incredibly fun activity, Ton Blom for his great assistance in concrete lab experiments and Arjan Thijssen for conducting the MIP experiments. Special thanks to Dr. Timo Nijland for his precious guidance on optical microscopy. I also feel grateful to all my colleagues at TNO, among others: Sacha Hermanns, Ron Lautz, Juan Felipe Garzon for helping me with experiments and making my stay at TNO a wonderful experience. I would like also to thank all my colleagues of the Materials and Environment section at TU Delft, that were always willing to help.

More importantly, I would like to express how grateful I am to the people that were always on my side, even if they were far away. First of all, to my friends in Greece: Christos, Thanos and Konstantinos, who are now a family to me. To the most amazing people that I met here in Delft, that I was so lucky to get to know in the 1st year of our studies and will always keep as close as possible: among others Harikrishnan Sushin, Karim El Laham, Giorgio Caumo, Eldhose Paul. Finally, an immense thank you goes to Polina, for believing in me and making this journey more beautiful.

*A.I. Mylonas
Delft, July 2021*

Summary

In the Netherlands, yearly 33 Mton new concrete (roughly 15 billion m³) is produced while 12 Mton concrete waste becomes available. Recycling of the yearly 12 Mton concrete waste results in roughly 7 Mton coarse recycled concrete aggregate (CRCA) and 5 Mton fine recycled concrete aggregates (fRCA). Currently, fRCA is not used in structural concrete, but only for low grade applications.

This research aims to investigate the effect of recycled concrete aggregates (RCA) incorporation on the performance of structural concrete mixtures. Three streams of fRCA were considered in this research and two deliveries of each source were examined. River sand was replaced by 25% fRCA, which was found to be the optimal amount that does not require cement increase. Both deliveries were used in order to identify potential differences. Additional concrete mixtures with simultaneous replacement of river sand by 25% fRCA and river gravel by 30% CRCA were evaluated. Parallel work was conducted during an 8-months internship at TNO, where optimization of mortar mixtures with full replacement of river sand by fRCA was investigated. This was performed by considering the water demand of solid constituents (binder and fRCA) and packing of fRCA. Optical microscopy was used for closer inspection of the microstructure of fRCA.

Fresh properties of studied mixtures were measured. Assessment of the mechanical performance of concrete mixtures was expressed by means of compressive strength and elastic modulus. Long term behavior was also investigated by shrinkage deformation measurements up to 95 days after casting.

Results show that substantial rise in cement content is necessary for obtaining the desirable flow and high levels of compressive strength, when full replacement of fRCA is performed. Regarding concrete mixtures with 25% fRCA, increase in air content was measured. Entrapped air is strongly dependent on the porosity of adhered cement paste on RCA, content of 0-0.25 mm fraction as well as agglomeration and presence of impurities in as received fRCA. This affects negatively their mechanical performance. Additional porosity resulting from CRCA incorporation was responsible for further reduction in mechanical properties of concrete mixtures. Mixtures with RCA showed three times higher mass loss at the age of 95 days.

*Antonios Ioannis Mylonas
Delft, July 2021*

1

Introduction

"Excellence is an art won by training and habituation. We do not act rightly because we have virtue or excellence, but we rather have those because we have acted rightly. We are what we repeatedly do. Excellence, then, is not an act but a habit."

Aristotle
Greek philosopher and polymath
384 BC - 322 BC

This master thesis is the result of the work performed during the past year, in order to obtain the Master of Science degree in Civil Engineering at the Technical University of Delft. The work contained herein was carried out as a collaboration between the Microlab at the section of Materials and Environment, Faculty of Civil Engineering and Geosciences at Delft University of Technology and TNO.

1.1. Research background

The entire building process involves multiple stages from extraction of material, manufacturing, assembly and use and maintenance of structures. All steps require consumption of huge amounts of energy and natural resources, transportation of raw materials and various activities for operational use and repair of the structure. Each one of the activities throughout the process has a major impact on carbon dioxide emissions and depletion of raw materials. Once the structure has reached the end of its design life, it has to be demolished. Construction waste is, then, produced. A linear building process suggests disposal of waste in landfills or partial recovery in low-grade applications. On the other hand, cyclic building economy promotes recycling of waste.

Since the industrial revolution, the linear model of production and consumption is well established worldwide. Population growth comes hand in hand with the rapidly growing construction sector and demand for construction materials, placing it now among the world's largest producers of waste. A crucial need for the transition to new circular solutions emerges from this situation. The concept of circular economy in the building sector, as well as recycling of construction and demolition waste (CDW) are analyzed in the following subsections.

1.1.1. Circular Economy

Several definitions of circular economy have been proposed. The European Parliament refers to circular economy as a model of production and consumption, which involves sharing, leasing, reusing, repairing, refurbishing and recycling existing materials and products as long as possible. The term encompasses a) extension of life cycle of products, b) reduction of waste and c) establishment of added value [2]. According to Eberhardt et al. [1], circular economy is a regenerative system in which resource input, waste and emissions are minimized by restricting (efficient resource use), extending service life and closing material loops (cycling).

Thus, both definitions highlight the emerging need of preserving natural resources and extending life cycle of materials by recycling. The value of a circular approach is recognized globally, offering environmental, societal and economic advantages to humanity. Available policies towards sustainability are widely diverse considering the variety of products and services that require different treatments and methods. In the new global economy, circularity has become a central issue for the building industry. This research specifically focuses on the enhancement of the transition from traditional linear building economy to the circular one by recycling CDW. Linear building process embodies the concept of "cradle to grave", whereas circular building economy switches to "cradle to cradle" cycle, giving birth to new ready-to-use materials from waste (Figure 1.1).

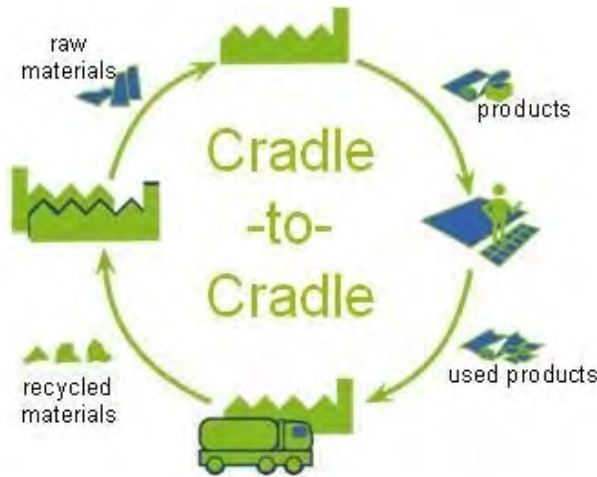


Figure 1.1: Circular building economy - "Cradle to cradle" process [3].

1.1.1.2. Construction and Demolition Waste (CDW)

Construction and Demolition Waste (CDW) comprises of multiple building materials from demolished structures, such as wood, masonry, gypsum, metals, concrete, plastic, glass or cardboards and excavated soils. As an increasing number of structures is reaching the end of their service life, proportional amounts of waste are produced. Most commonly, this waste is disposed in large landfills, possibly burdening soil and atmosphere with non-biodegradable and hazardous materials that contaminate the environment. CDW is the largest stream waste in EU, demonstrating relatively stable rates over time. According to European Environmental Agency, it is estimated that 374 million tons of CDW is produced per year in the European Union in 2016. In 2008, Waste Framework Directive (WFD) set the recovery target of 70 % of CDW in 2020. Already in 2016, many EU countries achieved this goal, with rates varying among EU members from 10 % to 90 % recycling, as depicted in Figure 1.2 [4], [5].

Reuse of CDW mainly relates to backfilling and reuse in low-grade applications, such as road sub-bases, questioning the efficiency of recycling in the building industry. The exact source of CDW is most of the times completely unknown, combining concrete of various grades, ages and compositions. This uncertainty about the quality of these recycled aggregates or the potential health risks for workers is a major hindrance in re-using CDW. According to EU Construction and Demolition Waste Protocol & Guidelines, published in 2018, this uncertainty restricts further development of recycling infrastructures in the European Union [5]. Therefore, an emerging need of creating a common protocol for utilization of CDW recycling exists. This action will be in line with EU initiative of carbon neutral economy by 2050, by contributing in the reduction of production and excavation procedures for raw materials.

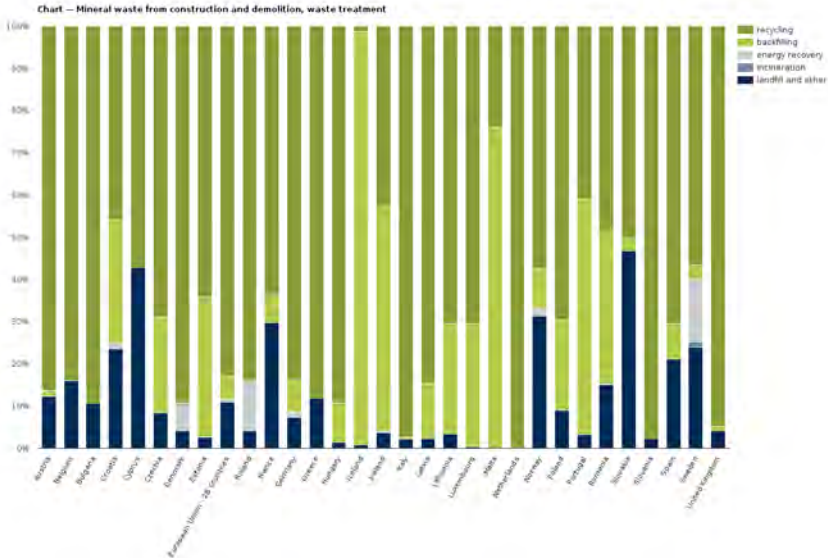


Figure 1.2: Recycling, backfilling, energy recovery, incineration and landfilling as a percentage of total mineral CDW [5].

One of the most common techniques of processing CDW is crushing waste into fractions forming coarse and fine aggregates. Coarse Recycled Concrete Aggregates (CRCA) have been commonly utilized in low-grade applications and in plain and reinforced concrete without having any harmful effect. A number of recommendations have been published, such as RILEM 1994, which allows the full replacement of natural gravel with CRCA on the condition that the latter meets certain specifications [6]. On the contrary, challenges associated with incorporation of fine Recycled Concrete Aggregates (fRCA) in structural concrete justifies the scarcity of guidelines and practical applications. They are mostly used as substitutes to virgin fine aggregates in downcycling applications, such as stabilization of soils and as a filling material for waste treatment plants [7]. Only few examples exist in literature about replacing natural sand with fRCA in structural concrete and the use of fRCA is even not allowed for structural concrete by several standards [8]. This research aims to tackle this bottleneck and investigate the potential of using fRCA in structural concrete.

1.2. Problem statement

As explained in 1.1, fRCA is primarily used in downcycling applications, since they are often associated with degradation of the mechanical properties of structural concrete. Use of fRCA for high-end and durable concrete products is commendable,

but it has to be acknowledged that the price to pay might be even higher. The majority of the successful studies of structural concrete with fRCA involves moderate to high cement increase and in a few cases, controlled quality of the recycled material (laboratory based crushed concrete). This directly rises the question of sustainability, since recycled aggregates may contribute to saving natural raw materials, but can enlarge carbon footprint and energy consumption in the stage of cement manufacturing.

Therefore, it is crucial to create structural concrete with the optimal fRCA replacement ratio, which keeps cement content the same or even lower compared to regular concrete designs and guarantees use in structural purposes. Additionally, since knowledge about the parent concrete is insufficient, an arising necessity exists to make use of available fRCA and identify potential quality indicators that will predict the properties of concrete with fRCA. Once the obstacle of fRCA incorporation is addressed, the simultaneous use of CRCA and fRCA will minimize the use of raw materials in concrete with recycled concrete aggregates (RCA).

1.3. Significance of the research

It is of great importance to make utilization of fRCA in structural concrete feasible, preserving natural sand and enhancing recycling of CDW. Overcoming the barriers of limited use of fRCA in structural concrete will have a major positive environmental and economic impact, preventing depletion of raw materials and minimizing the amounts of waste being disposed at landfills. It has been shown that reuse of CDW can save up to 600 million euros per year for the European Companies [8].

The main motives that demonstrate the importance of this research are summarized below:

- Carbon footprint: Building and construction industry are now responsible for 39 % of the total carbon dioxide emissions, as shown in Figure 1.3. The majority of the pollutants (28 %) originates from operation of buildings, namely heating, cooling and lighting. Remaining 11 % relates to the embodied carbon or so-called “up-front” carbon, which is incorporated into materials and construction processes throughout the whole building life cycle. EU strategy is aimed towards a zero-net emission economy by 2050 [9]. This is in line with Europe’s commitment to immediate global action under the Paris Agreement. The World Green Building Council in 2019 has formulated as ambition a reduction of embodied carbon by 40 % by 2030 and a net zero emission buildings by 2050 [10]. Minimizing the extraction of raw materials will significantly reduce energy consumption and consequently, carbon emissions.
- Raw material preservation: Sand is the second most used natural raw material globally, with water leading in the list. More than 50 billion tons of aggregates

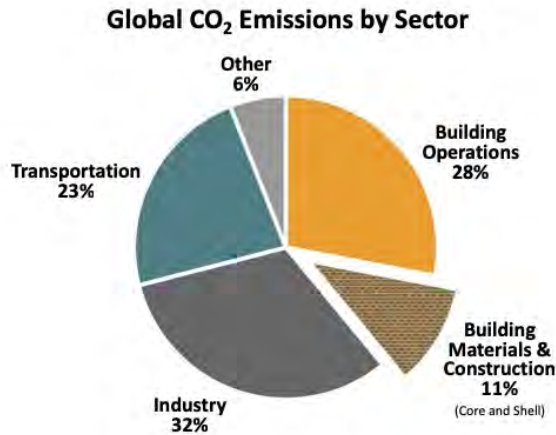


Figure 1.3: Embodied carbon in various activities in construction building process [10].

are needed for the building industry per year at the moment already, which is expected to rise considerably in the upcoming years. Since the demand is still increasing, it may lead to entire riverbeds and beaches being stripped bare, and farmlands and forests torn up. A powerful example is one of the largest sand mines in Poyang lake in China. Rapid urbanization and population growth increased the demand in concrete by 438 % in China alone over the past two decades, according to the United Nations Environmental Program. It is estimated that Poyang lake mining site produces 9 % of the total sand demand in the country, making it probably the world's largest sand mining site. This intense mining has caused desertation or flooding of parts of the coasts of the lake and landscape has altered dramatically, as demonstrated in Fig. 1.4 [11].

- Landfilling waste: CDW occupies approximately 20 % to 30 % of the total landfilling waste [5]. This is a considerable amount of waste produced by destruction of buildings and deteriorated infrastructures. In addition to that, it has been found that waste originates, also, from materials that have been purchased but have not been used. Bossink et al. detected this phenomenon in the Netherlands, where it was estimated that a total average of 9 % of purchased building materials is disposed as waste, accumulating landfills with non-degradable materials [12]. Fig. 1.5 shows the distribution of waste generated by economic activities and households in 2018, illustrating that construction waste occupies more than one third of the total waste generation.
- Costs: Potential cost reduction might occur by use of fRCA in structural concrete. Tosic et.al (2015) claimed that the cost of natural aggregates (NA) is 3 € / ton against 11.5 € / ton for fRCA [13]. Braga et.al (2019) found that NA and

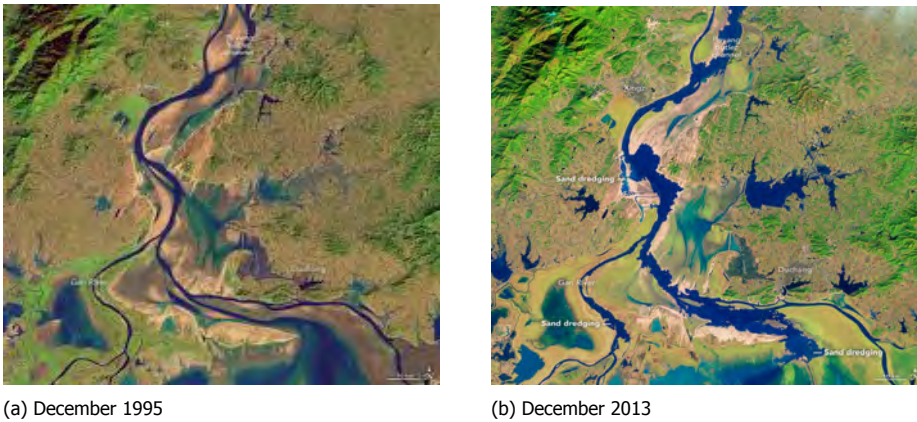


Figure 1.4: Landscape alteration due to excessive sand mining in Poyang Lake, China [11].

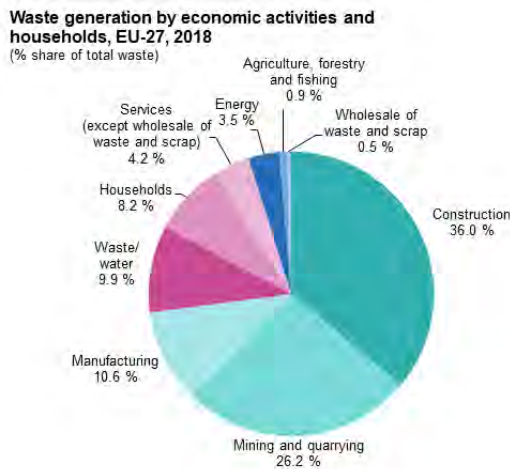


Figure 1.5: Waste generation by economic activities and households in EU members in 2018 [5].

fRCA cost 4 € / ton and 4.5 € / ton, respectively [14]. Aforementioned values do not take into account transportation costs. Therefore, contingency plans about decreasing overall economic costs, taking into account transportation costs but also costs due to e.g. avoided CO₂ / primary material or land use may make the costs of fRCA competitive with natural sand in the near future. The key-point in decreasing the cost of fRCA lays on financial motives by governmental policies. In some Member States, including Belgium and the Netherlands, the use of RCA is made an economically attractive option through government measures including levies on virgin materials and taxes on landfilling waste.

1.4. Description of the project

This study is part of Dr. Marija Nedeljkovic's Postdoc project, from which findings about the optimization of use of fRCA in cement based mortars will be derived. This thesis provides a continuation of this project by upscaling mortars with optimal fRCA amount to concrete level. Three different sources of fRCA were used provided by the three recycling companies and two separate deliveries were received by each company. The first delivery of fRCA was at 19/02/2019 and a second one was received at 04/01/2021. The effect of fRCA incorporation was evaluated using both fRCA deliveries. Additional concrete mixtures were designed with the optimal fRCA replacement ratio and the maximum allowed gravel replacement by CRCA.

This project was carried out in the framework of the Research Program of the Materials innovation institute (M2i) supported by the Dutch government. The project engages with the investigation of fRCA as an alternative raw material to Dutch river sand and the potential of incorporating fRCA in structural concrete. The partners involved in this project are: TNO, M2i, Rijkwaterstaat, CUGLA, AVG, Caron Recycling (CRH) and TweeR. The funding is provided by all aforementioned partners in different proportions except for CUGLA, which was included in a later stage for additional study purposes on superplasticizer (SP). TNO in cooperation with scientists from TU Delft (Post-doc researcher Dr. Marija Nedeljkovic) joined their forces to deliver the project results. AVG, Caron recycling and TweeR, also, supplied the project with necessary amounts of fRCA. CRCA used in this study were, also, provided by TweeR.

1.5. Aim of the research

The aim of this research is the development of concrete mix designs with the optimal amount of fRCA and CRCA that do not require cement content increase and maintain structural integrity.

1.6. Research objectives

The activities of the research are driven by the following research objectives:

1. Gain insight in fRCA and concrete with fRCA incorporation by reviewing research studies found in literature
2. Gain better understanding of quality of fRCA by investigating physical properties of fRCA delivered by 3 recycling companies located in the Netherlands
3. Propose a concrete mix design by determining the optimal incorporation ratio of fRCA that does not require increase of cement content

4. Evaluate performance of concrete with RCA by measuring fresh and mechanical properties of concrete

1.7. Research questions

The primary research questions that will be answered in this research are listed below:

1. What is the max fRCA replacement percentage that does not require cement increase and can reach the target strength class of compressive strength??
2. Which modifications are necessary when incorporating fRCA and upscaling mortars to concrete?
3. What is the effect of using both fRCA and CRCA in structural concrete?
4. What are the fRCA quality indicators for good performance of structural concrete?

1.8. Hypothesis

The probable outcome of the research is the determination of a rather low fRCA replacement percentage that does not require cement increase and can potentially compete with conventional concrete. Due to the nature of RCA, it is expected that the use of SP in higher dosages will be necessary. Additional porosity caused by the old cement paste attached to RCA is directly affecting the density of the mixture and consequently, the main mechanical properties. In this context, the key factor is the quality of the delivered RCA and the investigation of three different types of fRCA will offer a greater understanding in the correlations of RCA and the performance of concrete.

1.9. Assumptions and Scope

- **One major limitation is that the research only focuses on concrete mixtures with Ordinary Portland Cement (OPC) CEM I 42.5 N.**

Despite the fact that in the Netherlands, CEM III is most commonly used in practice, CEM I was used for comparison purposes with available global research on the topic.

- **Investigation of the maximum fRCA replacement percentage without increasing cement content is done only on mortars.**

The effect of fRCA is emphasized on mortars, where coarser aggregates are not present.

- **The concrete mixtures were designed for environmental class of XC3 and strength class of C30/37.**

XC3 environmental class and C30/37 concrete grade are widely used in the industry of concrete production.

- **The maximum allowed CRCA percentage was introduced to concrete mixtures and the effect was evaluated.**

Similarly, the optimal CRCA percentage could be determined. However, the research deliberates on identifying the optimal amount on fRCA and maximize the total RCA content afterwards.

- **Only compressive strength, elastic modulus and shrinkage will be determined as mechanical properties.**

A more complete research may broaden to the scope of durability issues of concrete with RCA, since these properties stem from porosity of the concrete matrix and its constituents.

- **100 % fRCA replacement was done only on mortar level, since cement increase was high and thus, it was not considered as a practical solution for concrete production for industry purposes.**

Mortars with 100 % fRCA replacement followed a completely different approach, adjusting the design for each fRCA type.

- **Curing of specimens will be done in a curing room in TU-Delft's Stevin Laboratory.**

With a temperature of 20 °C and RH of approximately 95 %.

1.10. Outline of the thesis

In chapter 2, a literature review will be given on available studies of concrete with RCA. The variations in results and approaches will give a better understanding and

knowledge gaps in this research field. Parameters that affect the fresh and mechanical properties of concrete with RCA will be identified.

The experimental program will be explained in detail in Chapter 3. The materials used in the study will be clearly defined and test set-ups will be described.

Results will be visually presented in Chapter 4. The effect of fRCA incorporation, as well as the batching and CRCA effect will be studied. Multiple comparisons with the reference concrete will explain the behavior of concrete with RCA. Finally, correlations between properties of fRCA and concrete properties will be drawn.

Conclusion from observation of the test outcomes will be drawn in Chapter 5. Additionally, guidelines for concrete mix design with fRCA will be presented. Finally, remarks on the research and consequently, future recommendations will be proposed.

The thesis outline is visually presented in the flow chart of Figure 1.6.

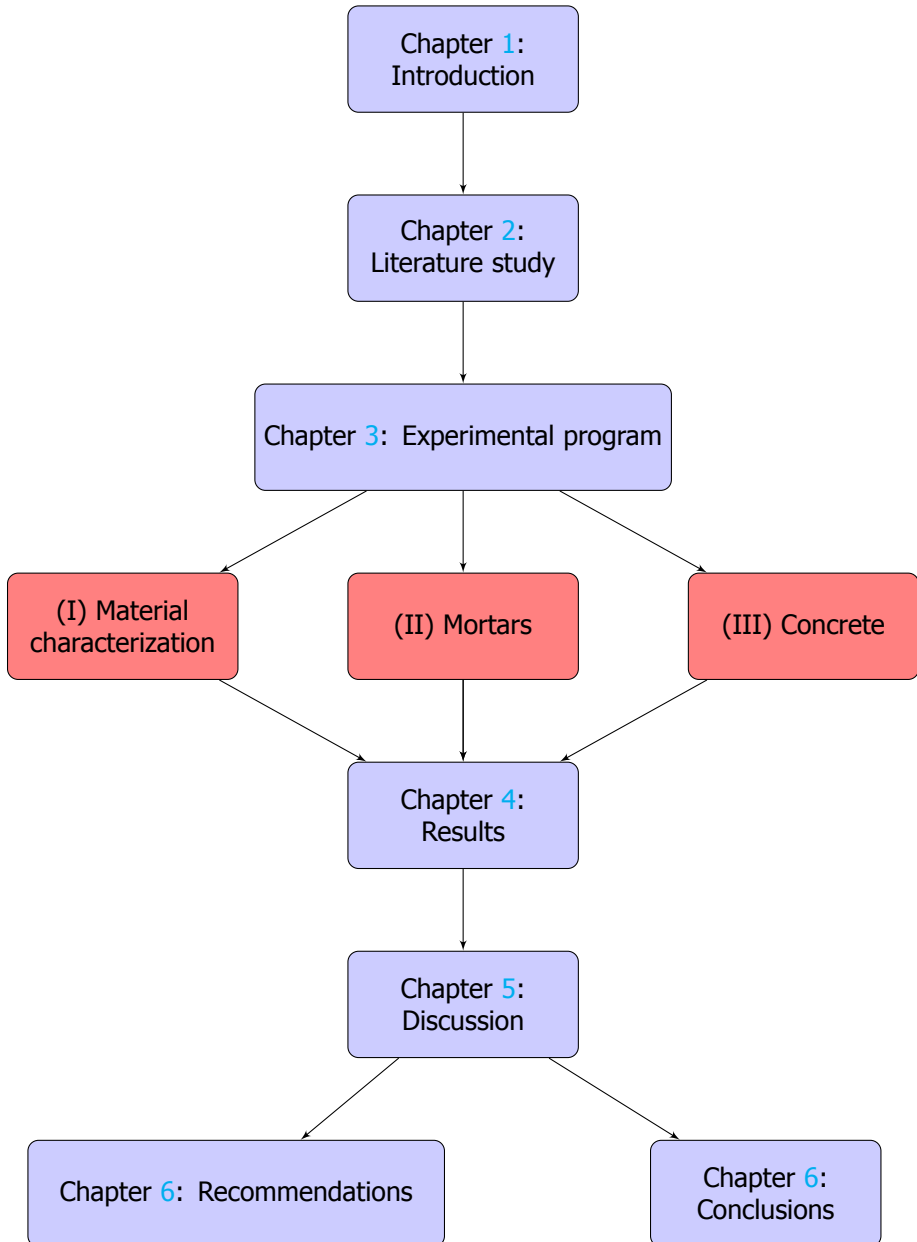


Figure 1.6: Thesis outline

2

Literature review

”The only true wisdom is in knowing you know nothing.”

Socrates
Greek philosopher
470 BC - 399 BC

There is a large volume of published studies describing the role of fRCA and CRCA in structural concrete production. In order to ensure structural reliability of concrete, a variety of fresh and mechanical properties need to be evaluated and comply with the specifications. Different approaches exist in the literature and the generalisability on this issue is hard to achieve. A number of published studies and the results of fresh and mechanical properties will be presented in chapter 2 and will provide a clear picture of what the main challenges in concrete with RCA are. The properties that will be reviewed are: workability, air content, compressive strength, elastic modulus and drying shrinkage.

2.1. Fresh properties of concrete with RCA

2.1.1. Workability

Workability is a very important property of fresh concrete mixture that guarantees ease of placement and compaction without any segregation. Except for w/c ratio and use of chemical admixtures, a strong link between aggregates used in the mixture and workability exists. The major points found in literature that are associated with workability of concrete with fRCA are presented:

- **Effect of moisture state of fRCA:** The moisture condition of fRCA used in the mixture directly influences foremost the initial slump of concrete. The most common states that fRCA can be found are oven dry, air dry, saturated surface dry (SSD) and wet condition. Depending on the moisture state, fRCA have either the ability to absorb water until saturation or contribute to fluidizing the concrete matrix. The majority of studies have investigated the effect of moisture state of fRCA on workability of concrete. On the one hand, presaturation of fRCA was performed. On the other hand, oven dried or air dried fRCA were added in the mixture. In the latter case, the total amount of water was added at time zero with all other constituents of the concrete mix. Differences in results and effects of the moisture state of fRCA are given in a few examples. According to Zhao et al. [24], the saturation state of fRCA used in mortars influences the workability obtained for a constant w/c ratio. This study showed that for the selected w/c ratios, dried fRCA resulted in higher slump compared to fully saturated fRCA. Since the effective water for lubrication of the cement paste is kept constant, it was concluded that water is not fully absorbed by fRCA and part of the water content was used up for obtaining higher workability of mortars. On the contrary, fully saturated fRCA have entrapped water in their internal porosity, which cannot escape and come in contact with cement paste. Therefore, it decreases the initial slump of the mixture. Recent cases reported by Poon et al. [25] also support this hypothesis. RCA were used in air dry, oven dry and saturated surface dry state and in various replacement ratios in concrete mixtures. Water content was adjusted to account for the same effective water in respect to moisture content of RCA. The authors observed that all oven dried RCA resulted in higher initial slump, validating the mechanism that was mentioned by Zhao et al. [24]. Slump loss was also evaluated, illustrating that oven dried RCA go through the water absorption process and thus, a quicker slump loss was recorded. This tendency is illustrated by the findings of Djerbi Tegguer [26], who proved that water absorption kinetics is the key player in RCA. Regarding natural aggregates, 24 h immersion in water is adequate for obtaining constant water absorption capacity. On the other hand, adhered mortar on RCA creates additional capillarity mechanisms that require more time in order to fill up all pores. Graphs in Figure 2.1 highlighted that a constant water absorption plateau was achieved after 144 h of immersion, demonstrating that water absorption kinetics and workability loss appear to be closely linked.

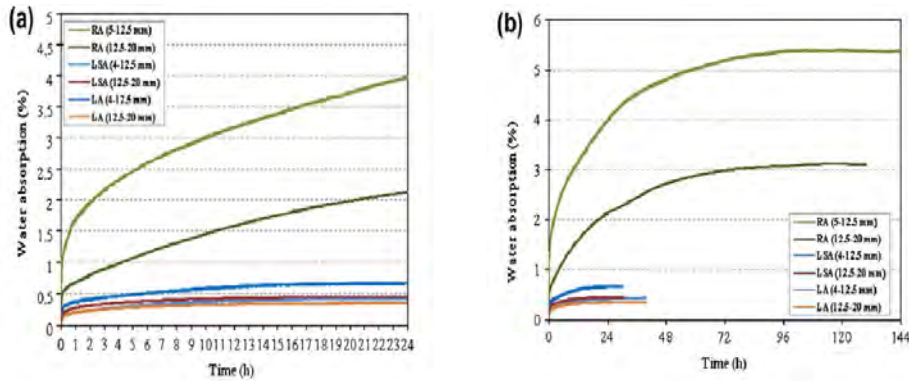


Figure 2.1: Water absorption kinetics in recycled aggregates (RA) for (a) 24h and (b) 144h [26].

- Effect of SP:** Li et al. examined the compatibility of common carboxylate superplasticizers (SP1) with fRCA concrete mixtures [23]. An especially developed polycarboxylate SP with addition of retarding and mud-inhibitor properties (SP2) was evaluated in comparison. It was apparent due to highly absorbent RCA, large amounts of both SP were used in concrete mixtures with 50 % v/v fRCA. Lower amounts of SP2 were used, resulting in slightly higher slump compared to SP1 mixtures, highlighting the suitability and effectiveness of the innovative SP. Pereira et al. [27] used regular lignosulfonate-based SP with additions and a modified polycarboxylate solution SP. Graphs, presented in their study in Figure 2.2, visualize a linear reduction in effectiveness of SPs when fRCA replacement ratios are increasing. In addition, lignosulfonate-based SP performed slightly more efficiently. This was explained by the authors based on the mechanism of lignosulfonate SP (electrostatic repulsion) and polycarboxylate SP (steric hindrance).
- Self-compacting concrete (SCC):** Carro - Lopez et al. [28] studied the fresh properties of self-compacting concrete with various fRCA incorporation ratios. fRCA replacement percentages of 20 %, 50% and 100 % were examined in concrete mixtures with $w/c = 0.46$ and SP in 1.7 % of the mass of cement. The evidence presented far supports the idea that increasing fRCA replacement ratio results in decreasing workability of mortar mixtures. The reduction rate for 50 % and 100 % fRCA incorporation is more severe and after a short period of time, self-compacting concrete mixtures lose their SCC properties.
- Fine content and particle shape:** As it has been reported, fRCA is found to contain large amounts of fines, which is mostly dependent on crushing technique applied in CDW. According to Celik et al. [29], high fine content gives rise to water requirements for adequate wetting of particles surface and obtaining the desired workability of concrete. A notable example of the effect of fine content and particle shape of fRCA (0-2 mm) on flow is provided by

Westerholm et al. [30]. Rheological parameters, such as yield stress and plastic viscosity, were evaluated by an automatic viscometer and values were interpreted for flowability of the mixtures. The authors observed that the relation between fine content above 16 % and yield stress is linearly increasing, resulting in less flowable mixtures. In addition, grading curves of fRCA were modified to match the particle size distribution (PSD) of natural sand in order to eliminate that parameter and examine the particle shape effect. The differences in plastic viscosity recordings can be attributed to irregularity and angularity of fRCA particles that increase particle friction and thus, resistance to flow is internally enhanced. Bouarroudj et al. [31] validated the aforementioned results in viscosity parameters measured for mortars with fRCA. Moreover, fRCA were used in different moisture states (full 24 immersion, dried fRCA, 24 WA + 5 % etc.). Plastic viscosity was higher compared to reference mortar only in 24h fully immersed fRCA. The authors, again, concluded that the remaining states had not reached total water absorption capacity of fRCA and thus, provided the mixture with additional flowability.

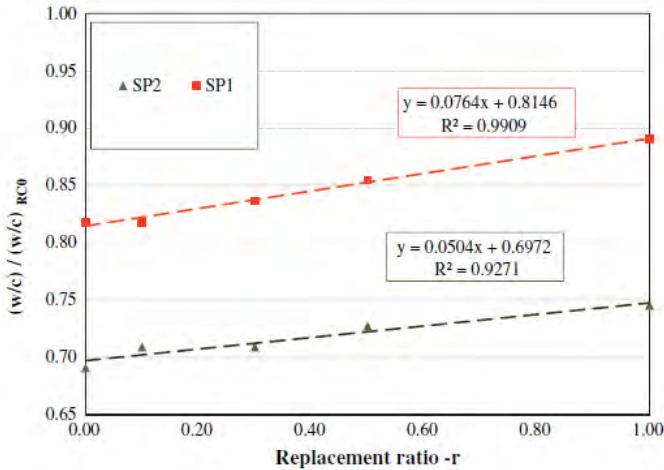


Figure 2.2: Water reduction in relation to fRCA replacement ratios and type of SP [27].

The existing research results demonstrate that workability of fRCA concrete can be influenced by moisture state of recycled aggregates, water absorption, type of SP as well as fine content. Due to continuous water absorption process by fRCA, quicker slump loss is reported for concrete with fRCA in comparison to conventional concrete mixtures. No unanimous approach has been concluded, though, for achieving the desired workability and maintaining flowable properties.

2.1.2. Air content

Despite of the fact that air content of fresh concrete is a very important factor to identify a dense mixture, there is a relatively small body of literature that is concerned with air content results in concrete with fRCA. Results of air content will determine expected loss in strength. A number of studies have postulated a convergence between the fRCA incorporation ratio and the entrapped air in concrete mixtures.

In Bouarroudj et al. study [31], moisture state of fRCA, used dried and after full 24h immersion, was examined in mortar mixtures. Both mortars with fRCA showed a considerable increase of air content in comparison to mortar mixes with natural aggregates. More specifically, dried fRCA had a 7 % air content, whereas fully immersed fRCA mortars dropped down to 4.5 %. The authors attributed this finding in presence of empty pores that were not filled during mixing for dried fRCA. In any case, mortars with fRCA contained particles with rougher and more porous surfaces than natural aggregates resulting in 700 % and 450 % increase in air content, respectively. The partition of air content that fRCA contributed was found to be 2.5 %, since volumetric air content of the cement paste with the given constituents in mortar mixtures was measured to be 4.5 %. Chinzorigt et al. [32] used fRCA in SSD state before mixing with other constituents. The replacement ratios for mortars were 10 %, 30 % and 60 %. The exact same mortar designs were applied for carbonated fRCA in order to evaluate the efficiency of this treatment method and all mortars with fRCA were compared to a reference mixture. As depicted in Figure 2.3, higher recordings in air content were registered for all mortars with fRCA in the range of 2.9 % to 5 %. As the fRCA incorporation percentage increases, the same trend is observed for entrapped air reaching the maximum value for 60% fRCA replacement. Carbonation treatment was not successful for reducing air content.

In contrast to earlier findings, no such evidence of direct relationship between fRCA replacement percentages and air content was detected. Revilla-Cuesta et al. [22] examined concrete mixtures with fRCA and CRCA in various percentages (25 %, 50 %, 75 % and 100 %). In this study, the linearly increasing trend in Figure 2.3 was not confirmed. All mixtures resulted in air content ranging from 3.75 % to 4.80 %. The minimum value was recorded for 25 % fRCA, whereas maximum value was measured for 0 % fRCA (concrete mixture with CRCA only). The authors observed no apparent relation between fRCA incorporation and air content, but attributed the discrepancies in present chemical admixtures and ongoing reactions.

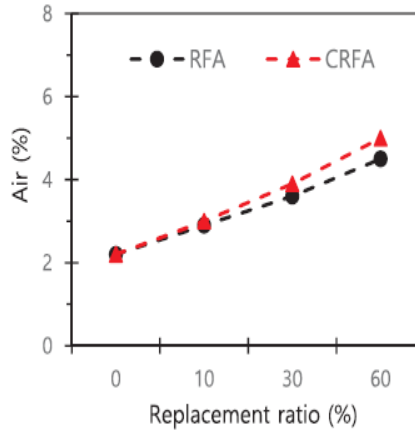


Figure 2.3: Air content in relation to fRCA replacement ratio for both Recycled Fine Aggregates (RFA) and carbonated Recycled Fine Aggregates (CRFA) [32].

These results are similar to those reported by Bogas et al. [19]. In their study, three fRCA concrete mixture groups were evaluated: i) no SP and no entraining agent (EA), ii) SP and no EA and iii) both EA and SP for evaluation of freeze thaw resistance. The fRCA replacement ratios were 20 %, 50 % and 100 %. For the first group, 50 % fRCA resulted in highest entrapped air, whereas 100 % fRCA had similar measurement to reference concrete. Use of SP in 2nd group, resulted in similar values and as expected, use of EA increased entrained air and content measured. Ju et al. [34], on the other hand, concluded a straightforward effect of fRCA on air content. 100 % fRCA replacement resulted in 30 % increase in air content (5.5 %) compared to reference concrete (4 %). In addition, effect of supplementary cementitious materials (SCM), such as fly ash (FA), ground granulated blast-furnaced slag (GGBS), was examined for fRCA concrete mixtures. Optimal mixture proved to be 15 % substitution of OPC binder by FA. For instance, in 50 % fRCA concrete mixtures, air content was decreased from 4.9 % to 4.2 %, whereas in 100 % fRCA concrete mixtures, entrapped air was lowered from 5.5 % to 4.2 %.

2.2. Mechanical properties of concrete with RCA

2.2.1. Compressive strength

The mechanical performance of concrete incorporating fRCA as replacement of natural sand is an emerging field of study. Scientists have attempted to conclude an upper limit that does not compromise the compressive strength of concrete. Undoubtedly, a unique value does not exist, since the mechanical properties not only depend on the quality of RCA (e.g. parent concrete, density, water absorption, adhered paste, particle size distribution (PSD), fine content, contamination etc.), but also, on size fraction, water and cement content and replacement ratio. The topic of compressive strength can best be treated under the following key-aspects:

- **Replacement ratio:** Puente et al. [53] selected target concrete strength classes that could be potentially achieved by 12 % and 24 % fRCA replacement. fRCA originated from both laboratory crushed concrete of a known strength class and composition and a recycling plant made by various concrete debris. Both samples succeeded in reaching the desired strength class. The authors attributed these results to enhancement of fRCA paste interface by interlocking of aggregates and proved that quality rather than origin of construction concrete waste is a driving factor. However, the majority of studies has detected a decreasing trend as the substitution ratio of fRCA increases. A collection of results is presented in Figure 2.4.
- **Filler effect:** A considerable number of studies support that an optimal replacement percentage might exist when fRCA are incorporated in structural concrete. That is based on the fine content and PSD of fRCA, which can potentially function as additional filler and provide better packing. Khalid et al. [35], in this context, found that this phenomenon occurred at 20 % fRCA replacement in mixtures with various w/c ratios (from 0.4 to 0.6). High fine content in fRCA provoked filler effect that counteracted the porosity of the recycled aggregates. This is exemplified in the work undertaken by Katz [36], who has proposed that mechanical performance of fRCA concrete may be sustained because of old adhered paste on aggregates that can contain unhydrated cement particles. These particles can potentially be reactivated and contribute to the total amount of paste. Evangelista et al. [37] observed similar strengths despite of the increasing fRCA replacement and came in agreement with the previous possible explanation.
- **Treatment effect of fRCA:** The effectiveness of the carbonation treatment technique has been exemplified in the study by Le et al. [39]. In this case, replacement ratios of 33 %, 66 % and 100 % were tested. Untreated fRCA concrete resulted in accumulating loss in compressive strength of 3 %, 18 % and 26 %, respectively. This loss was compensated by carbonation treatment of fRCA limiting the maximum compressive strength loss to 6 % with a total

fRCA replacement. Another example of a potential treatment of fRCA for limiting the mechanical properties loss is given by Pandurangan et al. [38]. The authors used three treatment methods for removal of adhered paste (acid, mechanical and thermal) in order to improve the bond strength between recycled aggregates and concrete matrix. Untreated fRCA presented a 14 % loss in compressive strength, whereas for treated fRCA and irrespective of the treatment method, the maximum loss was limited to 9 %.

- **Particle size fraction replacement:** Li et al. [39] distinguished various fractions of fRCA into 5 groups and studied the effect of replacing natural sand fractions with the respective fRCA. Compressive strength compared to reference mortar was maintained only when coarser fractions of sand were replaced (2.36 mm – 4.75 mm). As the lower limit of fraction range was decreased to 1.18 mm, 0.6 mm, 0.3 mm and 0.075 mm, consistent accumulating loss in strength was obtained. This is, primarily, attributed to increased water content necessary for maintaining the desirable flow and additionally, to presence of old adhered cement paste on recycled aggregates. Interfacial Transition Zones (ITZs) between fRCA and old adhered paste introduce extra weak interface links in mortar matrix.
- **Moisture state:** According to Ji et al. [40], the moisture state, at which fRCA are present, is directly related to the effective w/c ratio in concrete matrix. The authors studied fRCA concrete samples in three different states, oven dry, air dry and SSD state. Based on the assumption that only part of the water might return to lubrication of paste on air dry and SSD aggregates, SSD state resulted in the lowest effective w/c ratio and consequently, to the highest compressive strength.

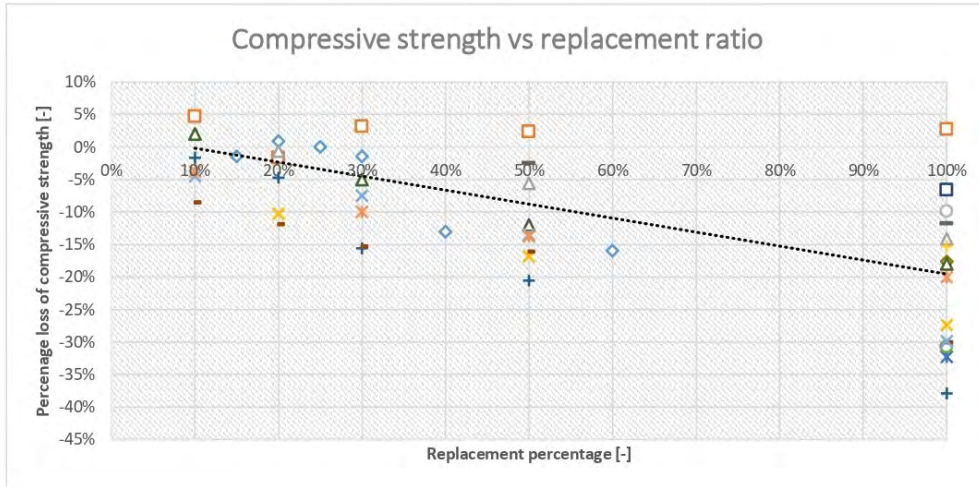


Figure 2.4: Relationship between compressive strength loss and fRCA replacement ratio found in literature [18],[19],[20],[21],[24],[34],[35],[37].

2.2.2. Tensile splitting strength

Wang et al. [41] evaluated the tensile splitting on specimens with simultaneous incorporation of CRCA and fRCA. Substitution rates of 50 % and 100 % were employed for fRCA and the recycled material originated from two different sources. All 4 samples showed slight decrease in tensile splitting strength in comparison to reference sample with no apparent decreasing trend relative to the replacement ratio. According to Ju et al. [34], the results of their study illustrated the beneficial effect of FA in 15 % replacement of OPC binder. Mineral admixtures, such as GGBS and FA were tested in various percentages to evaluate their effect on mechanical performance of fRCA concrete mixtures with 50 % and 100 % fRCA. The optimal mineral admixture and percentage replacement of binder was found to be FA in 15 %, which showed a trend of slight increase in tensile strength. A collection of results found in research studies is presented in Figure 2.5, where the trendline highlights a minor reduction in splitting strength with increasing fRCA replacement ratio.

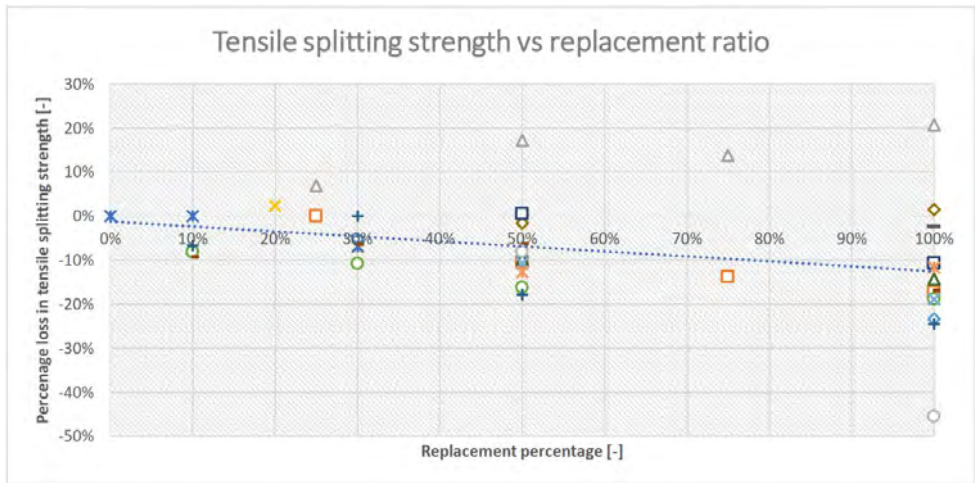


Figure 2.5: Relationship between tensile splitting strength loss and fRCA replacement ratio [27],[34],[37],[42],[43],[44].

The effect of fRCA was exemplified in Zhao's et al. [24] study, as total replacement of natural sand by fRCA resulted in a large reduction in flexural strength. In addition, dry and fully saturated states of fRCA were evaluated. Mortars with dried fRCA performed better in terms of flexural strength, which was explained by microscopic analysis, illustrating that a larger ITZ occurred between saturated fRCA and the cement paste, as it is clearly shown in Figure 2.6.

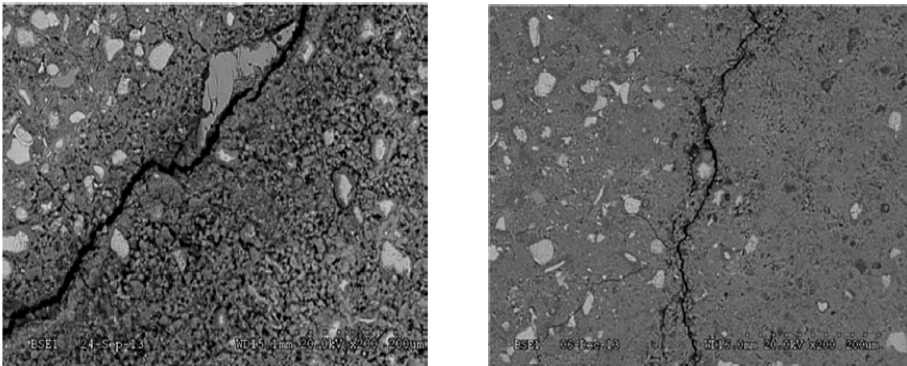


Figure 2.6: BSE images of (a) saturated fRCA mortars and (b) dried fRCA mortars [24].

2.2.3. Elastic modulus

Elastic modulus of concrete is directly dependent on the quality of aggregates used, the stiffness of aggregates, the total porosity and the strength of the bond be-

tween these phases [37]. The majority of studies have reported that elastic modulus of concrete with fRCA is considerably influenced demonstrating decrease rates ranging from 1.2 % to 30 % [27],[37],[41],[44],[45],[46]. An overview of these studies attribute the reduction in elastic modulus to the higher porosity of old adhered paste/mortar and the presence of weak ITZs between these two phase [32],[37],[43],[45],[46]. Evangelista et al. [37] reported that in low fRCA replacement percentages, e.g. 30 %, no significant reduction in elastic modulus is observed, whereas full replacement leads to 18.5 % decrease. The authors claim that mortar stiffness is just one factor among others that influences the modulus and this effect is intensifying only in higher percentages. Another example is the study by Bendimerad et al. [47], who observed reduction of 4 GPa in elastic modulus at the age of 1 week when 30 % of natural sand is replaced by fRCA. Similarly, Velay – Lizancos et al. [8] reported that even low replacement ratios up to 30 % resulted in decrease of E_{cm} . Monitoring of the evolution of modulus over time highlighted that in the early ages hardly no difference is present among reference concrete and concrete mixtures with fRCA. Chinzorigt et al. [32] investigated fRCA replacement ratios up to 50 % and observed reduction of elastic modulus of 17 % or less. The authors, also, used CO₂ treatment of fRCA and concluded that it has very small effect on improving elastic modulus of concrete mixtures with fRCA. A summary of the results of E_{cm} of concrete with fRCA is displayed in the following Figure 2.7.

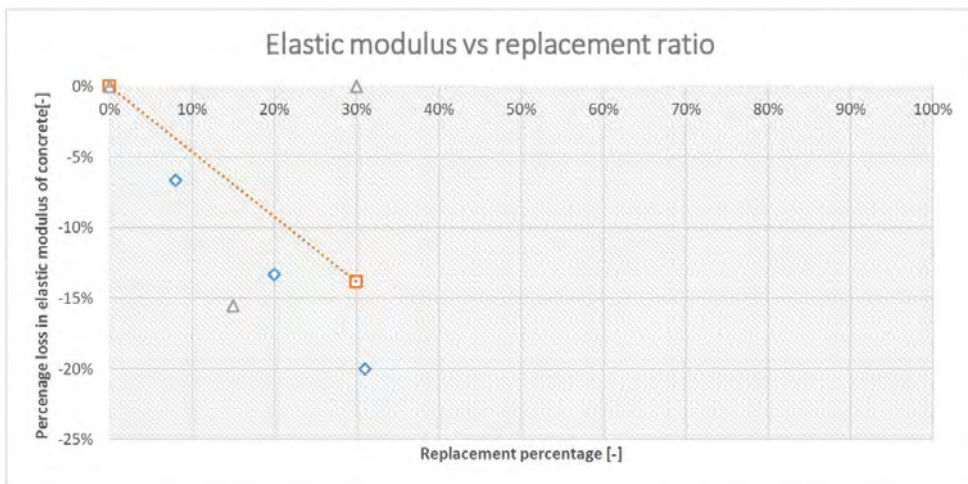


Figure 2.7: Elastic modulus of fRCA concrete in relation to fRCA incorporation ratio [8],[32],[47].

2.3. Time-dependent properties of concrete with RCA

2.3.1. Shrinkage

2

The long-term properties of concrete mixtures with fRCA have also been investigated and it has been shown that a strong impact of fRCA incorporation on shrinkage of concrete exists. Shrinkage measurements in concrete mixtures with RCA have an increase in the range from 0.67 % to 57.14 % [48]. This effect is primarily explained in literature by the weaker restraint provided by recycled aggregates [55],[50], higher porosity and lower elastic modulus of concrete with RCA [32],[47],[51], higher water absorption leading to accumulating loss of free and absorbed water [52] and consequently, to higher capillarity [51]. Gesoglu et al.[52] investigated shrinkage in SCC mixtures with total replacement of fine and coarse natural aggregates by fRCA and CRCA respectively. Results highlighted increased shrinkage in concrete mixtures with RCA reaching almost double maximum values in comparison to reference concrete. This tendency was connected to the presence of old adhered paste/mortar on RCA, which gives rise to water absorption and thus, loss of amount of water overtime. The effect of fRCA in comparison to CRCA is exemplified in the study of Chinzorigt et al. [32]. The authors investigated a mixture including only CRCA and compared this with simultaneous CRCA and fRCA concrete mixture. The latter displayed higher shrinkage, leading to the conclusion that additional old adhered paste on the fine fraction contributes to higher values. In addition, CO₂ treatment of the recycled aggregates was not effective in terms of shrinkage. In a similar case, Puente de Andrade et al. [53] confirmed the direct relationship between fRCA replacement ratio and shrinkage of concrete mixtures. More specifically, highest substitution ratio (50 %) resulted in the highest recorded shrinkage. All shrinkage measurements were in agreement with mass loss recordings. According to Pedro et al. [21], shrinkage of concrete mixtures incorporating RCA display higher increases for old ages rather than early ages. Higher RCA replacement ratios yielded in elevated shrinkage values and total replacement of natural coarse and fine aggregates led to maximum values of approximately -520 $\mu\text{m}/\text{m}$, as depicted in Figure 2.8. The authors, also, investigated mixtures with RCA originating either from laboratory crushed concrete or from demolition waste. The results illustrated that the source of RCA did not have any considerable effect on the outcome.

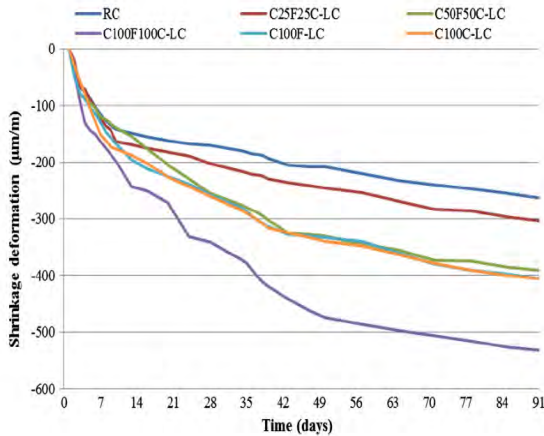


Figure 2.8: Shrinkage deformation of concrete mixtures with fRCA and CRCA originating from laboratory crushed concrete [21].

2.4. Synopsis

To conclude this section, there is a growing body of literature that recognizes the importance of concrete with RCA and identifies the challenges in this topic. Concrete mixtures with RCA tend to show significant differences in terms of both fresh and mechanical properties relatively to traditional concrete. The most probable explanations for this behavior stem from the source of RCA, higher fine content, introduction of additional porosity, lower stiffness due to adhered old paste/mortar and existence of multiple ITZ's.

Although a wide range of studies exist on concrete with RCA, results are inconsistent and conclusions are not unanimous. For instance, the majority of the published studies correlate higher replacement ratios with decreasing performance, but yet a few results are contradicting. A few studies have been able to draw on any systematic research into concrete with RCA and establish the property of concrete that is mostly affected. A sound reasoning to the existing controversial results is the large variety of construction concrete waste that can be used as RCA. Unknown origin of the crushed materials may result in great discrepancies on the performance of concrete. No strict quality controls for RCA exist, which increases the probability of their contamination. Therefore, the quality of RCA is not guaranteed. This study will try to tackle these uncertainties and contribute to understanding of RCA incorporation in concrete mixtures by a number of investigated parameters.

The optimized mortar mixtures with fRCA will be selected from the work of M. Nedeljkovic [58] and will be upscaled to concrete level in the present study. Mortar mixtures were created with $w/c = 0.5$ and $\text{sand/cement} = 3$. Optimization of the mortar mix designs lays on the basis of keeping the cement content the

same as reference mortar. River sand will be replaced at 0%, 25%, 50%, 75% and 100% with fRCA. A specially designed polycarboxylate SP will be used that was developed in cooperation with CUGLA. Additional constituents in this tailor-made SP will assist with defoaming effect and potentially, reduce air content of the mixtures. In practice, concrete mixtures with air content above 3 % are difficult to finish and considerable strength will be lost. This parameter will be a driving factor for approving or eliminating mortar mix designs. The dosage of SP will be adjusted for every mixture in order to achieve desirable consistency levels. As it was apparent from previous studies, the moisture state of fRCA is of high importance. Thus, the presaturation and drying of fRCA and their effect on the performance of mortars will also be examined. Moreover, partial removal of subfraction 0-0.250 mm will be investigated. Finally, mixing sequence will be altered.

The optimal fRCA replacement ratio on mortar mixtures was selected from [58] and mortar mix designs were upscaled to concrete mixtures in this study. Additional concrete mixtures with fRCA and CRCA were investigated. Optimal fRCA replacement ratio was fixed and natural gravel was substituted by 30 % CRCA by volume. This is not an arbitrary value, since this is an upper limit for designing concrete with CRCA according to EN 206. This limit applies to general environmental class and type A1 coarse recycled concrete aggregates, namely CRCA with density higher than 2200 kg/m^3 .

3

Experimental program

”The beginning is the most important part of the work.”

Plato
Greek philosopher
428/427 BC – 348/347 BC

Let us now move on to describing in detail the materials and experiments used in this study. The experimental program is divided into three headings i) characterization of RCA, ii) mortar testing and iii) concrete experiments.

The first step in this process was to measure the physical properties of RCA. Moisture content, water absorption and SSD densities were essential parameters before proceeding with mortars and concrete mixtures. The involved procedures are explained in section [3.1](#) and [3.2](#).

On completion of this stage, a thorough investigation of the optimal mortar mix design was carried out, which is described in section [3.3](#). In order to understand the effect of fRCA on mortars, multiple replacement ratios were evaluated and compared with a reference mixture. The optimal fRCA percentage was selected and a number of mortar mixtures were prepared for testing fresh (flow, air content) and mechanical properties (compressive strength, flexural strength). MIP was used to assess the distribution of pores and the total porosity of mortars with fRCA. Optical microscopy was also used to examine the microstructure of fRCA mortars.

After finalizing the previous stage, the optimal mortar mix design was upscaled to concrete. Additional concrete mixtures with fRCA and CRCA were investigated.

The testing process, described in section 3.4, started with workability and air content experiments. Compressive strength of the concrete mixtures was measured at three ages (7,28,56 days). Additionally, elastic modulus tests were performed and shrinkage was recorded.

3.1. Characterization of fine Recycled Concrete Aggregates (fRCA)

3

In this research study, reference river sand with 93 wt.% of SiO_2 and three types of fRCA of unknown concrete were used. fRCA were provided by three different recycling companies located in The Netherlands. **AVG** (located in South Holland), **Caron Recycling** (located in the North of the country) and **2R** (located in West of the country) delivered the necessary quantities of fRCA. Each company delivered fRCA two times (February 2019 and January 2021) in order to investigate the effect of quality of different fRCA batches from the same company. The reference sand is labeled as sand A. The first deliveries of fRCA are respectively named as sand B, C, D, whereas the second deliveries are labeled as sand NB, NC and ND. The recycling technique was rotor crusher (fRCA B) or jaw crusher combined with a cone crusher (fRCA C, D). The crushing steps differ, as fRCA B was produced with 1 single crushing step, whereas fRCA C and D were produced with 3 crushing steps. fRCA B, NB, NC and ND were delivered fresh without any indoor or outdoor storage of the material. This becomes highly apparent in Figures 3.1, 3.2, 3.3 where fRCA C and D show intense agglomeration forming big chunks of aggregates.

The investigated fRCA can be assumed that they constitute representative samples of the major Dutch fRCA, considering the geographical spread of the companies in the country. In addition, use of two fRCA deliveries broadens the investigation of existing recycled sands and raises repeatability of the process.



(a) fRCA B



(b) fRCA NB

Figure 3.1: First and second delivery of fRCA B



(a) fRCA C



(b) fRCA NC

Figure 3.2: First and second delivery of fRCA C



(a) fRCA D



(b) fRCA ND

Figure 3.3: First and second delivery of fRCA D

3.1.1. Moisture content and water absorption

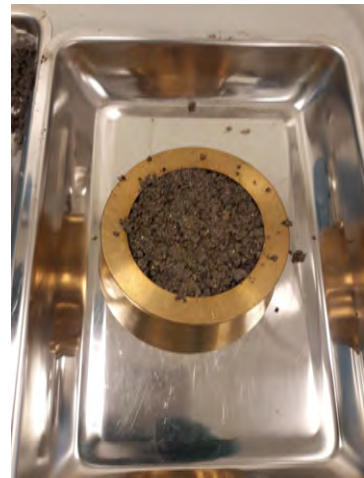
As received fRCA were dried in a ventilated oven at 105 °C for 24 h according to NEN EN 1097-5 [59]. For each source of fRCA, three samples of at least 1 kg were measured and moisture content was recorded after successive weighing in 1 h intervals and until no difference by more than 0.1 % is observed.

Water absorption was measured according to the pycnometer method for aggregate particles passing the 4 mm tests sieve and retained on the 0.063 mm test sieve followed by the standard NEN EN 1097-6 [60]. The dry aggregate sample is first immersed in water bath for 24 h in the pycnometer, which is gently rolled so that entrapped air is released. Subsequently, the SSD state was reached by drying the sample with hot air, as shown in Figure 3.4. The sample is, then, placed in a metallic cone (Figure 3.4), which is slowly lifted, while the aggregates are forming a pyramid. Multiple trials were done to ensure the SSD state of fRCA particles. The SSD state was visually confirmed when the desired shape was achieved according to Figure 3.5. After drying the sample in a ventilated oven for 15 min, water absorption is calculated regarding the mass difference between SSD and oven dry state.

3



(a) Application of hot air on the fRCA sample



(b) Cone testing of fRCA sample

Figure 3.4: Drying and preparing fRCA sample for water absorption determination.

3.1.2. SSD density

SSD density of fRCA is determined according to NEN EN 1097-6 [60]. As described in subsection 3.1.1 and shown in Figure 3.5, the SSD state was achieved by applying hot air on the sample, so that surface moisture evaporates. The sample was, then, dried completely and SSD density is calculated taking into account the differences in the recorded masses. This method cannot be considered as accurate as the Helium Pycnometer Method for measuring physical densities of the aggregates, as it is dependent on visual inspection and rough definition of the SSD state.

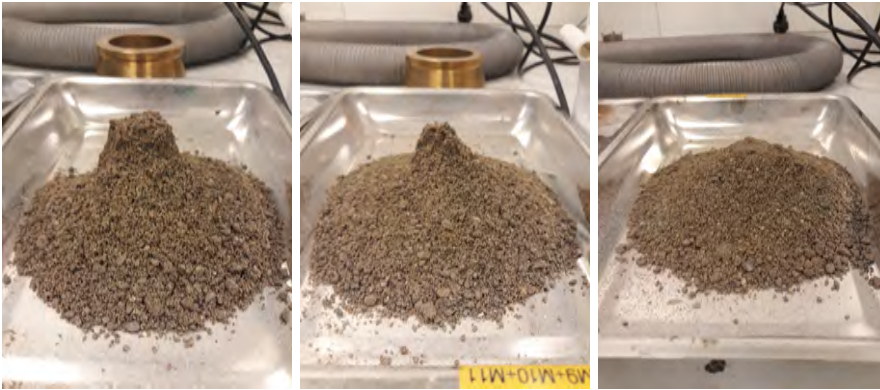


Figure 3.5: Shape of aggregate sample after cone testing. SSD state is reached in the last picture.

3.1.3. Particle size distribution

Dried fRCA samples were divided into various fractions using a sieve tower, as shown in Figure 3.6 Three random samples of various mass were collected. The selected fractions comprise <0.063 mm , $0.063-0.125$ mm, $0.125-0.25$ mm, $0.25-0.5$ mm, $0.5-1$ mm, $1-2$ mm, $2-4$ mm, >4 mm. The fine aggregates were specifically evaluated for the fine content (<0.25 mm). This is an important parameter defined by regulations of concrete mix design. The descending in size fractions of fRCA NB, NC, ND are clearly presented from left to right in Figures 3.7,3.8, 3.9, respectively.

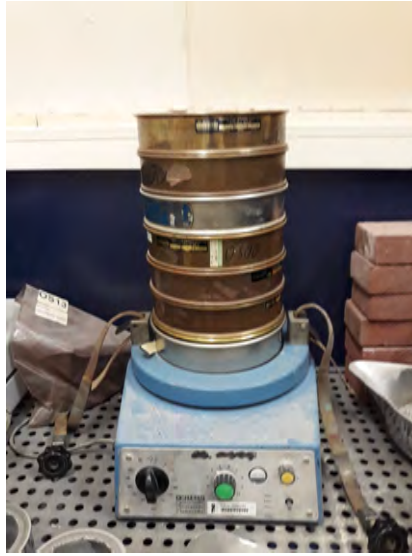


Figure 3.6: Sieve tower for particle size distribution of fRCA.



Figure 3.7: Various fractions of fRCA NB - From left to right : >4 mm, 2-4 mm, 1-2 mm, 0.5-1 mm, 0.25-0.5 mm, 0.125-0.25 mm, <0.125 mm.



Figure 3.8: Various fractions of fRCA NC - From left to right : >4 mm, 1-4 mm, 0.5-1 mm, 0.25-0.5 mm, 0.125-0.25 mm, <0.125 mm.



Figure 3.9: Various fractions of fRCA ND - From left to right : >4 mm, 1-4 mm, 0.5-1 mm, 0.25-0.5 mm, 0.125-0.25 mm, <0.125 mm.

3.2. Characterization of Coarse Recycled Concrete Aggregates (CRCA)

CRCA from unknown concrete origin were, also, investigated in this study. The material was provided by **2R**, the same company that provided fRCA D and ND. For reference gravel, river gravel of 4-16 mm was used. CRCA was dried for further use in physical characterization. As received and dried CRCA are shown in Figure 3.10.



(a) As received CRCA



(b) Dried CRCA

Figure 3.10: Coarse Recycled Concrete Aggregates (CRCA)

3.2.1. Moisture content and water absorption

CRCA was delivered with its natural moisture. Similar to fRCA in 3.1.1, CRCA was dried in a ventilated oven at 105 °C for 24 h according to NEN EN 1097-5 [59].

Three samples were randomly collected from the delivered material for measuring moisture content. After multiple weighing in 1 h intervals and achieving deviation in mass no larger than 0.1 %, moisture content was calculated as the average result of the recordings.

Pycnometer method for aggregate particles passing the 31.5 mm test sieve and retained on the 4 mm sieve according to NEN EN 1097-6 [60], was adopted for determination of the water absorption of coarse aggregates. First, a sample of minimum 2 kg was collected in agreement with the standard. The dried sample was immersed in water bath in the pycnometer. After 24 h, the sample is removed from water and left to drain. The drained test portion is placed in dry cloths, which are used to dry the surface of the aggregates. The SSD state is assumed to be reached, when surface moisture is completely removed (Figure 3.11).



(a) Moisture is absorbed from the surface



(b) No further surface moisture

Figure 3.11: Preparation of test portion of CRCA for water absorption measurement

3.2.2. SSD density

NEN EN 1097-6 [60] was followed for the determination of SSD density. A representative test portion was collected to evaluate SSD density of CRCA. As described in 3.2.1, SSD state is reached after removing surface moisture. After drying the sample, SSD density is calculated by subtracting the difference in masses of the two states.

3.2.3. Particle size distribution

Three randomly collected test portions of different masses of dry CRCA were sieved in fractions of >16 mm, 8-16 mm, 4-8 mm and <4 mm. The present fractions in

descending diameter size order in CRCA are shown in Figure 3.12.



Figure 3.12: Various fractions of CRCA

3.3. Mortars

3.3.1. Mortar series

Ordinary Portland cement CEM I 42.5 N was used in all mortar and concrete mixtures (ENCI, the Netherlands). The composition of the cement, measured by X-ray fluorescence (XRF) was the following (by mass): CaO 63.8%, SiO₂ 20%, Al₂O₃ 4.8%, Fe₂O₃ 3.3%, MgO 2.0%, SO₃ 3.1%, K₂O 0.5%, Na₂O 0.2% [58].

CUGLA superplasticizer (SP) based on polycarboxylates in combination with defoamer was added as a chemical admixture. SP dosage was 0.3% in order to reach the target flow of 140-150 mm [58].

Two series of mortars were investigated:

1. **Series 0** constitutes of multiple mixtures towards achieving the optimal parameters for mortar mix designs, investigated in the study of M. Nedeljkovic et al. [58]. The mixing sequence, moisture state of fRCA and partial removal of the fine content were investigated. According to findings of the experiments [58], the optimal fRCA replacement ratio was 25%. In addition, as received fRCA with their original PSD were used and the modified mixing sequence was applied. The water content has been also corrected relative to the water present in the SP. All mortars had the same effective water-to-cement ratio of 0.5 and the cement-to-sand ratio (1:3). Mortars with fRCA were evaluated in comparison to a reference mortar mixture and were upscaled to concrete level.
2. **Series 1** comprises optimization of mortar mixtures with 100 % fRCA replacement, that was conducted during the author's internship at TNO. This was done by taking into account the water demands of solid constituents and volumetric packing of as received fRCA. Effect of Fly Ash (FA), as mineral admixture, was investigated in terms of improving properties of mortar mixtures. FA was added as substitute for cement at 30 wt%.

Mortar mixtures from **Series 1** will be analyzed in detail. In total, 8 mixtures were investigated and are presented in summary below. The detailed mix designs are shown in the Appendix:

1. Mortar mixtures with 100% fRCA B, fRCA C and fRCA D. These are labeled as: **NB**, **NC**, **ND**. An additional mortar mixture with 100% fRCA D and increased aggregate content was investigated. This was labeled as **NF**. For these mixtures, CEM I 42.5 N was used as binder.
2. Portland cement was replaced at 30 wt% by FA in all aforementioned mortar mixtures. These mixtures are labeled respectively as: **NBFA**, **NCFA**, **NDFA** and **NFFA**.

3.3.2. Flow measurement

The consistency of mortar mixtures was evaluated by flow table according to NEN EN 1015-3:1999 [61]. A truncated conical mold with bottom diameter of 100 mm, top diameter of 70 mm and height of 60 mm was filled with the fresh mortar mixtures. Each mixture was placed in two consequent layers, and each layer was compacted with a tamper for 10 short strokes to ensure uniform filling of the cone. After letting the mixture rest for 15 s, the mold is slowly lifted and the table is jolted for strokes at a constant frequency of approximately 1 drop per second. The flow is measured with a caliper in two perpendicular directions and the average value is recorded.

3.3.3. Air content

Air content of mortar mixtures is measured with standardized pressure method according to NEN EN 1015-7 [62]. A sample cylindrical container of 0.75 L is filled in two layers, and each layer is compacted with 10 strokes using a tamper. Excess mortar is removed by a palette knife. The rim of the container is carefully cleaned to ensure watertight sealing of the pressure cover assembly. The experiment starts with inserting water from one valve, until all air is expelled through the other valve. Subsequently, the valves are closed and air pressure is introduced using the air pump mechanism until the calibration point of the apparatus. Stabilization of the needle is done by gently tapping the pressure gauge. Finally, the test handle is pressed and held until a stable value is obtained. The reading of the air content is taken with accuracy of 0.1 % and $\pm 1\%$ of measuring error.

3.3.4. Flexural and compressive strength

Three mortar samples per mixture were cast in molds of $160 \times 40 \times 40 \text{ mm}^3$ and curing was carried out in a curing room of 95 % RH. At 28 days, mortar prisms were tested for flexural strength under three point bending according to NEN EN 1015-11 [63]. After breakage of the specimens, two cubic halves of $40 \times 40 \times 40 \text{ mm}^3$ derived from each prism were tested under compression. Average results and standard deviations were recorded.

3.3.5. Porosity tests

Total porosity of mortar samples was evaluated according to RILEM CPC 11.3 procedure [64]. The mortar prisms of $160 \times 40 \times 40 \text{ mm}^3$ were first dried in a ventilated oven at $105 \text{ }^\circ\text{C}$, until a constant mass m_1 is obtained. The specimens were next transferred to a vacuum tank with an air pressure not higher than $100\text{-}250 \text{ N/m}^2$. The second stage involves transferring water from an adjacent tank, and the specimens are fully submerged under water. The test is performed, first, under vacuum

and subsequently, atmospheric pressure is applied. Under these conditions, the mass of the sample is measured m_2 . The final step is to record the mass m_3 , while the sample is submerged in water and pressure is removed. The total porosity by immersion under vacuum is calculated as such :

$$A_{vc} = \frac{m_2 - m_1}{m_2 - m_3} \times 100 \quad (3.1)$$

3

3.3.6. Mercury Intrusion Porosimetry (MIP)

The hardened mortar mixtures were taken for Mercury Intrusion Porosimetry (MIP) experiments. The samples were, first, immersed at 28 days in an isopropanol solution for 72 h, which halted cement hydration. The samples were, then, inserted into a ventilated oven for 10 min so that isopropanol completely evaporates. The last step in sample preparation was to insert the samples under vacuum in a freeze dryer, with a temperature of around - 16 °C. The weight loss was recorded with weekly measurements, until two successive recordings differed no more than 1 %.

The sample was removed from the freeze dryer and an amount of ± 8 g is inserted in an air-tight sealed penetrometer. The mass of the sample and the penetrometer was recorded. The MIP device consists of a low- and a high-pressure unit. First, the sample was introduced in the low-pressure unit, where mercury will penetrate into the pores of mortar until a pressure of approximately 100 kPa. Following the recording of the combined mass of the intruded sample and the penetrometer, the high-pressure unit allowed mercury to intrude smaller pore sizes until a pressure of approximately 250 MPa. The accompanying software, Auto-pore IV9500, produced a data file including pore size distribution and total intruded mercury volume.

3.3.7. Optical microscopy

Thin sections of mortar mixtures of **Series 1** were prepared for investigation under optical microscopy. Before starting the preparation for thin section, the samples were dried out for 15 min to ensure evaporation of free water and stop of hydration. This was done at 21 days after casting the mortar mixtures and cured at 65 % RH climate room. First, the sample was sawn off using a water cooled cutting blade. Afterwards, the section was placed in the polishing machine, where a polished surface was obtained. The thickness of the sample was further reduced on a thin section grinder and a fine grinding with 1000 grit was done. The last step includes epoxy impregnation under pressure into the pores of the specimen. Final inspection of the section is done under microscopy validating the desirable thickness and visibility of the morphological characteristics of the samples. An example of a polished section is given in Figure 3.13.



Figure 3.13: Polished section of a mortar mixture of Series 1

3.4. Concrete

The optimal mortar mix designs from **Series 0** were upscaled to concrete. Mortars from **Series 1** were considered to be very demanding in terms of cement increase and water absorption of fRCA and thus, not practical for industrial purposes. Therefore, they were not upscaled to concrete level. Concrete mix designs were performed according to norm NEN EN 206 [65] and mixtures were designed for a strength class of C30/37. Target consistency class was F4 (>150 mm in slump test) and XC3 environmental class was selected (NEN 8005 [66]). Dosage of SP was adjusted for each concrete mixtures as a percentage of cement weight so that the desirable consistency class is achieved. The maximum aggregate size is restricted to $D_{max} = 16\text{mm}$ and grading must lay in Zone I. According to NEN 206-1 [65], the following equation was used to estimate strength of concrete:

$$f'_{cube} = f'_{ck} + 1.65 \times \sigma = 37 + 1.65 \times 4 \cong 43.6\text{MPa} \quad (3.2)$$

where : f'_{cube} is the average cube strength (e.g. 28 days), f'_{ck} is the characteristic strength of concrete and σ is the standard deviation.

According to Dutch practice, concrete cube strength at day "n" can be estimated with the following equation:

$$f'_{cube} = \alpha \times N_{28} + \frac{b}{w/c} - c \quad (3.3)$$

where α , b , c are constants for type of cement CEM I, N_{28} is the nominal strength of CEM I 42.5 N at 28 days and w/c is the water to cement ratio.

From Equation 3.3, the unknown w/c can be derived as follows:

$$w/c = \frac{b}{f'_{cube} - \alpha \times N_{28} + c} = \frac{33}{43.6 - 0.85 \times 46.2 + 62} \rightarrow w/c = 0.5 \quad (3.4)$$

Environmental class XC3 allows $(w/c)_{max} = 0.55$ and thus, the calculated value $w/c = 0.5$ complies with the regulations. Cement content C , according to environmental class X3, must be at least $C_{min} = 280Kg/m^3$. Considering that it is desirable to keep the cement content as low as possible and simultaneously, achieve the target strength class, it was decided upon $C = 350Kg/m^3$.

Three concrete series were defined in this study:

1. Reference concrete mix **A100** with 100% sand A. Concrete with 25% fRCA from the first delivery (fRCA B, C, D). These concrete mixtures were labeled as: **B25**, **C25** and **D25**, respectively.
2. Concrete with fRCA from the second delivery (concrete with 25% fRCA NB, NC, ND) – Effect of 'batching'. These concrete mixtures were labeled as: **NB25**, **NC25** and **ND25**.
3. Concrete with fRCA (25%) from the second delivery (fRCA NB, NC, ND) and 30% CRCA. An additional reference concrete mixture with 100% sand A and 30% CRCA (labeled as **A70**) was created. The remaining recycled mixtures are **NB25/30**, **NC25/30** and **ND25/30**.

For all concrete mixtures, the modified mixing sequence was applied, as mentioned in 3.3. This means that all natural fine and coarse aggregates together with cement are first mixed for 1 min. Afterwards, water and SP is added and mixed with other constituents for additional 2 min. Finally, RCA (either fRCA or both fRCA and CRCA) are added and mixed for 2 more min. The mixing speed is low for all stages. The modified mixing sequence is shown in 3.14.

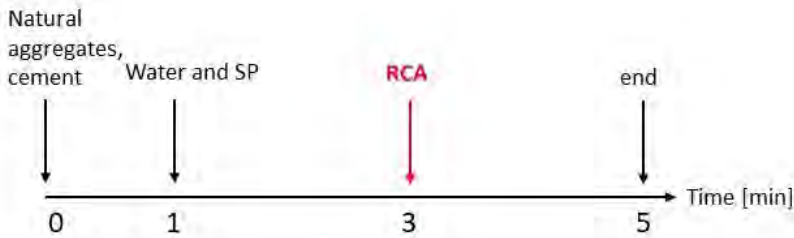


Figure 3.14: Modified mixing sequence applied for concrete mixtures

3.4.1. Workability

Workability of fresh concrete mixtures was tested with the slump test according to NEN EN 12350-2:2009 [67]. A truncated conical mold with 200 mm base diameter, 100 mm top diameter and 300 mm height is filled with concrete in fresh state in three consequent layers. Each layer occupies approximately one third of the mold volume and is compacted with 25 strokes using a tamping rod. The bottom layer is compacted throughout its depth, whereas the second and top layer is compacted in a way that the strokes just penetrate into the underlying layer. Excess material is removed by leveling the surface of the top layer. The assembly is left for 15 s and the mold is raised steadily in 5 s. The distance between the top surface of the mold and the top point of the fresh concrete mixture is recorded as the slump value. The slump experiment is clearly shown in Figure 3.15.



Figure 3.15: Slump test set up for fresh concrete mixtures

3.4.2. Air content

Air content of fresh concrete mixture is measured according to ASTM C231/C231M-10 [68]. A cylindrical measuring bowl with a total volume of 8 L is used for filling in the material. The interior of the container is dampened with a wet cloth. Freshly mixed concrete is then introduced in three equal layers, which are compacted in the same way as described in 3.4.1. A thorough cleaning of the rims of the filling container is required so that pressure-tight sealing with the cover assembly is ensured. Water is introduced from one petcock, until all water emerges from the opposite petcock and all air is expelled by gently jarring the assembly. The valves are, then, closed and air pressure is introduced in the chamber by using the pumping mechanism on top of the cover assembly, until the measuring needle reaches the calibration point. Finally, air is released by pressing the top button and the air content value is taken, when the measuring needle at the gauge stabilizes. If no stable recording is observed, the experiment must be repeated due to leakage. The configuration of the air content experiment is depicted in Figures 3.16.

3



(a) Introduction of freshly mixed concrete



(b) Cover assembly

Figure 3.16: Air content experiment of fresh concrete mixtures.

3.4.3. Compressive strength

Cubic molds of $150 \times 150 \times 150 \text{ mm}^3$ were cast to be tested under compression according to standard NEN EN 206-1 [65]. Fresh concrete was introduced in two layers in the cubic molds and each layer was compacted using a vibration table for approximately 10 s (Figure 3.17). After leveling and skimming off the excess material, a plastic sheet cover was placed on the surface of the samples. The cubes were demolded after 24 h (Figure 3.17) and stored in the curing room (with 95 % RH, $T = 20 \text{ }^\circ\text{C}$). Three (3) cubes were tested at each age of 7, 28 and 56 days. The machine for compression tests has a loading capacity of 5000 kN and the loading rate 13.5 kN/s.



(a) Introduction of freshly mixed concrete in two layers



(b) Plastic sheet cover on concrete cubes for 24 h immediately after casting

Figure 3.17: Casting concrete cubes for compression tests

3.4.4. Elastic modulus & Poisson's Ratio

Static modulus of elasticity is determined for the hardened concrete mixtures according to NEN-EN 12390-13:2013 [69]. Rectangular molds of $400 \times 100 \times 100 \text{ mm}^3$ were used for casting the freshly mixed concrete in two layers. Similarly, each layer was compacted by vibration for approximately 10 s. After leveling and skimming off the excess material, a plastic sheet cover was placed on the surface of the samples. The prisms were demolded after 24 h and stored in the curing room (with 95 % RH, $T = 20 \text{ }^\circ\text{C}$). Three (3) prisms per concrete mixture were tested at 28 days. Four (4) LVDT's parallel to the loading direction were placed at fixed points of the specimen for measuring the vertical strains, whereas two (2) perpendicular LVDT's recorded horizontal strains for deriving Poisson's ratio (ν). The loading sequence starts with loading the specimen until 10 % of their corresponding compressive strength at 28 days. Afterwards, three cycles of loading and unloading are performed between 10 % and 20 % of the ultimate value. When the latter values are reached, the load is held for a maximum period of 20 s and loading/unloading follows. The loading rate for all load sequences is 1 kN/s. An accompanying computer software records all

LVDT's measurements. Average strains are used for calculations. Using the fundamental equation of elastic materials $\sigma = E \times \varepsilon$, elastic modulus E_{cm} of concrete is derived, whereas Poisson's ratio ν comes from the division of horizontal and vertical strains. The test set up is shown in Figure 3.18.



Figure 3.18: Experimental setup for elastic modulus tests of concrete

3.4.5. Shrinkage & Mass loss

Molds of 75 x 75 x 280 mm³ (Figure 3.19) were cast in order to measure drying shrinkage according to ISO 1920-8:2009 [70]. The molds constitute of special tap points at the top and bottom of the assembly, that are incorporated inside the specimen after demolding. Likewise, fresh concrete was introduced in two layers and each layer was compacted at the vibration table for approximately 10 s. After leveling and skimming off the excess material, a plastic sheet cover was placed on the surface of the samples. The prisms were demolded after 24 h and stored in the climate room (with 55 % RH, T = 20 °C) (Figure 3.19).

Special tap points are embodied in the specimens that allow accurate placement in the measuring gauge, as depicted in Figure 3.20. Successive daily measurements are taken for the first two weeks and values are frequently recorded until approximately 60 days. The device measures an arbitrary value, as a starting point at day 1, and gradual decreases are recorded. Shrinkage strains are derived by subtracting the differences in recordings and obtaining the length change. In parallel to shrinkage measurements, consecutive weighings of the samples are recorded and mass percentage loss is calculated.



(a) Shrinkage molds of $75 \times 75 \times 280 \text{ mm}^3$



(b) Curing and storage of concrete specimens for shrinkage at 20°C and 55 % RH

3

Figure 3.19: Dimensions of molds and hardened shrinkage concrete specimens



Figure 3.20: Measuring gauge device for shrinkage of concrete

4

Results

"Eureka!"

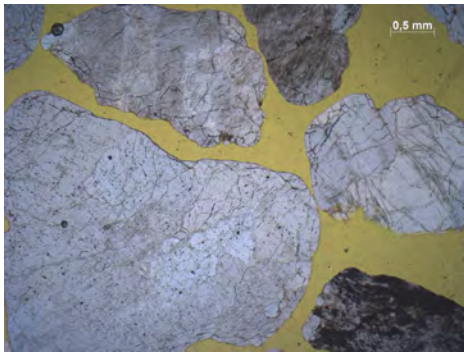
Archimedes

Greek mathematician, physicist, engineer, inventor, and astronomer
287 BC - 212 BC

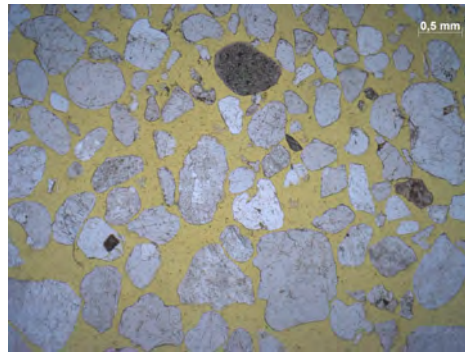
This chapter presents the results of the experimental program described in chapter 3. The physical properties of fRCA and CRCA are presented in section 4.1. Afterwards, the results of mortars optimization from Series 1 will be given in section 4.2. As mentioned previously, mortars from Series 0 were optimized in the work of M. Nedeljkovic et al. [58] and details of the experimental results will not be repeated. The optimized mortar mixtures from Series 0 were upscaled to concrete level and the findings will be presented in section 4.3.

4.1. Recycled materials

The appearance of grain size fractions 0.0632 mm and 24mm of fRCA in comparison to river sand is shown in Figure 4.1. Differences in particle shape of river sand and fRCA are illustrated. Rounded grains are observed for river sand, whereas fRCA demonstrates more angular shape. fRCA can be found either in single aggregate particles or in composite form. Single aggregate particles are mostly composed of quartz and calcite. Composite grains consist of dense or loose cluster of particles linked by old cement paste. Denser composite aggregates are seen in microphotographs (c) and (e) for fRCA B and C respectively. A good example of loose clusters is illustrated in microphotograph (g). Large amount of voids is observed, which can be attributed to a high aggregate-to-binder ratio or poorly compacted concrete. This will cause weak internal coherence and consequently, less stiff aggregates.



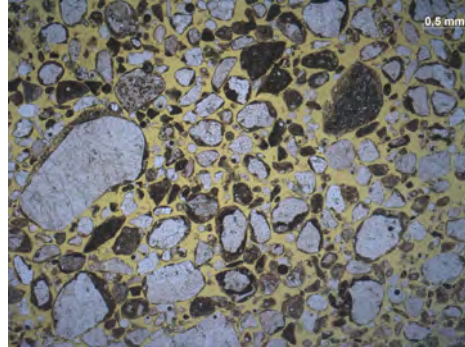
(a) River sand A (fraction 2-4 mm)



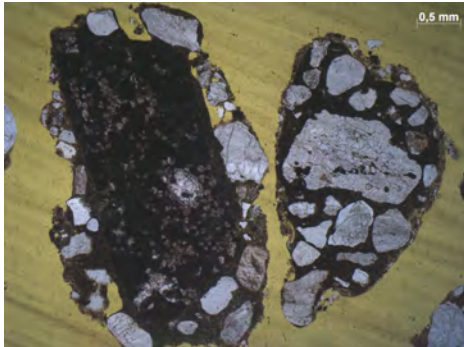
(b) River sand A (fraction 0.063-2 mm)



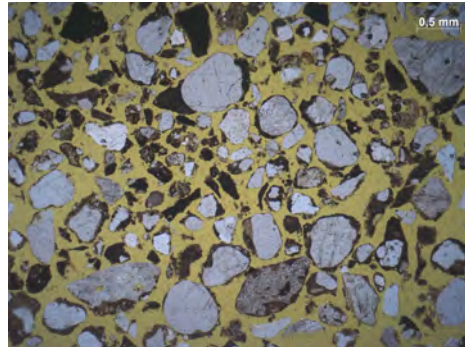
(c) fRCA B (fraction 2-4 mm)



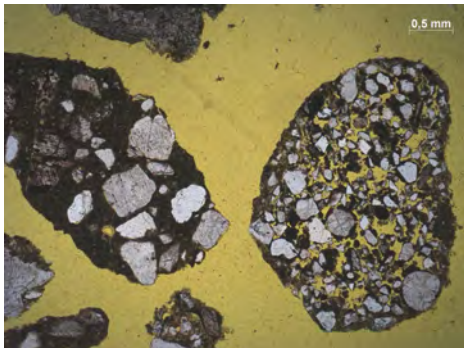
(d) fRCA B (fraction 0.063-2 mm)



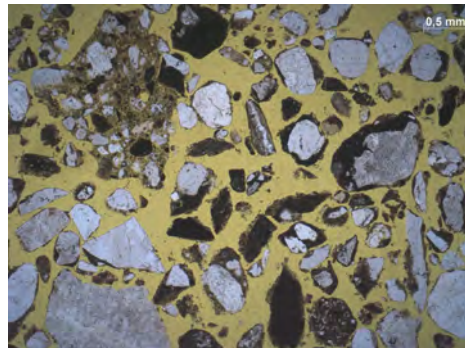
(e) fRCA C (fraction 2-4 mm)



(f) fRCA C (fraction 0.063-2 mm)



(g) fRCA D (fraction 2-4 mm)



(h) fRCA D (fraction 0.063-2 mm)

Figure 4.1: Microphotographs of 0.063-2 mm and 2-4 mm fractions of river sand A and fRCA B, C, D [15]

The physical properties of natural and recycled concrete aggregates are the starting point for mortar and concrete mix design. As depicted in Figure 4.2, moisture content of RCA differs significantly from natural aggregates. Highest moisture content is measured for fRCA B. This is in line with water absorption capacities of RCA. Figure 4.3 highlights the considerably higher water absorption of fRCA compared to natural sand. Similar values are obtained for fRCA B and C in both deliveries, whereas 2nd batch of fRCA D displayed a substantial increase in comparison to 1st batch.

Regarding coarse aggregates in this study, the same tendency exists. CRCA contains larger moisture content in comparison to zero moisture content of natural river gravel, according to Figure 4.2. Moreover, water absorption was 9 times higher than river gravel with a value of almost 4.5 %, according to 4.3.

4

SSD density results are presented in Figure 4.4. Natural river sand displays the highest density of 2647 kg/m³. Decreased densities are measured for all types of fRCA. The lowest value is obtained for fRCA ND reaching a value of 2350 kg/m³. The values are in agreement with the differences in densities measured for fRCA in literature, where the majority lays below 2500 kg/m³. In addition, most of the studies reported densities of natural sand higher than this limit and a significant difference between fRCA and natural sands [16], [17], [22]. Major decrease is, also, observed for CRCA. The density of the latter is 2142 kg/m³ in comparison to 2650 kg/m³ of natural gravel.

Figure 4.5 shows the particle size distribution of natural aggregates and RCA. It can be seen that all materials comply with the regulation limits set by EN12620 [71]. All types of fRCA, with a dominantly angular shape, have finer particle size distribution compared to river sand. fRCA B and NB have almost identical curves. Slight differences are observed for fRCA C and NC, whereas a small difference is reported for fRCA D and ND. All types of fRCA show lower passing percentage at the 1 mm nominal sieve. Similarly, CRCA in Figure 4.5, follow a finer particle size distribution curve than river gravel. Attention is drawn on the 4 mm nominal sieve, where CRCA has residual material passing the fine aggregates limit and consequently, adding up to the fine aggregate percentage.

The opposite behavior exists for fine content (<0.25 mm), except for fRCA B and NB. From Figure 4.6, it becomes obvious that the fine content is significantly increased for fRCA C, NC, D and ND relative to river sand, fRCA B and NB. The fine content mainly depends on the attached old cement paste, the recycling crushing technique and the number of steps [15], as well as on the type of construction waste. fRCA B originates from residuals of precast concrete elements and are produced with 1 crushing step. Since fRCA type C and D are produced with 3 crushing steps and a variety of less stiff construction material is present, it is reasonable to obtain higher fine content. The deviation in fine content between the two deliveries can be justified by the heterogeneity of fRCA.

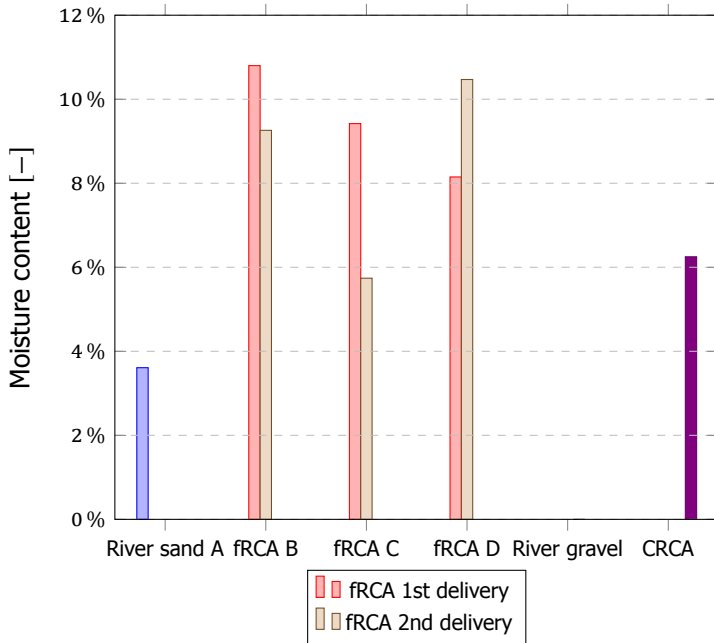


Figure 4.2: Moisture content of natural and recycled aggregates

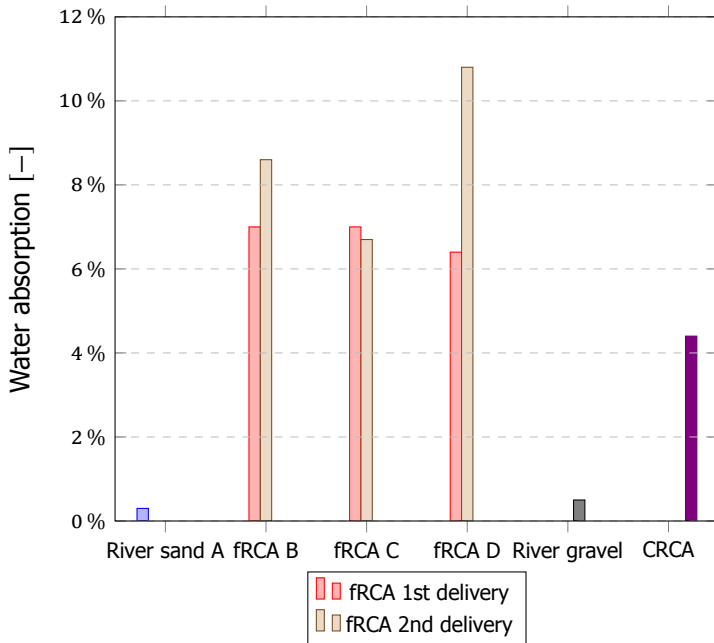


Figure 4.3: Water absorption of natural and recycled aggregates

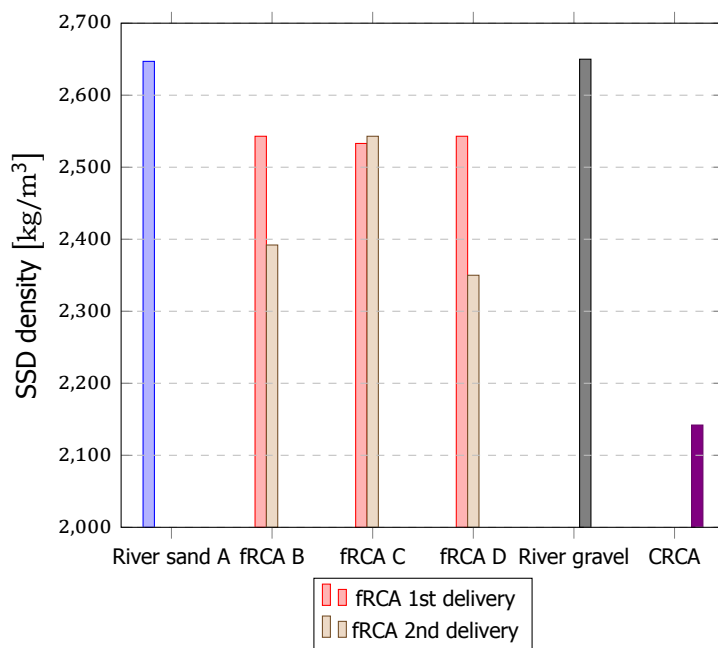


Figure 4.4: SSD density of natural and recycled aggregates

A thorough physical and chemical characterization of river sand A, fRCA B, C and D was performed by M. Nedeljković et al. [15]. A summary of these properties is listed in Table 4.1.

Property	River sand A	fRCA B	fRCA C	fRCA D
Water soluble sulfates (wt.%)	0	0.16	0.14	0.1
Acid soluble chlorides (wt.%)	0	0.04	0.04	0.04
Old cement paste (wt.%)	0	19	25.8	16.2
Quartz content (wt.%)	94.1	57.7	62.7	72.1
Calcite content (wt.%)	0	8.7	7.6	3.8
Amorphous content (wt.%)	0	25.1	21.9	19
Reactivity (J/g of sand)	0	0.71	0.72	0.51
BET Surface area (m ² /g) of 0-0.250 mm fraction	0.7	8.9	6.4	7.8
D50 (μm) of 0-0.250 mm fraction	125	41	71	50

Table 4.1: Physical and chemical characterization of studied sands [15]

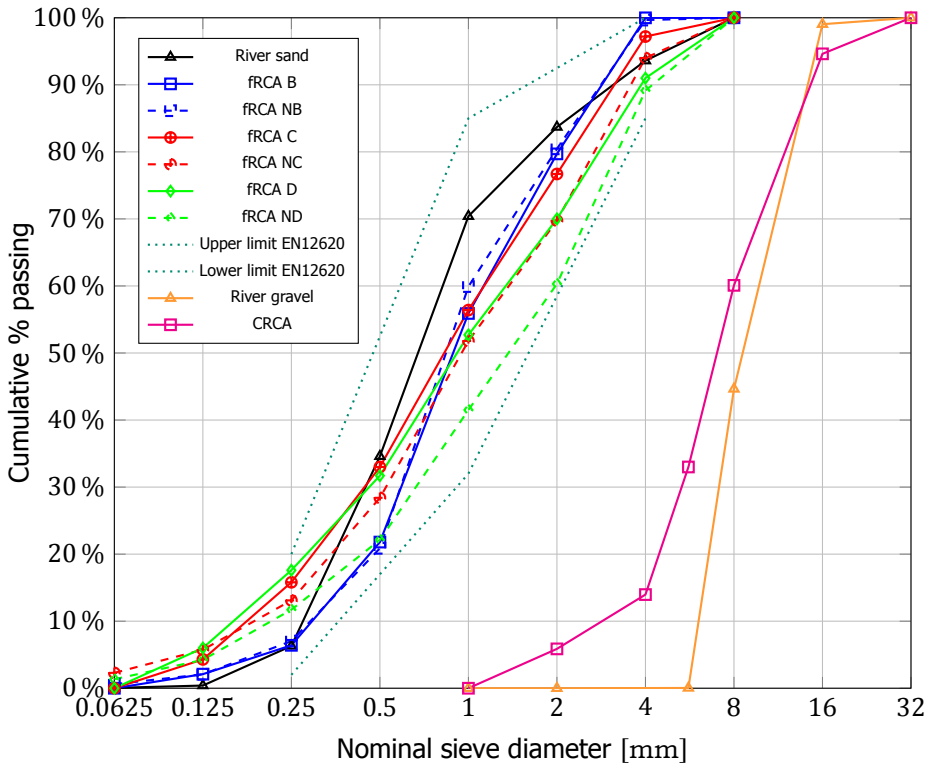


Figure 4.5: Particle size distribution of fine and coarse aggregates

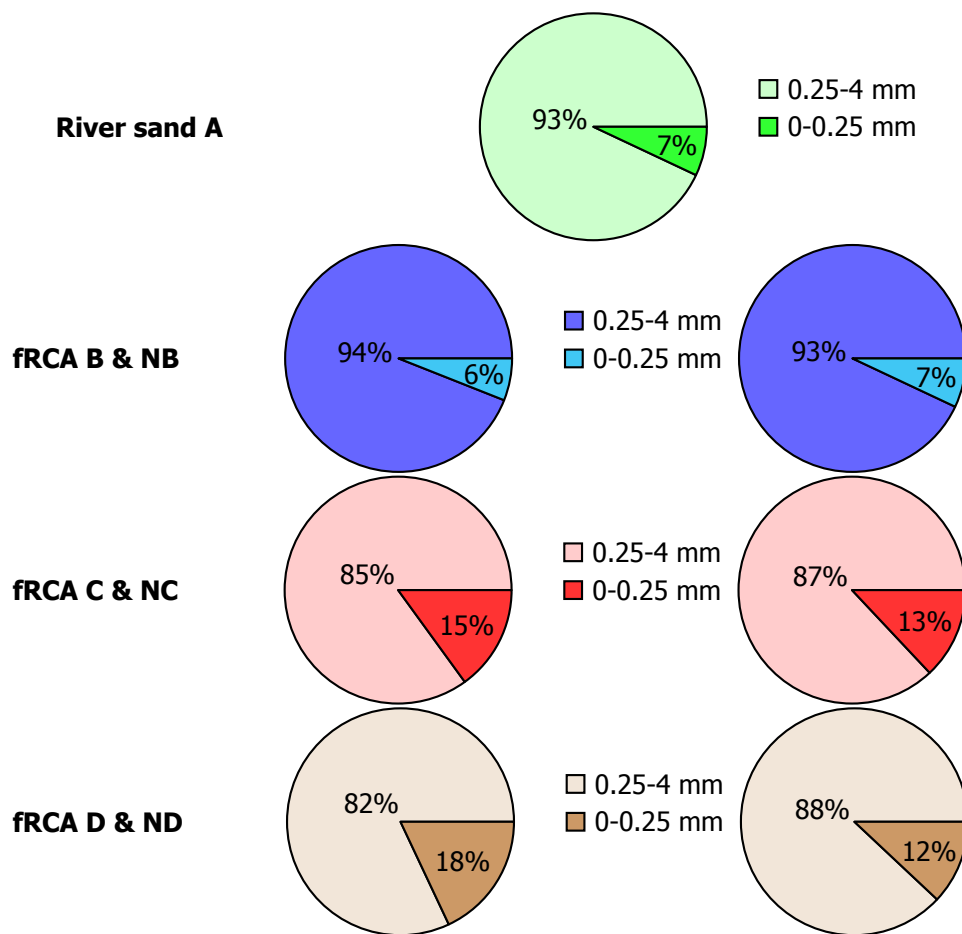


Figure 4.6: Fine content 0-0.25 mm for fine aggregates

4.2. Mortar level

The results of the experimental program for mortars of Series 1 incorporating 100% fRCA are presented in this section ¹. First, fresh properties, such as fresh density, air content and flow will be presented. Afterwards, compressive and flexural strength of mortars, as well as porosity results will be shown. Finally, optical microscopy results will be presented.

4.2.1. Fresh density

Figure 4.7 shows the fresh densities of mortars with fRCA. Very similar values are observed among the mortar mixtures. The maximum fresh density is approximately 2050 Kg/m³ and reached for NC. As it can be seen in the graph, mortars with FA demonstrate lower fresh densities, except for ND, which shows a slight increase.

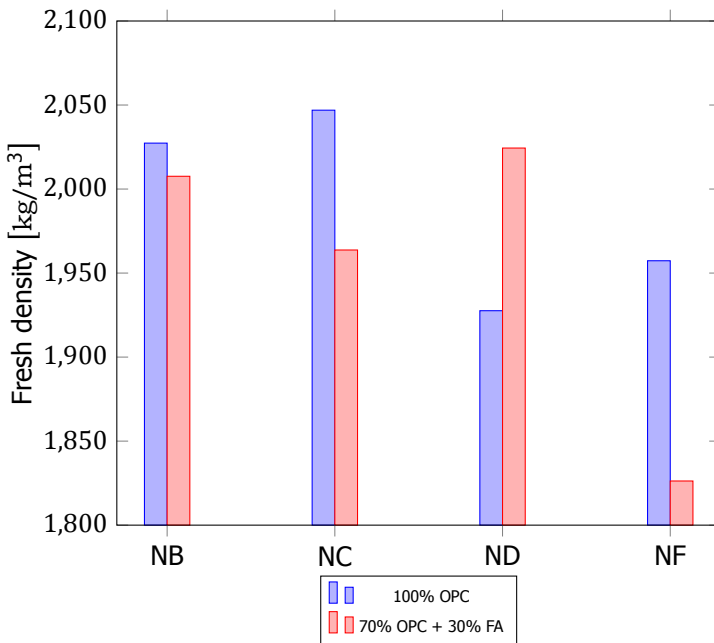


Figure 4.7: Fresh density of mortar mixtures of Series 1

4.2.2. Flow

Figure 4.8 provides the results obtained from the flow table test. As it is apparent from the graph, the target flow around 150 mm was reached for all mortar mixtures.

¹Results about mortars of Series 1 are obtained during the author's internship at TNO

This flow level guaranteed a workable mixture.

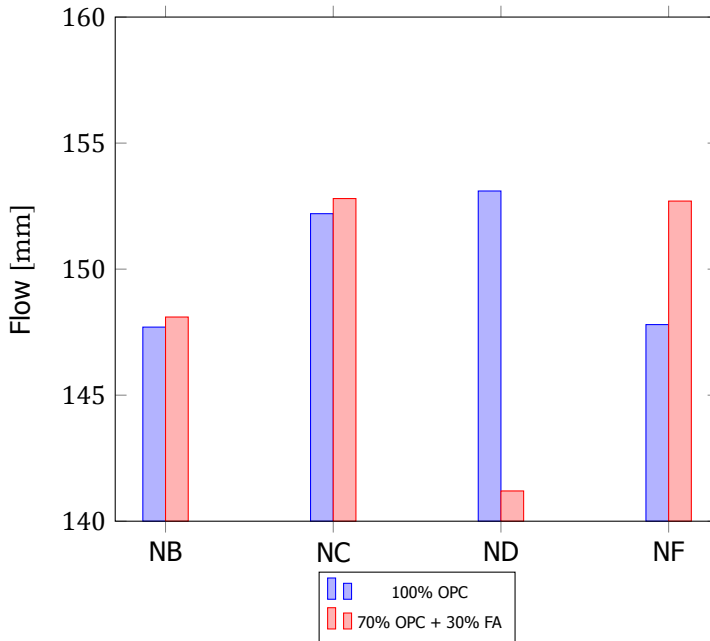


Figure 4.8: Flow of mortar mixtures of Series 1

4.2.3. Air content

Figure 4.9 presents the air content of fresh mortar mixtures of Series 1. What stands out in this graph is that all mortar mixtures with fRCA resulted in elevated air content values ranging from 8.5 % to 12 %. What is also interesting in this graph is that mortars NF and NFFA resulted in considerably higher content in comparison to mortars ND and NDFA. That can be probably attributed to additional pores originating from fRCA since in mortar NF the aggregates occupy a larger volume (0.68 in NF to 0.58 in ND). In turn, increased air content was measured for mortars ND and NF relative to NB and NC. This comes in agreement with the water absorption values depicted in Figure 4.3. Additionally, there is a clear decreasing trend in air content for mortars with FA. Fly ash has a positive effect on air content and resulted in reduced values ranging from 5.5 % to 8.5 %.

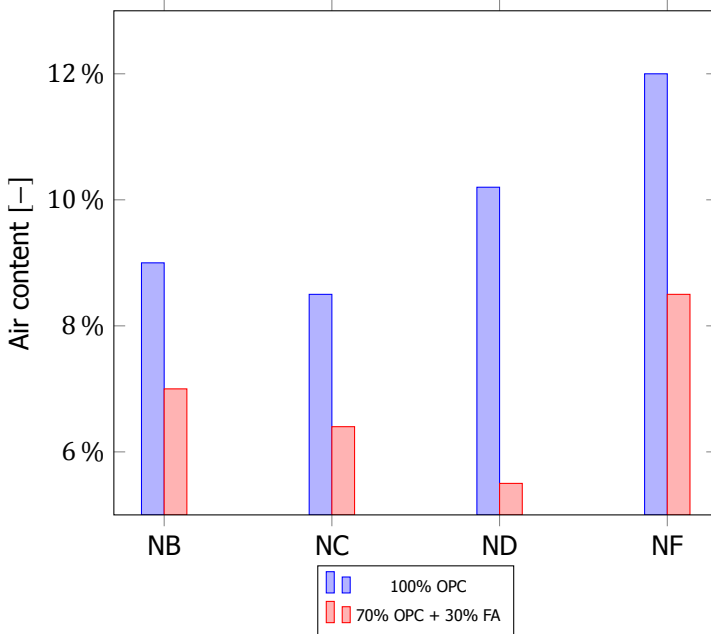


Figure 4.9: Air content of mortar mixtures of Series 1

4.2.4. Compressive strength and flexural strength

Figure 4.10 presents the compressive strength of the mortar mixtures at different ages. What is striking about the data in this table is that an apparent relation between the aggregate fraction and the strength results exists. A closer look to mortars NF and NFFA illustrates that the lower paste fraction results in a significantly lower compressive strength. Furthermore, the best performance is detected for mortar NB reaching a value of 32.4 MPa at 28 days. No considerable differences are observed for mortars NC and ND. That is supported by the almost identical binder paste fraction in spite of the fact that w/c ratios are different. This will be explained further in Table 4.2. However, mortar mixture NF had a considerably lower compressive strength, since the binder paste fraction is also lower.

Proceeding now to mortar mixtures with 30% FA, it is surprising that NBFA, NCFA, NDFA had comparable compressive strengths with mortars NB, NC and ND, since FA reacts a lot slower than CEM I 42.5 N. That observation is not made when a comparison is done for NF and NFFA, where compressive strength is reduced significantly. That discrepancy can be potentially attributed to the higher aggregate fraction governing the performance of mortar mixture. Figure 4.11 shows clearly that slower strength development is observed for mixtures with FA.

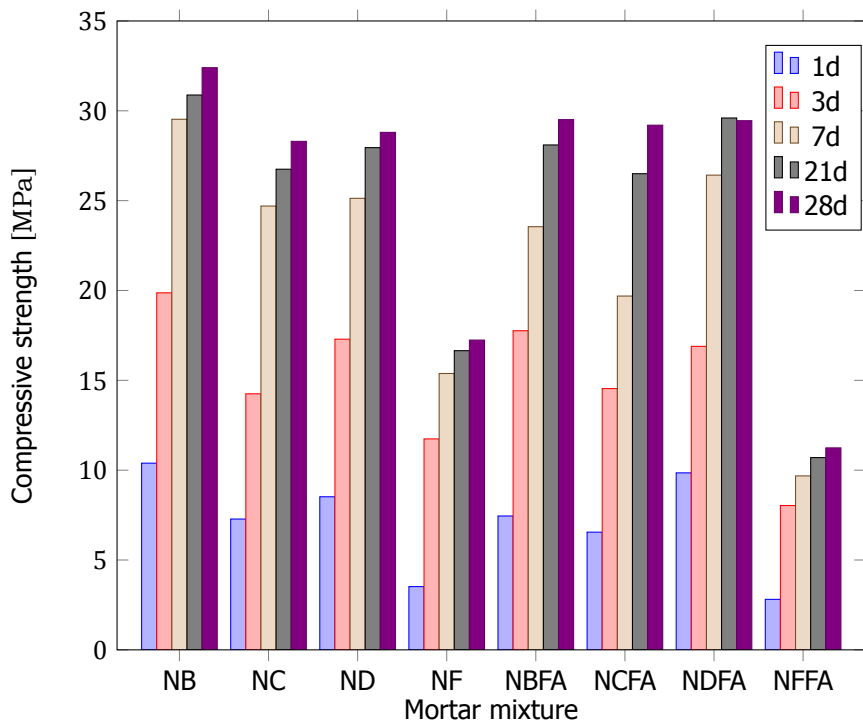


Figure 4.10: Compressive strength of mortar mixtures

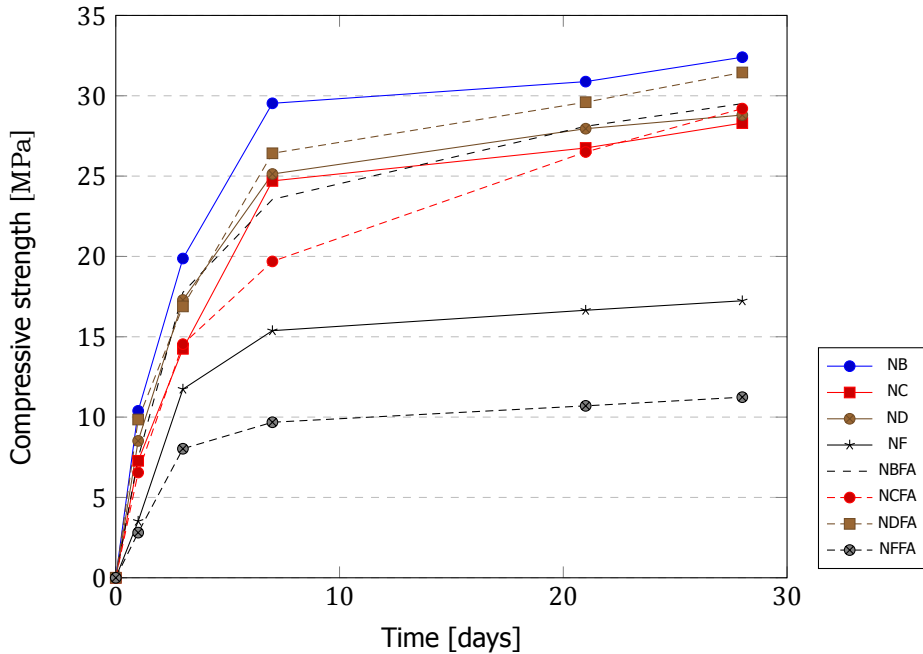


Figure 4.11: Compressive strength time development

The same tendency is observed in flexural strengths in Figure 4.12 at three different ages. The maximum value is 8.0 MPa for mortar NB at 28 days. Similarly to compressive strengths, mortars NC and ND has a slightly lower flexural strength at 28 d, whereas mortar NF is significantly lower due to the increased aggregate fraction. Regarding mortars with 30% FA, it is surprising that NCFA stands out and performed even better than NC. However, the difference is not large and it can be claimed that an equal level of flexural strength was reached. For the remaining mortar mixtures, a reduction of approximately 20 % is observed for NBFA and NDFA, whereas the decrease approached 50 % for NFFA.

Fig. 4.14 shows the relationship between compressive and flexural strength of mortars of Series 1 at 28 days. Data collected from the experimental results in this graph revealed that compressive strength is approximately 4 times higher than flexural strength in all mortar mixtures.

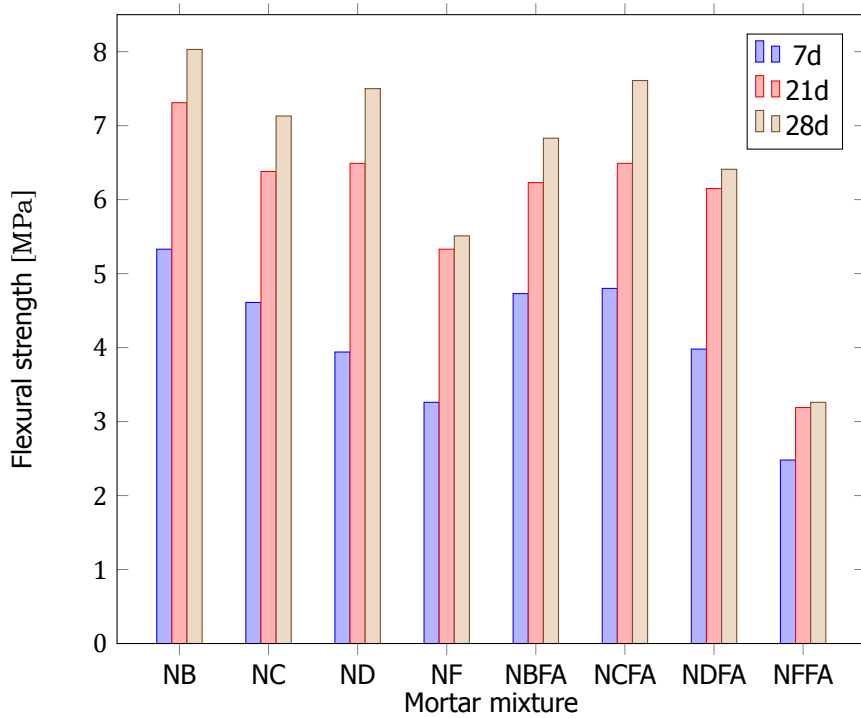


Figure 4.12: Flexural strength of mortar mixtures of Series 1

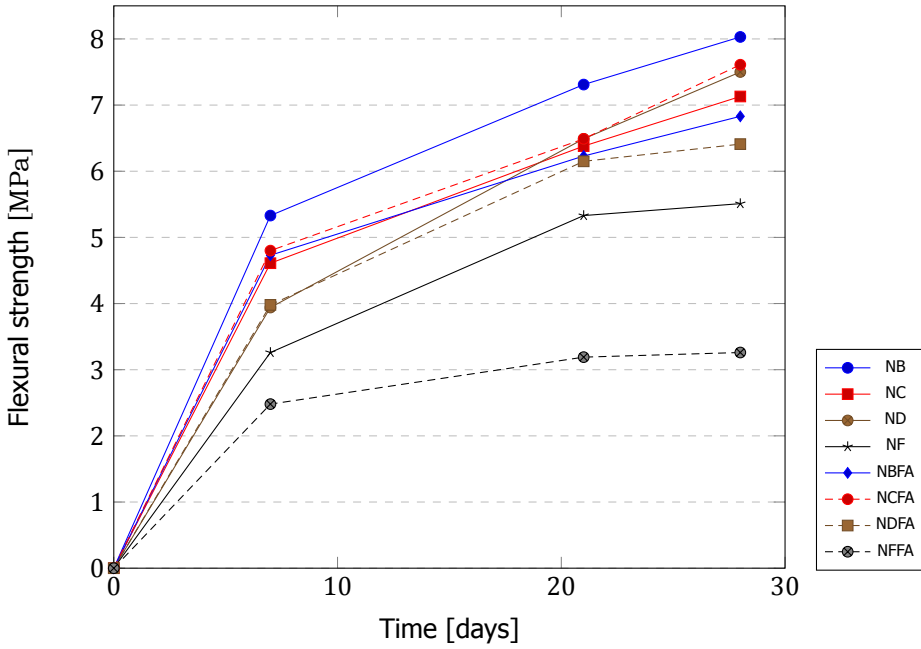


Figure 4.13: Flexural strength time development of mortar mixtures of Series 1

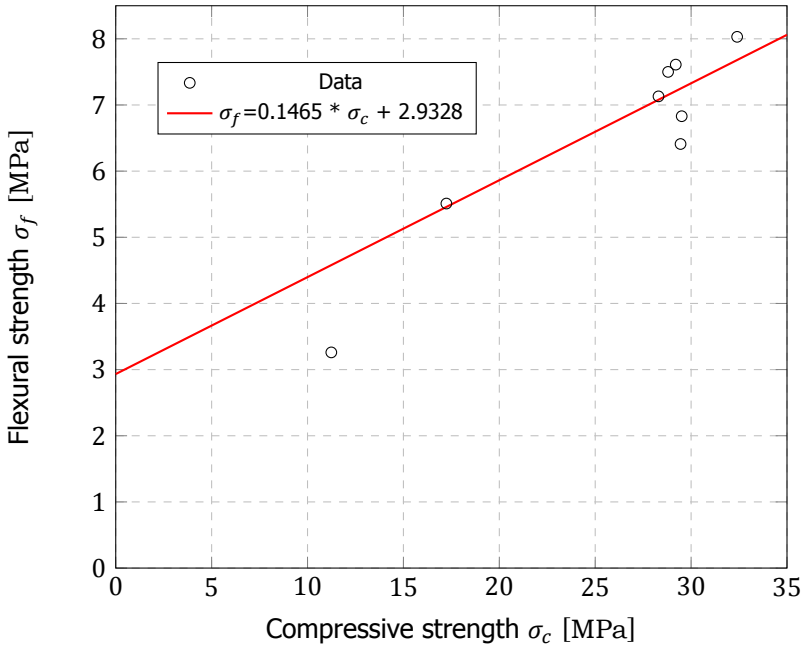


Figure 4.14: Relationship between compressive and flexural strength of mortar mixtures of Series 1 at 28 days

4.2.5. Porosity

Results obtained from porosity experiments at 7 and 21 days are presented in Figure 4.15. Similar porosity is measured for mortars with different source of fRCA. The highest values at 21 days are obtained for mortar ND and NF laying around 33%. Furthermore, porosity is reduced with longer curing time. With regard to mortars with FA, a more significant decrease over time is observed. Additionally, mortars with FA demonstrated a considerable increase in porosity in comparison to NB, NC, ND and NF respectively. For instance, porosity of NB was 32 %, whereas NBFA reached a value of 42 %.

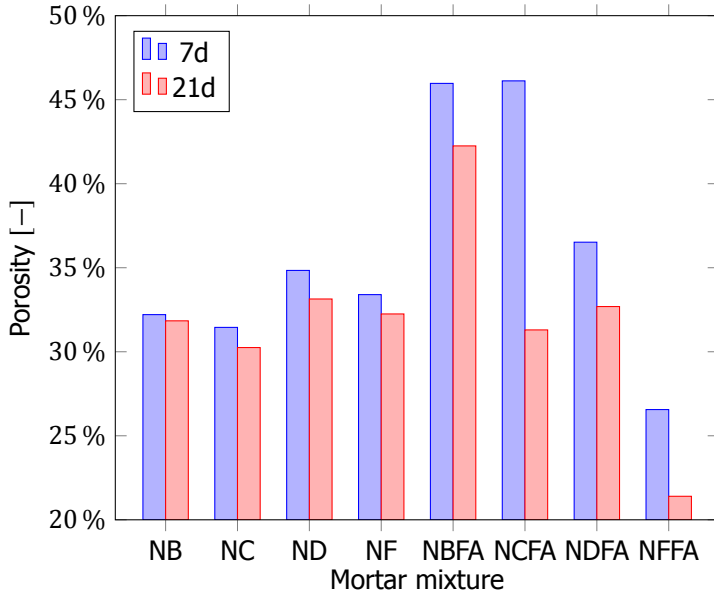


Figure 4.15: Porosity of mortar mixtures of Series 1

4.2.6. Microscopic analysis

According to the mix designs provided in the Appendix, w/c ratios are calculated theoretically. The first assumption was that the total water absorption capacity of fRCA is reached and water is completely in the pores of fRCA. On the other hand, the second hypothesis was that no water was absorbed by the fRCA pores and the entire quantity contributes to the binder paste. The two calculated w/c ratios are labeled as min. wcr. and max/ w/c in the Table 4.2. The third column of the table was obtained from optical microscopy, where samples were compared with reference samples and wcr. was extracted. What is interesting from these results is that no consistency is observed. The general conclusion is that water is not fully absorbed by the fRCA pores and a part of that water contributes to lubrication of the paste. The quantification of that part of the water is not easy to define, since it directly depends on the capillary pores of fRCA, interconnectivity of the pores and the water absorption kinetics.

More accurate results are obtained when comparing air content from air content experiment and optical microscopy. A quantification of the air content using optical microscopy was performed and the values are presented in the Table 4.3. Surprisingly, these results demonstrate that a very close approach was reached for air content results from both methods regarding mortars NB, NC, ND, NF, NBFA and NDFA. However, discrepancies occur for mortars NCFA and NFFA, where optical microscopy showed a higher air content.

Mortar sample	min. wcr	max. wcr	wcr from opt. microscopy
NB	0.38	0.58	0.55
NC	0.46	0.65	0.50
ND	0.33	0.58	0.55
NF	0.40	0.81	0.55
NBFA	0.45	0.67	>0.50
NCFA	0.54	0.75	0.55
NDFA	0.42	0.69	0.4-0.45
NFFA	0.49	0.98	0.50

Table 4.2: Comparison of wcr calculated from mix designs and from optical microscopic analysis

Various photographs of the microstructure of mortar mixtures of Series 1 were taken using optical microscopy. A few examples of the most interesting findings are presented in Figures 4.16, 4.18 and 4.17.

In Figure 4.16, presence of carbonated paste is observed on the upper edge of mortar mixtures NBFA and NDFA. Since the mortar mixtures were cured in a sealed climate room, carbonation originates from the parent concrete, which is adhered on the surface of fRCA. Turning now to Figure 4.17, internal porosity of fRCA and formation of ITZs are illustrated. The porosity inside a particle of fRCA is highlighted in mortar NDFA on the left picture. Interconnectivity of the capillary pores allowed

Mortar sample	Air content from experiments	Air content from opt.microscopy
NB	9	10
NC	9	8
ND	10	10-12
NF	12	15
NBFA	7	5-7
NCFA	6.4	10
NDFA	5.5	5-7
NFFA	8.5	10

Table 4.3: Comparison of air content measured experimentally and derived from optical microscopic analysis

4

epoxy to penetrate into the pores of fRCA and give a clear picture of the additional porosity that exists due to old adhered cement paste. This is also observed on the fRCA particle on the top right part of NFFA mortar in Figure 4.17. ITZ between fRCA particles and the new paste is visible by the bright surrounding light. The intensity of this zone is not considerably high and thus, it can be said that ITZ width is not very high. Finally, in Figure 4.18, a quick qualitative air content evaluation can be made. For both mortars NB and NC, it is apparent that large entrapped air bubbles exist and are distributed throughout the new binder paste. Agglomeration of fRCA is one possible hypothesis that causes this elevated air, but no evidence has been found in previous studies for this phenomenon.

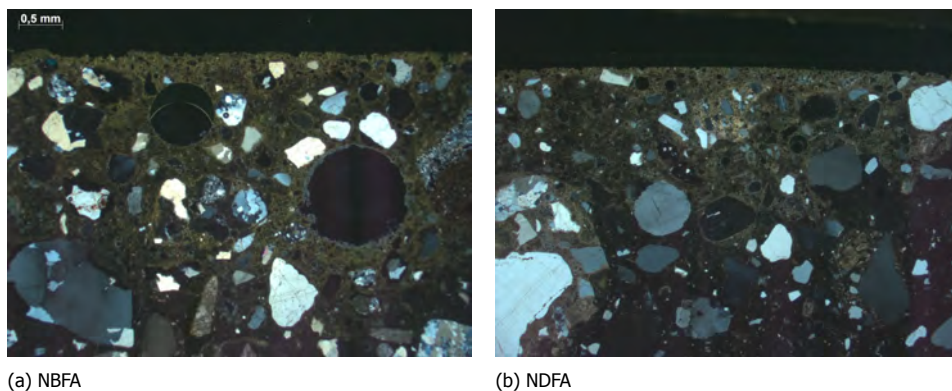
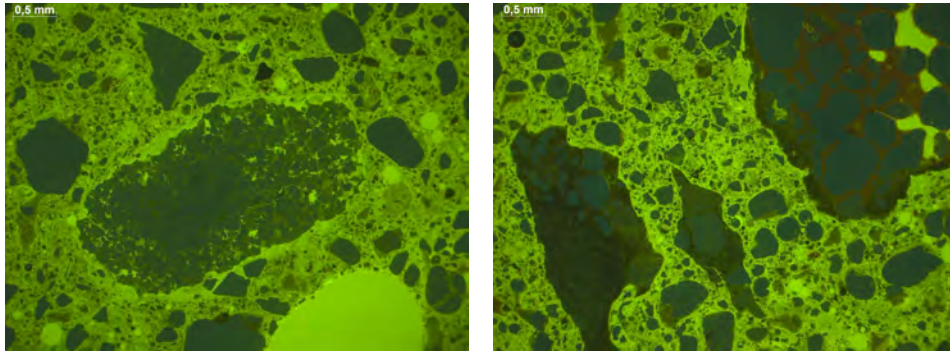


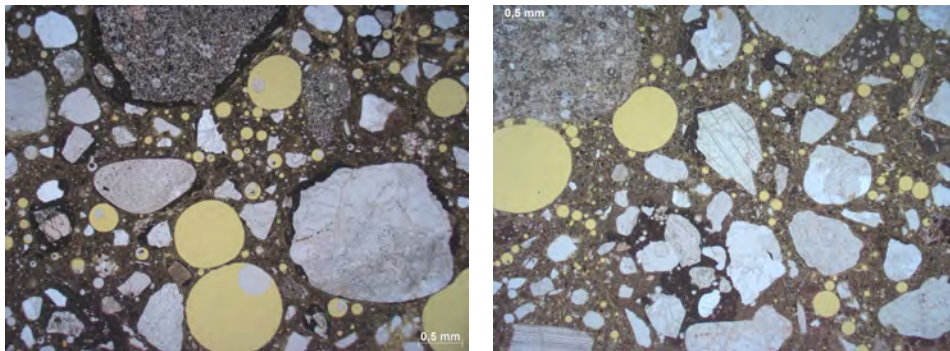
Figure 4.16: Carbonated paste in mortar mixtures (a) NBFA and (b) NDFA



(a) NDFA

(b) NFFA

Figure 4.17: Old adhered paste on fRCA and presence of ITZs in mortar mixtures (a) NDFA and (b) NFFA



(a) NB

(b) NC

Figure 4.18: Presence of entrapped air in mortar mixtures (a) NB and (b) NC

4.3. Concrete level

Having concluded with mortar mixtures of Series 1, we now turn to upscaling mortar mixtures of Series 0 to concrete level. Mortars from **Series 1** were considered to be very demanding in terms of cement increase and water absorption of fRCA and thus, not practical for industrial purposes. Therefore, they were not upscaled to concrete level. In the next section, the principal findings of concrete mixtures investigation will be presented. Fresh and mechanical properties, as well as shrinkage and effect of fRCA, batch effect and addition of CRCA on these properties will be demonstrated in the following paragraphs.

4

4.3.1. Slump

As previously stated, the target consistency class was F4. According to findings from M. Nedeljkovic et al. [58], 0.2% SP dosage was necessary for reference mortar A100, whereas mortars with 25% fRCA required 0.3% SP dosage for the target flow of 140-150 mm. This dosage was examined for concrete A100, as well as for mixtures with 25% fRCA of both deliveries and proved to be successful for slump values higher than 150 mm. However, simultaneous incorporation of fRCA and CRCA required adjustment of SP. A balance between air content and desirable slump levels was attempted to be achieved. This investigation resulted in 0.4% SP dosage for A70. The remaining mixtures NB25/30, NC25/30 and ND25/30 were produced with 0.5% SP dosage by cement weight.

The optimized concrete mix design with the modified mixing sequence, adjusted SP dosage and as received fRCA resulted in stable concrete mixtures. No excessive bleeding or segregation was identified by optical observation of the mixtures. ND25 is given as an example of a stable concrete mixture that retained its shape after removing the cone (Figure 4.19).



Figure 4.19: Stable concrete mixture after slump testing

Figure 4.20 presents the results of slump tests for fresh concrete mixtures. First of all, as it can be seen from the bar chart, the consistency class F4 was achieved for all concrete mixtures. A100 and A70 act as reference concrete mixtures and are presented on the left part of the graph. Slump around 155 mm was obtained for both of them. The lowest slump of 150 mm was measured for B25, whereas the peak value of 197.5 mm was reached for NC25.

Closer inspection to mixtures with 1st delivery of fRCA (B25,C25,D25) shows that C25 had the highest slump value. D25 had slightly lower slump compared to C25, whereas a considerably reduction was observed for B25. This trend is again illustrated by comparing mixtures with the 2nd delivery of fRCA (NB25,NC25,ND25). However, the lead is shared between NB25/30 and NC25/30 for mixtures with 25% fRCA and 30% CRCA.

The effect of batching on workability of concrete mixtures is also presented. Difference in slump between C25 and NC25, shown in Figure 4.20 illustrate the influence of 2nd fRCA delivery. NC25 was significantly more workable, approaching a 200 mm slump. Mixtures with fRCA B or D seemed to remain unaffected by this parameter.

Finally, no clear correlation is derived for the effect of simultaneous incorporation of fRCA and CRCA on workability. Similarities in slump are observed for A70 and ND25/30 compared to A100 and ND25, respectively. Contrasting results, though, are obtained for NB25/30 and NC25/30. In the first case, slump was substantially increased, whereas in the second case, the value dropped from 197.5 mm to 180 mm.

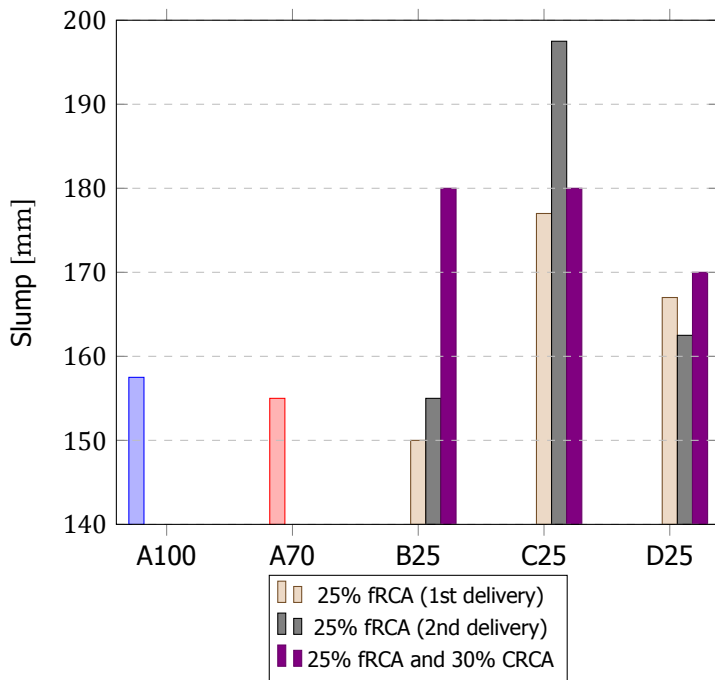


Figure 4.20: Slump of concrete mixtures

4.3.2. Air content

The air content experiment was performed as described in 3.4.2. After compacting the fresh mixture, a qualitative assessment of the mixtures was done. In Figure 4.21, the large difference of the surface between A100 and C25 can be seen. C25 had clusters of air bubbles and produced foam on the surface indicated that higher air content is expected. The foam could also come from unwashed sand. Unwashed sand means that impurities from different sources (contamination from environment, contamination from demolition works, contamination from soil, curing and hydrophobic agents) will be present on the FRCA particles as shown in Figure 4.22. Water with significant impurities present in it may have an effect (positive or negative) on air entrapment.



(a) (i)

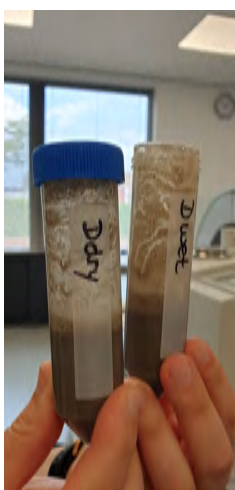


(b) (ii)

Figure 4.21: Surface of concrete mixtures (i) A100 and (ii) C25 after compaction



(a) (i)



(b) (ii)



(c) (iii)

Figure 4.22: (i) As received fRCA D in water and appearance of air bubble, (ii) Appearance of dirty water and foam when water is mixed with fRCA D, (iii) Visual observations of air bubbles on the top of the mortar container after compaction

The experimental results of air content are shown in Figure 4.23. From the chart, it can be seen that reference mixture A100 has the lowest air content. Regarding mixtures with RCA, there is a clear trend of increase in air content compared to A100.

Firstly, mixtures with 25% fRCA of 1st delivery demonstrated higher entrapped air. B25 had a slight rise, whereas for C25 and D25, air content was approximately three times higher than A100.

The effect of the 2nd delivery of fRCA on air content is also shown. A clear benefit of the 2nd delivery in the prevention of entrapped air is identified only for ND25 and D25. A considerable 50% fall of the air content of ND25 relative to D25 was measured. However, NB25 and NC25 showed a distinct rise in air content compared to B25 and C25 respectively.

An interesting outcome of this graph is derived by comparing mixtures with 25% fRCA and 30% CRCA. The effect of CRCA addition becomes apparent by comparing 2.3% air content of A70 to 1.4% air content of A100. An increasing trend is observed for all mixtures with both fRCA and CRCA. What stands out in this graph is the dramatic rise in air content by 62.5% of NC25/30 compared to NC25. NC25/30 reached a value of 7.8% entrapped air. Substantial increases are also observed for NB25/30 and ND25/30.

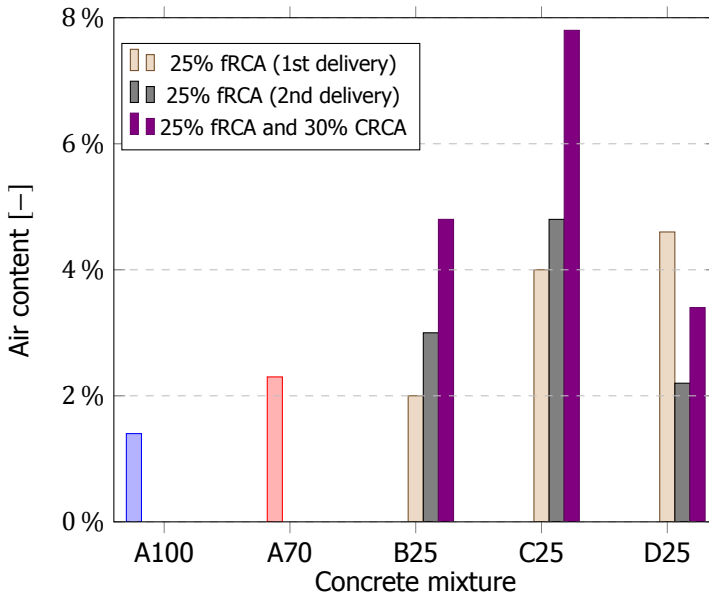


Figure 4.23: Air content in % of concrete mixtures

Figure 4.24 shows air content results for mixtures A100, B25, C25 and D25 for dried and as received fRCA. As previously mentioned for Figure 4.23, higher entrapped air was measured for all mixtures with fRCA in both moisture states. Use of dried fRCA resulted in 25% increase in air content for mixture B25, whereas a slight decrease is detected for mixture C25. The negative effect is highlighted for mixture D25. Use of dried fRCA in D25 led to 20% higher entrapped air compared to D25 with as received fRCA.

The effect of the tailor-made SP on the air content of concrete mixtures is also shown in Figure 4.24. For concrete mixtures with 25% fRCA and 30% CRCA, the SP dosage had to be adjusted so that a stable mixture with consistency class F4 would be developed and the air content would remain as low as possible. The graph illustrates the effect of SP on entrapped air of mixtures. The results are somewhat counterintuitive. For A70, increasing dosage from 0.2% to 0.4%, air content decreased from 3.2% to 2.3%. The positive effect is highlighted for ND25/30, which showed a drop from 6.5% to 3.4 % by increasing SP dosage from 0.4% to 0.5%. What is striking, though, is the opposite influence of SP dosage increase on air content of NC25/30, which rised by 20%.

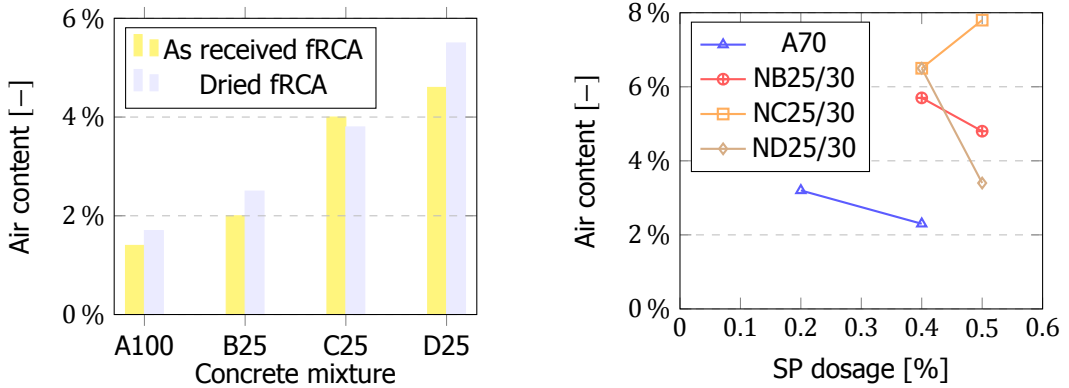


Figure 4.24: (i) Air content in concrete mixtures with as received and dry fRCA, (ii) Effect of SP on air content of concrete mixtures with 25 % fRCA and 30 % CRCA

4

4.3.3. Fresh and hardened density

Results of fresh and hardened density of all concrete mixtures are presented in Figure 4.25. The highest fresh density of $2,365 \text{ kg/m}^3$ is demonstrated for A100. A clear reduction is observed for mixtures with 25% fRCA from both deliveries. A direct comparison between mixtures with fRCA of the 1st and 2nd delivery reveals a positive effect of the 2nd fRCA batch on the fresh density of ND25. This concrete mixture reached a fresh density of $2,333 \text{ kg/m}^3$ approaching the value of A100. For NB25 and NC25 no significant differences are shown. Moreover, clear evidence for less dense mixtures with CRCA incorporation is shown in the graph. As we can see, presence of both fRCA and CRCA resulted in large reductions in fresh density and dropped the values approximately to $2,200 \text{ kg/m}^3$. Regardless of the fRCA source, very similar fresh densities were obtained for NB25/30, NC25/30 and ND25/30.

The pattern described for fresh density is also identified for the results of hardened density at 28 days in Figure 4.25. Similarly, the peak value is 2354 kg/m^3 for A100, whereas the lowest hardened density is approximately 2100 kg/m^3 for D25. What stands out in this data is the positive effect of the 2nd delivery of fRCA for ND25 compared to D25. Use of 2nd batch of fRCA D resulted in a significant growth in hardened density of the mixture from 2100 kg/m^3 to 2300 kg/m^3 . Lastly, mixtures with simultaneous replacement with fRCA and CRCA were poorer in terms of hardened density.

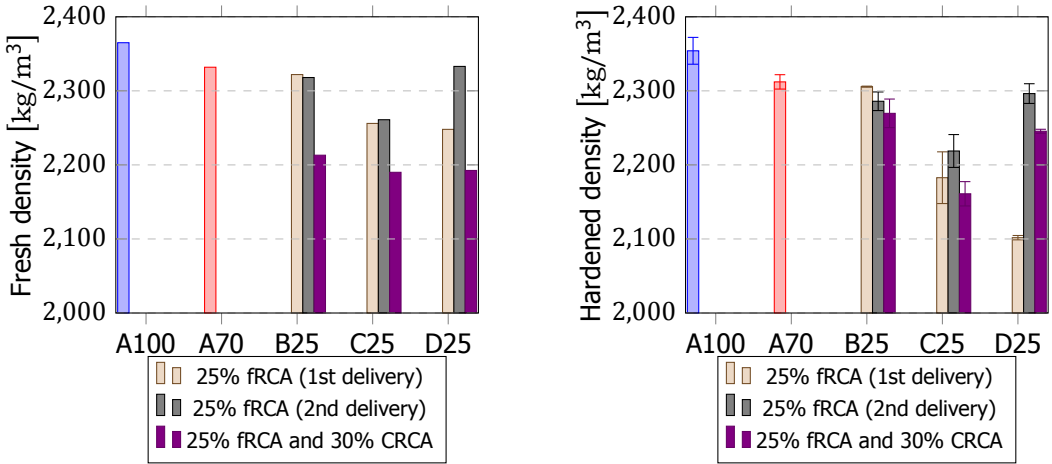


Figure 4.25: Fresh density and hardened density of concrete mixtures after 28 days of curing

4.3.4. Compressive strength

Figure 4.26 shows an overview of the results of compressive strength experiments at 7, 28 and 56 days. It is apparent from the graphs that all concrete mixtures with RCA had lower compressive strength compared to reference concrete mixture A100. The peak compressive strengths are reached for A100 and B25 with very slight differences at all ages. A breakdown of the results is shown in Figures 4.27, 4.28 and 4.29 for investigation purposes of the effects of fRCA and CRCA incorporation.

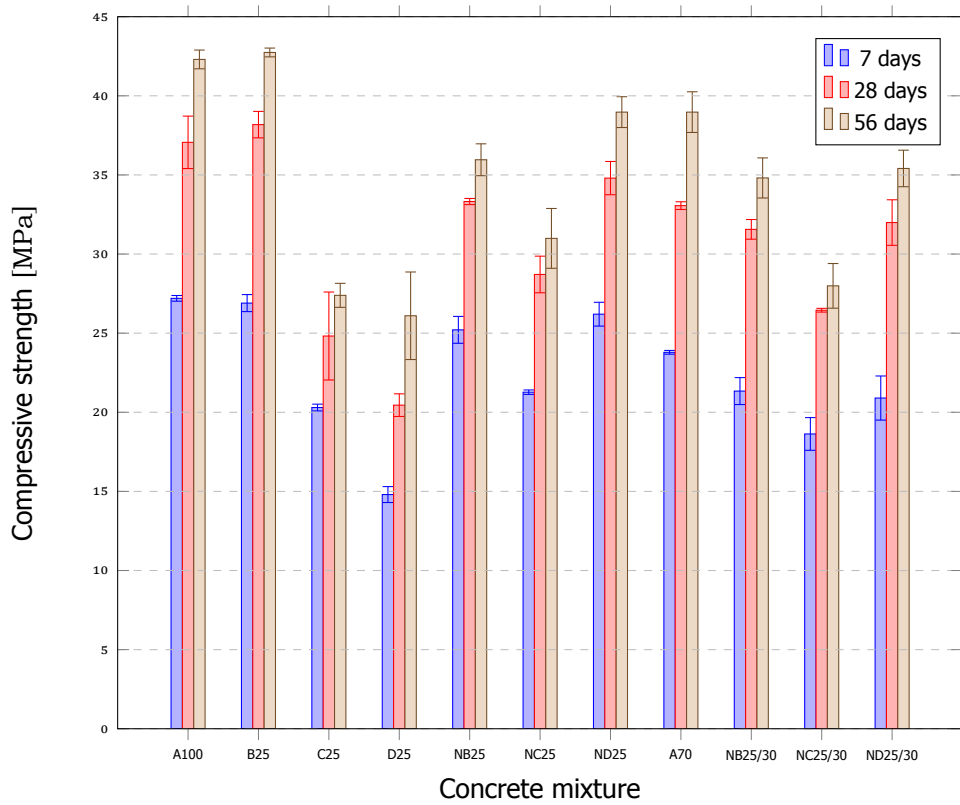


Figure 4.26: Compressive strength results

Figure 4.27 presents the compressive strengths at 7 days. Peak value is obtained for A100 reaching 27.2 MPa at 7 days. In general, RCA incorporation resulted in lower compressive strengths with loss percentages ranging from 1.1% to 45.5%. B25 performed equally with A100, whereas a sharp fall is observed for C25 and D25. The latter remained just below 15 MPa. If we now turn to mixtures with the 2nd delivery of fRCA, a clear positive effect is illustrated from the graphs. This trend is exemplified for mixtures D25 and ND25, where a 43.5% increase occurred. A closer inspection of mixtures with both fRCA and CRCA reveals the negative influence of CRCA addition on compressive strength. This is also demonstrated by A70, which was 12.5% weaker than A100. None of the mixtures with 25% fRCA and 30% CRCA achieved strength levels of A70 at 7 days. Additionally, in comparison to NB25, NC25 and ND25, significantly lower compressive strength with reduction rates up to 20% is observed for mixtures with both fRCA and CRCA.

Moving now to Figure 4.28, similar trends are observed. The most interesting aspect in this graph is that B25 surpassed A100 reaching 38 MPa and 37 MPa respectively at 28 days. In contrast to Figure 4.27, where NB25 had similar compressive strength to B25, a reduction of 13% in compressive strength was measured for NB25. Slight decline is also observed for mixtures NB25/30, NC25/30 and ND25/30 compared to NB25, NC25 and ND25 respectively.

In the same manner in Figure 4.29, compressive strength at 56 days follow the general pattern that was described for previous findings. Compressive strength of B25 was slightly higher than A100. On the other hand, D25 performed the worst of all mixtures, being just above 25 MPa. The same effects of 2nd delivery of fRCA, as well as addition of CRCA are identified.

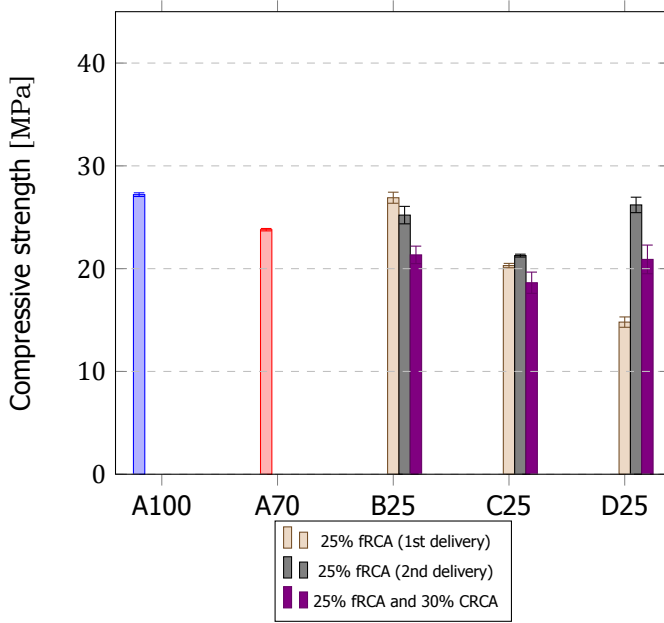


Figure 4.27: 7 days compressive strength

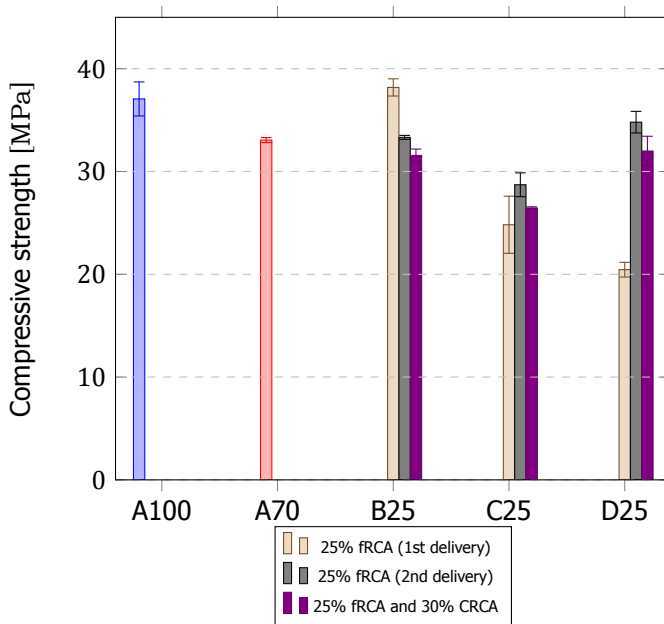


Figure 4.28: 28 days compressive strength

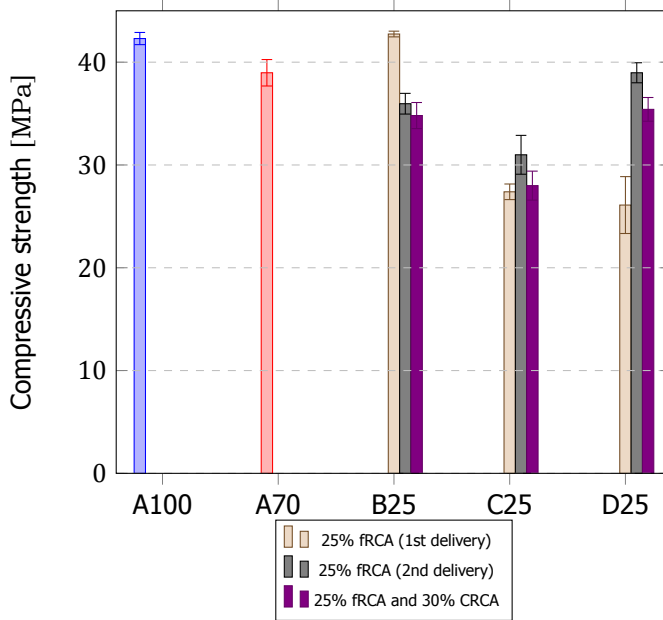


Figure 4.29: 56 days compressive strength

The strength development over time is presented in Figure 4.30. No significant differences are identified in the slopes of the graphs. The single most striking observation to emerge from the data comparison is the lower strength development of C25 between 7 and 28 days.

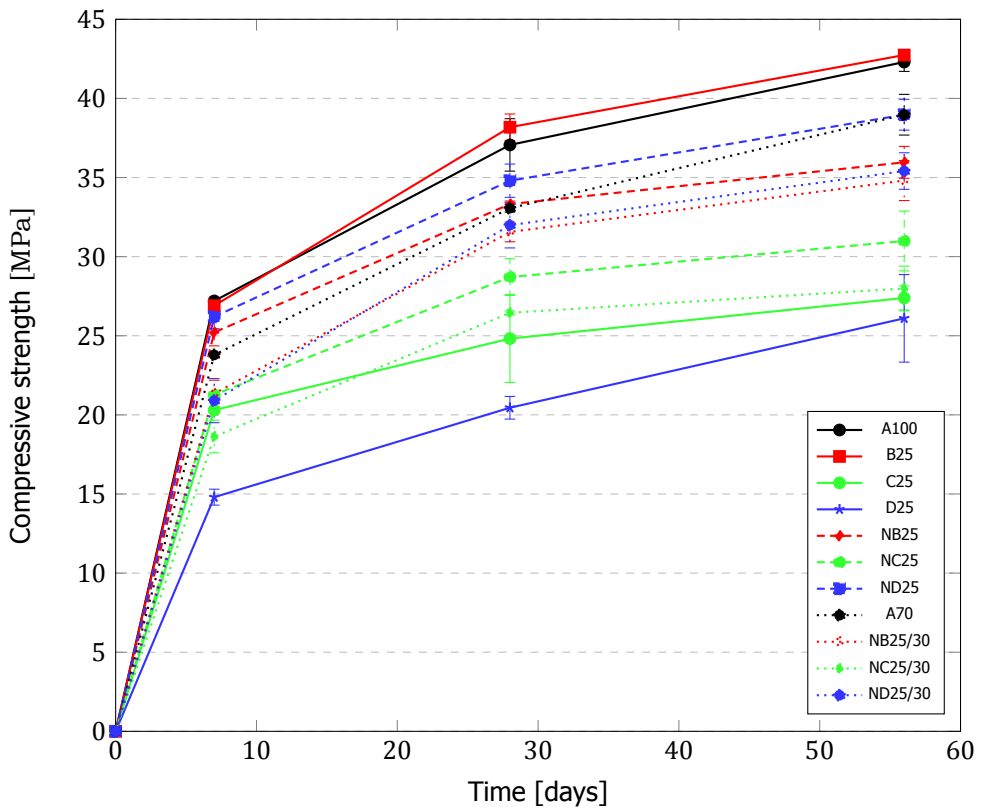


Figure 4.30: Compressive strength time development. Maximum strength is measured for B25 at 56 days, whereas minimum strength is obtained for D25. C25 and D25 show large standard deviations at 28 days.

4.3.5. Elastic modulus and Poisson's ratio ν

Figure 4.31 presents the elastic modulus test results. It is worth mentioning that only ND25 was tested under elastic modulus for mixtures using the 2nd delivery of fRCA. That is because it was identified that the effect of the 2nd fRCA batch proved to be significant only between D25 and ND25. First of all, reference concrete mixture performed the best with 37 GPa elastic modulus at 28 days. Likewise previous results, mixtures with RCA had lower performance compared to A100.

Comparing B25, C25 and D25 with A100, the general pattern of the previous outcomes is observed. One can clearly see that D25 had the lowest elastic modulus around 28 GPa. C25 showed slighter drop, whereas almost equal modulus were measured for B25 and A100, as expected.

If we now turn to ND25, the positive effect of the 2nd fRCA delivery is again identified. Elastic modulus increased from 28 GPa to 32.5 GPa. Despite no available data exist for NB25 and NC25, it is expected that slight differences would be measured.

As NB25 and NC25 results are not available, no direct comparison can be done for the effect of CRCA addition in these mixtures. However, the effect of simultaneous fRCA and CRCA incorporation becomes apparent by contrasting A70 to A100. Elastic modulus dropped by 23% reaching a value of 28.4 GPa compared to 37 GPa of mixture A100. No considerable difference is observed when CRCA was added to mixture with 25% fRCA D of 2nd delivery, as both values lay around 32 GPa.

In the same manner, Figure 4.32 shows Poisson's ratios ν of concrete mixtures at 28 days. What is interesting in this data and needs to be emphasized is that error bars of the results are quite large and values are not highly accurate. This is attributed to the alignment of LVDTs' during the elastic modulus experiments. However, some patterns are revealed by looking closer to mean values. Firstly, the peak value of 0.2 is reached for reference mixture A100. A substantial decrease, on the other hand, is observed for mixtures with 25% fRCA. The minimum values is 0.13 for C25.

The batching effect is also illustrated only for concrete mixtures with fRCA D. As it has been seen, D25 and ND25 are characteristic examples of the influence of the two deliveries of fRCA. ND25 showed a 20% increase reaching a value of 0.18 compared to 0.15 of D25.

As NB25 and NC25 results are not available, no direct comparison can be done for the effect of CRCA addition in these mixtures. Nevertheless, the differences in mixtures with fRCA and mixtures with both fRCA and CRCA are illustrated for A70 and ND25/30. What can be clearly seen from the graph is that there is again a substantial drop in Poisson's ratios for both mixtures.

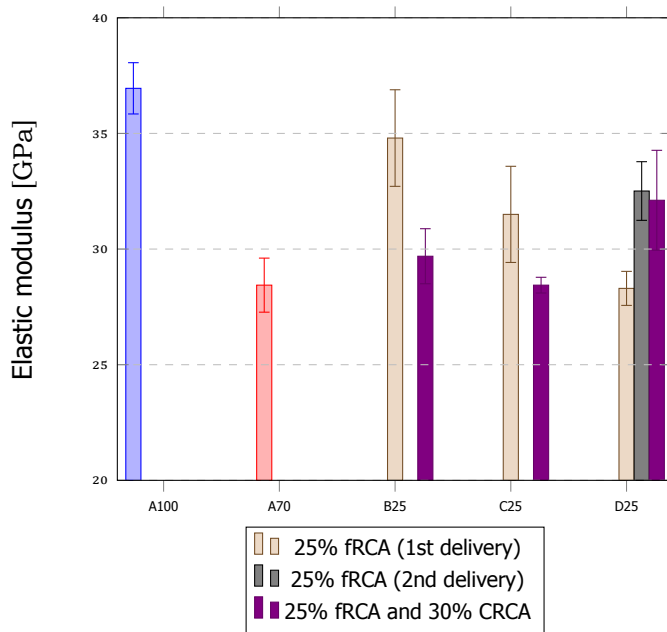


Figure 4.31: Elastic modulus E_{cm} of concrete mixtures at 28 days

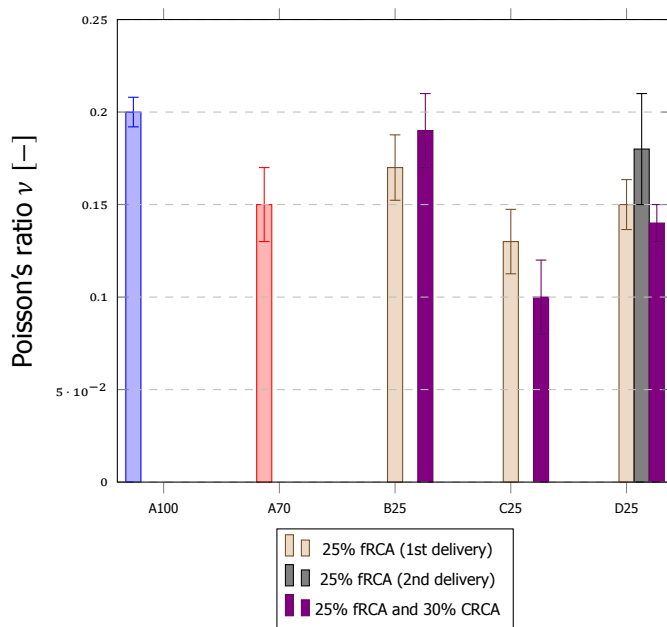


Figure 4.32: Poisson's ratio ν of concrete mixtures at 28 days

4.3.6. Shrinkage and mass loss

Figures 4.33, 4.34, 4.35 present shrinkage of mixtures with fRCA B, C and D respectively. The reference concrete mixtures A100 and A70 are also displayed. As it can be seen, the deformation increases over time in a non-linear manner. This increase occurs mainly in the early ages, tending to stabilize afterwards. Closer inspection of B25, C25, D25, as well as NB25, NC25 and ND25 shrinkage curves reveals that no substantial difference exist in shrinkage measurements. NC25 showed similar shrinkage compared to reference mixture A100. On the contrary, shrinkage of B25, C25 and D25 was significantly lower compared to A100 after the first 3-4 days.

Regarding the influence of the second delivery of fRCA, shrinkage seems to be slightly increased. In Figure 4.33, NB25 reached a value of approximately 420 $\mu\text{m}/\text{m}$ compared to B25, which just stayed below 300 $\mu\text{m}/\text{m}$. Similarly in Figure 4.34, NC25 showed a 50% rise relative to C25 at 95 days shrinkage. On the other hand, in Figure 4.35, no significant reduction between D25 and ND25.

The shrinkage results obtained for mixtures with 25% fRCA and 30% CRCA are also presented in Figures 4.33, 4.34 and 4.35. Firstly, the effect of CRCA addition is illustrated by comparing A100 to A70. The latter approached a value of 430 $\mu\text{m}/\text{m}$ at 95 days, whereas the former remained as low as approximately 400 $\mu\text{m}/\text{m}$, proving that no considerable difference exists. Moreover, it can be seen that mixtures with simultaneous fRCA and CRCA incorporation acquired the highest values among all concrete mixtures. The peak value was 440 $\mu\text{m}/\text{m}$ for mixture NC25/30. What is also interesting in these Figures is the correlation between A70 and mixtures NB25/30, NC25/30 and ND25/30. During the first approximately 20 days, curves were almost identical for NB25/30 and NC25/30 compared to A70. However, A70 remained on lower levels after this age point. No significant difference between the two groups was evident at 95 days and reduction no greater than 8% was observed.

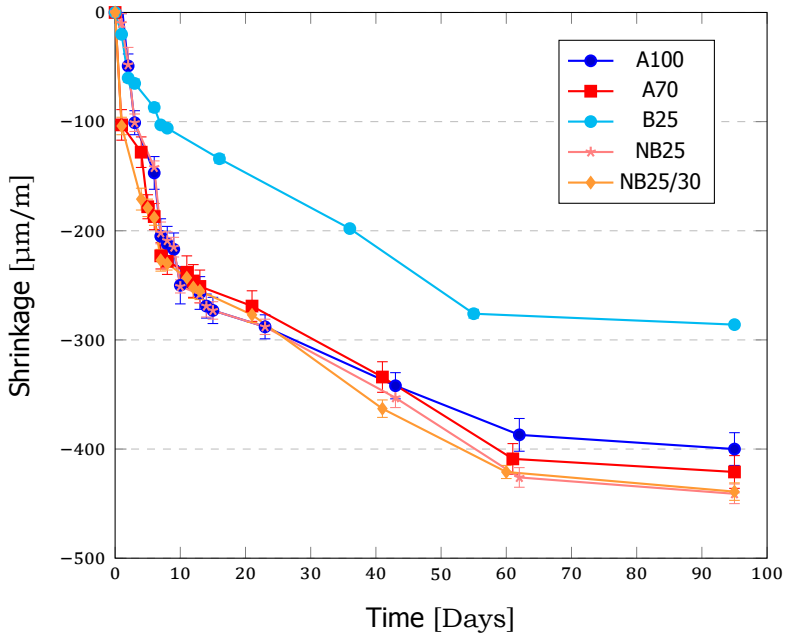


Figure 4.33: Shrinkage for concrete mixtures with fRCA B and CRCA. Comparison with A100 and A70.

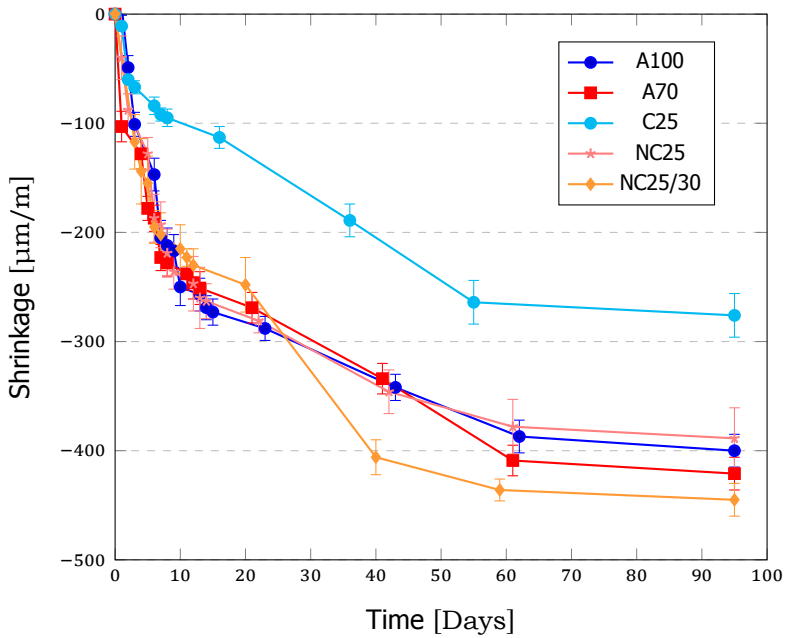


Figure 4.34: Shrinkage for concrete mixtures with fRCA C and CRCA. Comparison with A100 and A70.

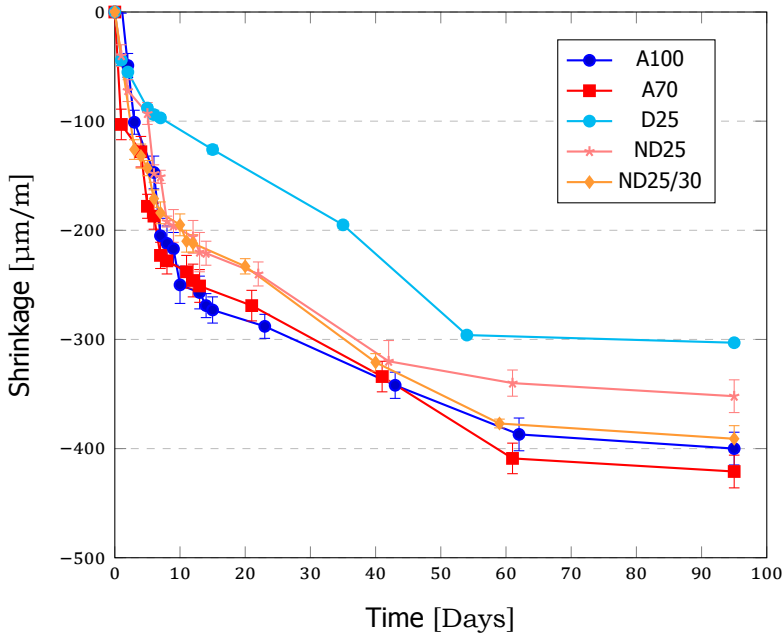


Figure 4.35: Shrinkage for concrete mixtures with fRCA D and CRCA. Comparison with A100 and A70.

Figures 4.36, 4.37 and 4.38 provide the results obtained for mass losses of the studied concrete mixtures. Unlike shrinkage results in Figures 4.33, 4.34 and 4.35, substantial increases in mass loss are observed for concrete mixtures with RCA. This discrepancy is highlighted by mixtures B25, C25 and D25, which showed considerably lower shrinkage measurements, but a significant increase in mass loss. Taking a closer look to mixtures with 25% fRCA for both deliveries, mass loss was found to be 3 times higher compared to reference concrete mixture A100. Regardless of the type of fRCA, all mixtures presented mass losses around 3%. The only exception to this outcome was NB25, which showed similar values to A100.

In contrast to previous findings about the effect of 2nd delivery of fRCA on shrinkage, no strong evidence of influence exists for mass loss for mixtures with fRCA NB, NC and ND. The most interesting aspect in Figure 4.36 is mixture NB25, which performed significantly better than B25. The mass loss for NB25 remained at the same levels as A100 and the two curves were almost identical.

The effect of simultaneous fRCA and CRCA incorporation on mass loss is presented in Figures 4.36, 4.37 and 4.38. To begin with, this is illustrated by comparing A100 and A70, which performed significantly worse and reached a double loss percentage of 2.6% at 95 days. A70 becomes now a relative reference concrete mixtures for NB25/30, NC25/30 and ND25/30. The results in mass loss are not in agreement with the shrinkage recordings of the aforementioned mixtures. Presence

of fRCA and CRCA had minor effect, since A70, NB25/30 and NC25/30 followed very similar curves at all ages. The single most striking observation to emerge from the data comparison is that a large reduction was identified for ND25/30 compared to A70.

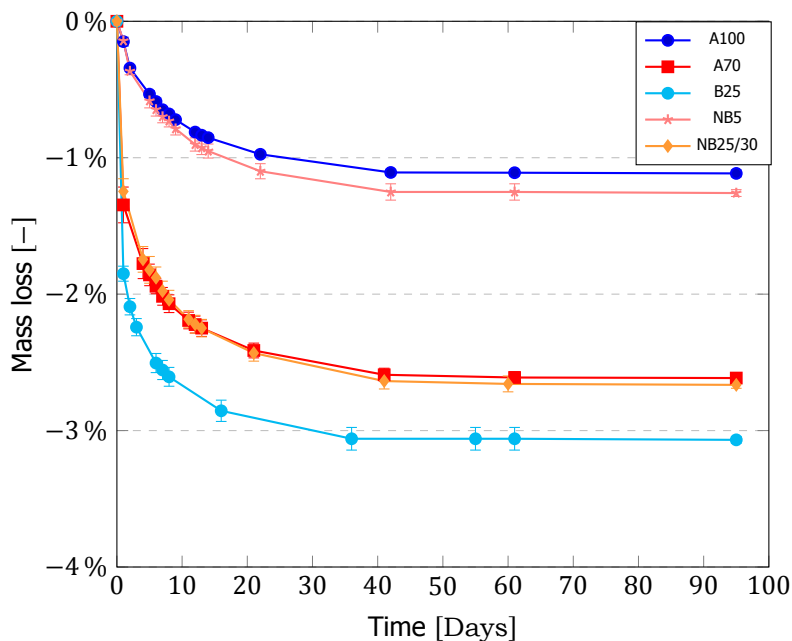


Figure 4.36: Mass loss for concrete mixtures with fRCA B and CRCA. Comparison with A100 and A70.

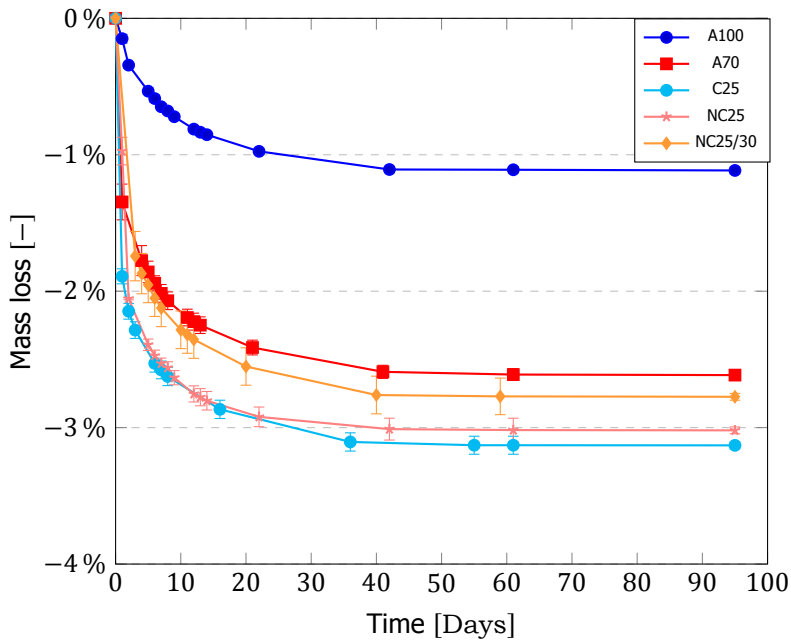


Figure 4.37: Mass loss for concrete mixtures with fRCA C and CRCA. Comparison with A100 and A70.

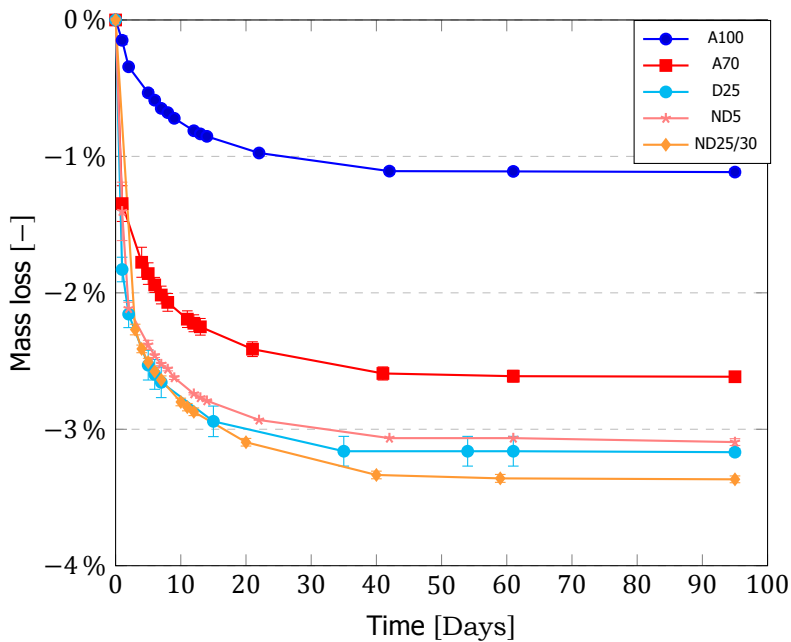


Figure 4.38: Mass loss for concrete mixtures with fRCA D and CRCA. Comparison with A100 and A70.

5

Discussion

"Nothing endures but change."

Heraclitus
Greek philosopher
535 BC – 475 BC

The previous chapter has presented detailed results of the experimental program. It is now necessary to collect these findings and provide explanations. Highlights of the results of fresh and mechanical properties of concrete mixtures will be analyzed and correlations between fRCA properties and their performance will be drawn.

5.1. Slump

Regarding SP admixtures, tailor-made design of SP used in this study made it possible to keep the SP dosage in very low levels. The use of SP at dosages ranging from 0.3%-0.5% by cement content largely helped to achieve consistent mixtures with RCA and adequate workability. Nevertheless, increased dosage of SP was necessary for mixtures with RCA compared to A100. That is attributed to high water absorption mainly of fRCA, angular particle shape and rough surface texture of RCA. Angular and irregular shapes increase friction between aggregates and cement paste and consequently, prevents flow of the mixture.

Slump results presented in Figure 4.20 clearly demonstrated that mixtures with 25% fRCA C and D with both deliveries reached higher slump values than mixtures

with 25% fRCA B. These results are likely to be related to a number of parameters.

1. **Content of fraction 0-0.25 mm.** fRCA C and D, shown in Figure 4.6, have considerably higher amount of 0-0.25 mm fraction compared to fRCA B. Moderate amount of fines has been found to have positive effect on workability of concrete [30].
2. **Water absorption of fRCA.** Inaccuracies and water absorption kinetics of fRCA cannot be ruled out as an explanation to this observation. As previously explained, the amount of water in mixtures was adjusted so that the effective w/c ratio would remain 0.5. In case water absorption values were overestimated, excess amount of water will contribute to fluidization of the mixtures. Errors during the procedure of water absorption experiments, described in 3.1.1, might occur, mostly regarding the SSD state of fRCA. These possible sources of error could have affected the workability of mixtures. Moreover, fraction 0-0.25 mm was not removed from the sample, possibly leading to slightly higher absorption values. Water absorption kinetics can also differ among fRCA B, C and D. During the short time period of mixing, internal pores of fRCA might not be completely filled with water and therefore, the effective w/c ratio is slightly higher. This possible explanation might be also supported by Table 4.2, where discrepancies are measured for w/c ratios experimentally and according to designs. It seems that total water absorption capacity was more unlikely to have been achieved. Optical microscopy observations revealed discrepancies compared to w/c ratios calculated according to mix designs and fRCA water absorption capacities.

5.2. Air content

According to previous results, mortars and concrete mixtures with RCA resulted in elevated air content. The investigated concrete mixtures reveal the effect of 25% fRCA, batching effect and simultaneous 25% fRCA and 30% CRCA incorporation on air content. Very interesting results were obtained for B25, NB25 and ND25, which were kept below 3% air content. These values would be generally accepted for concrete mixtures in practice, as the limit of 3% is not surpassed. High air content results in this study corroborate the findings of a great deal of the previous work in air content of mixtures with RCA. The following observations and possible explanations are drawn according to air content results:

- 1. RCA consists of aggregate particles that might introduce additional porosity.** This porosity is due to the presence of old adhered paste on the surface of fRCA, which varies in quality and density. As illustrated in 4.1, porous clusters of pure aggregates and cement paste present a large number of voids. These empty spaces can potentially entrap air and give rise to air content of the mixture. Higher air content for mixtures with simultaneous incorporation of 25% fRCA and 30% CRCA seems possible that is due to introduction of additional porosity on adhered mortar or cement paste on CRCA surfaces. However, no direct correlation is drawn between the amount of adhered paste on fRCA and air content results. According to 4.1, fRCA D has lower paste content compared to fRCA B, whereas D25 showed considerably higher air content than B25. This is possible attributed to the quality of attached paste (e.g. presence of badly compacted concrete, poor quality, higher w/c ratio) rather than the quantity.
- 2. Intense agglomeration due to storage.** This phenomenon is clearly observed in Figures 3.2 and 3.3 for fRCA C, NC and D, which were not delivered fresh after production. Weather conditions, such as high humidity or carbonation resulted in the formation of big chunks. These agglomerated particles offer extra porous areas than can entrap air, as shown in Figure 5.1. This effect is highly illustrated by ND25 in Figure 4.23, which showed significantly lower air content compared to D25. The 2nd delivery of fRCA D was not stored and agglomeration was not present. Since the source of fRCA and other properties were similar, this large discrepancy is attributed to the existence of agglomerates.
- 3. Presence of impurities in fRCA might reduce effectiveness of SP.** SP used in this study was specially designed with defoaming agents that have a positive effect on air content of mixtures with fRCA. The modified mixing sequence implemented for mortars of Series 0 and consequently, for all concrete mixtures counteracted the affinity of SP to entrain air when the standard mixing order was used. However, mixture NC25/30 in Figure 4.24 illustrates that the opposite effect is observed when SP dosage is increased. Despite

the beneficial effect of SP on air content in mixtures NB25/30 and ND25/30, fRCA C seems more likely to contain various impurities that act as obstacles to the defoaming agents of the tailor-made SP (Figure 5.1). Taking, also, into account that fRCA is not washed at the recycling companies, contamination from environment, demolition works, soil, curing and hydrophobic agents are not removed. It is reported that the foaming property of surfactants from SP can be affected by the impurities present in the host solution [58]. This phenomenon, though, cannot be extrapolated to all mixtures.

4. **Replacement of OPC binder by FA resulted in significant decrease in air content in mortars of Series 1.** As shown in Figure 4.9, a decreasing trend was revealed with 30% use of FA. This finding is consistent with that of Ju et al. (2020), who reported the positive effect of 15% FA use on air content of mortars with fRCA [34]. These relationships may partly be explained by the higher fineness and ball bearing effect of fly ash. Fly ash spherical particles may create a denser structure and increased packing, filling up the empty spaces that can entrap air.

5

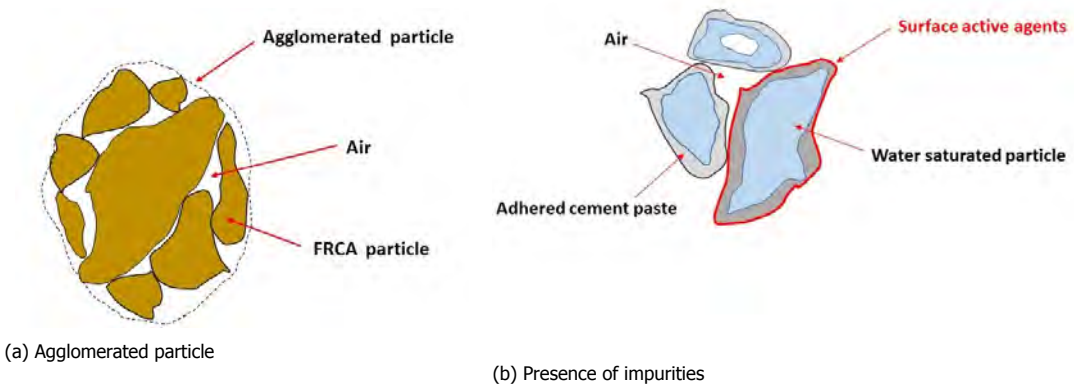


Figure 5.1: (i) Storage of material causes particle agglomeration and entrapment of air in empty spaces, (ii) Presence of impurities on the surface of fRCA particles

5.3. Compressive strength

Lower performance is illustrated for the majority of concrete mixtures compared to A100, as shown in Figures 4.26 and 4.31. The concrete mix design was successful for A100, as the strength class C30/37 was achieved at 28 days. Surprisingly, B25 performed slightly better than A100, reaching approximately 38 MPa at 28 days. The remaining mixtures stayed below 33 MPa at 28 days.

Air content is an important determinant of the mechanical performance of concrete mixtures. This behavior is observed in Table 5.1. The effect is highlighted

by D25, ND25 and ND25/30. ND25 showed considerable reduction in air content compared to D25 from 4.6% to 2.2% and remarkable rise in compressive strength by approximately 40%. This close correlation is presented in Figure 5.2. Results are not consistent, however, for C25 and NC25. The effect is possible negligible for these mixtures, since no great difference was observed in air content and compressive strengths, shown in Figure 5.2, are average values. It can thus be suggested that entrapment of air is responsible for lower mechanical performance of mixtures with RCA, since it introduces weak areas in the concrete matrix, reduces the effectiveness of force distributing mechanisms and cracks can propagate facing less resistance.

Concrete mixture	Air content [%]	Compressive strength at 28 days [MPa]
A100	1.4	37.06
B25	2	38.18
C25	4	24.82
D25	4.6	20.45
NB25	3	33.32
NC25	4.8	28.71
ND25	2.2	34.8
A70	2.3	33.06
NB25/30	4.8	31.56
NC25/30	7.8	26.45
ND25/30	3.4	31.99

Table 5.1: Correlation between air content and compressive strength of concrete mixtures

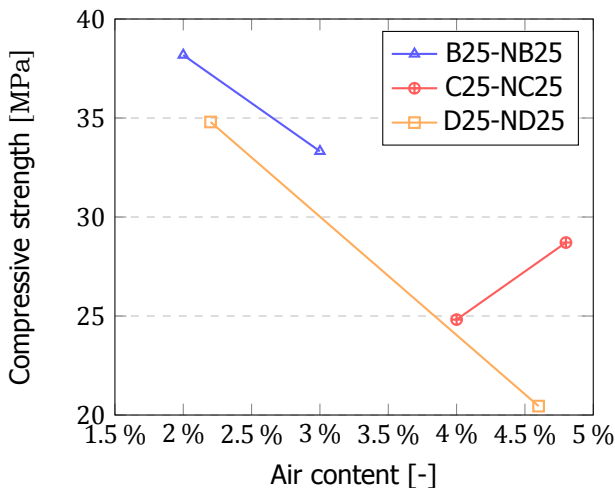


Figure 5.2: Air content effect on compressive strength of concrete mixtures with 1st and 2nd delivery of FRCA

Another possible explanation is the lower stiffness of RCA and porosity of adhered paste on fRCA. As explained previously in 5.2, the quality of parent concrete has major influence on the level of porosity and presence of additional ITZs in concrete matrix. Poor quality of parent concrete, on the one hand, results in porous clusters of fRCA aggregates with high porosity. On the contrary, good quality parent concrete is closely linked to denser microstructure of fRCA aggregates and therefore, lower porosity. Proportion of these particles will strongly affect the compressive strength. Microphotographs with UV light in Figure 5.3 illustrates the presence of porous aggregates in mortar NC and dense fRCA particles in mortar ND. Bright color on the periphery of the fRCA particle in mortar NC reveals the presence of porous ITZ, as well as higher porosity on the attached paste. On the other hand, stiffer aggregates exist in mortar ND demonstrating better quality of parent concrete. This may also be another possible explanation for the difference in performance of NC25 and ND25.

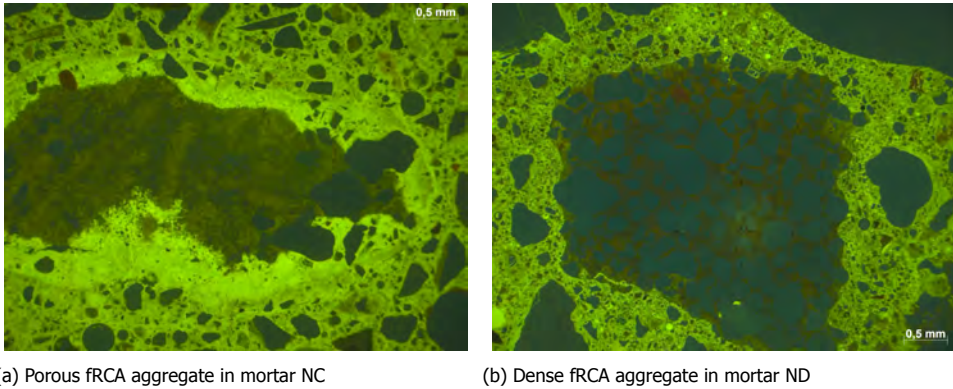


Figure 5.3: Microphotographs under UV light for (i) fRCA aggregate in mortar NC and (ii) fRCA aggregate in mortar ND

MIP experiments were conducted on the mortars derived from concrete mixtures A100, B25, C25 and D25 to determine the effect of the presence of additional porosity introduced by the attached cement paste on fRCA surface. The results are presented in Figures 5.4 and 5.5. In Figure 5.4, the pore size distribution is displayed. Slight increase is observed in the capillary voids for mortar mixtures B25, C25, D25 compared to A100. Higher content of especially small capillary voids from $0.01 \mu\text{m}$ to $0.05 \mu\text{m}$ are observed in mortar mixtures with fRCA. For medium and large capillary pore sizes, only C25 and D25 showed slightly higher values. No significant differences are observed for larger pore size diameters. In Figure 5.5, the total capillary pore volume is presented. Regardless of the mortar mixture with 25% fRCA, slightly higher porosity was measured. Additional 3% is observed for these mixtures compared to A100, which may be possibly attributed to the introduction of porosity in the attached cement paste on the surface of fRCA. The connection between this phenomenon and lower mechanical performance is observed, however, only for C25 and D25, as it was shown in Figure 4.26. This

might lead to the assumption that this additional porosity on the adhered paste on fRCA is not a governing factor for the performance of concrete mixtures with fRCA.

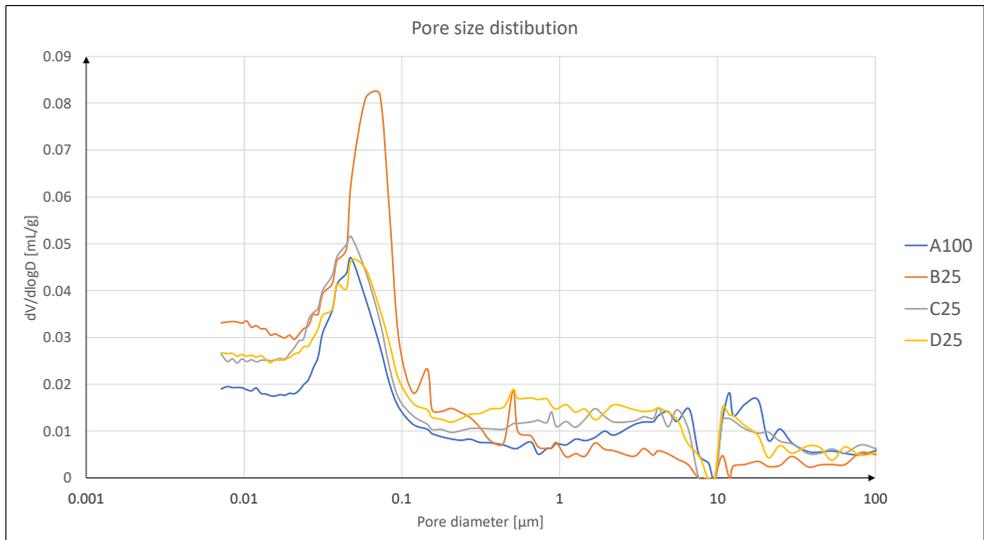


Figure 5.4: Pore size distribution of mortars derived from concrete mixtures A100, B25, C25, D25

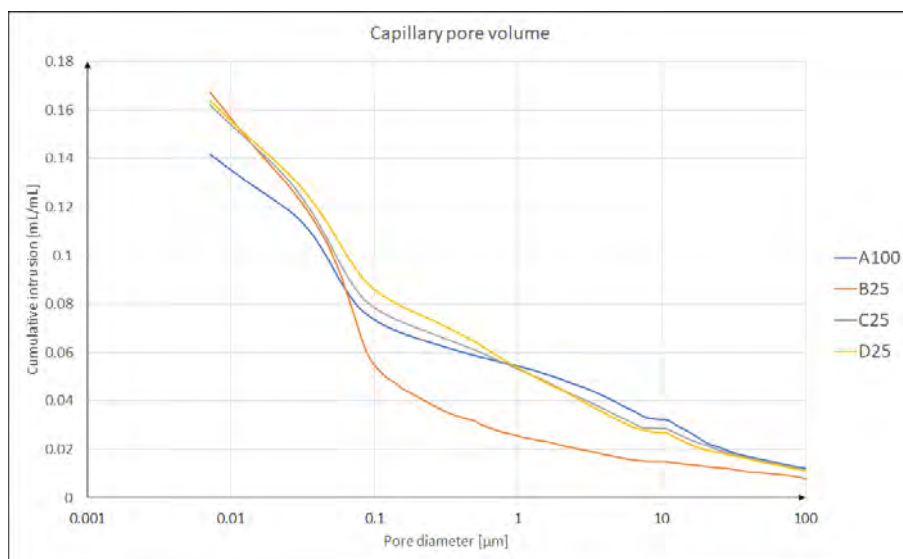


Figure 5.5: Total capillary pore volume of mortars derived from concrete mixtures A100, B25, C25, D25

5.4. Shrinkage

Unanticipated findings were obtained for shrinkage of mixtures with 25% fRCA according to Figures 4.33, 4.34 and 4.35. High water absorption requires larger amount of water, so that the desirable consistency class is achieved. Despite of the fact that the effective w/c ratio was fixed to 0.5 for all mixtures, additional water might not be absorbed by fRCA particles and thus, be present as free water. It was expected that this amount of water would evaporate after a long time period and considerably larger shrinkage would be measured for mixtures with 25% fRCA. What is striking, though, about these mixtures is that shrinkage deformation is not in agreement with mass loss recordings, as shown in Figures 4.36, 4.37 and 4.38. Mass loss was considerably higher for the majority of mixtures with 25% fRCA compared to A100, which indicates that large amounts of free water evaporated.

It is difficult to explain this result, but it might be related to the internal curing phenomenon of fRCA particles. These results reflect those of Pedro et al., who also found that evaporation of free water is compensated by water captured by RCA [21]. However, this phenomenon was observed only during early ages and the authors supported that the contribution of autogenous shrinkage in total drying shrinkage was eliminated. These results also corroborate the ideas of Medjigbodo et al. [46]. According to their study, RCA particles may function as internal water reservoirs, providing water for the continuation of hydration. This is attributed to interconnectivity of pores in fRCA and their water absorption capacity, that allows them to store and transfer water to adjacent cement paste. In this way, self-desiccation is mitigated. It is possible that larger amount of hydration products is

formed and as a result, voids are reduced and a denser microstructure is created [46].

Nevertheless, slightly higher shrinkage deformation is observed for mixtures with 25% fRCA and 30% CRCA. A very interesting outcome is derived by closer inspection between A70 and NB25/30, NC25/30, ND25/30. Presence of 25% fRCA, regardless of source, seems to have negligible effect on shrinkage deformation. That is possible explained by the fact that CRCA has a governing role on shrinkage due to higher replacement ratio and their lower stiffness. This explanation is supported by elastic modulus results in Figure 4.31. Weaker aggregates resulted in reduced overall stiffness of these mixes and lower resistance to deformation and consequently, lower elastic modulus values. These results reflect those of Manzi et al. (2013) and Menjibodo et al. (2018) [54], [46], who found the same effect of CRCA on shrinkage. It also needs to be mentioned that a potential error might exist in the moisture content measurements of CRCA. That is because samples for moisture content were selected only from one bucket of material. However, during production of concrete, it was apparent that CRCA stored in different buckets were fully saturated. Excess amount of water was removed before mixing the material, but it might be that the effective w/c ratio is slightly higher than 0.5.

Finally, the lower precision of the shrinkage measurements relative to mass loss measurements shall be taken into account. Measuring errors might have occurred especially for concrete mixtures B25, C25 and D25, where the path deviates after 3-4 days after casting, as shown in Figures 4.33, 4.34 and 4.35. Inaccuracies in the manual measurements of shrinkage deformation might be a possible explanation to the discrepancies between shrinkage results and mass loss. Weighing the samples on the mass scale provides significantly higher accuracy and the plateau, as expected, was reached after approximately 40 days.

6

Conclusions and future recommendations

"The oldest, shortest words— "yes" and "no"— are those which require the most thought."

Heraclitus
Greek philosopher, mathematician
580 BC – 496 BC

In the next chapter, the main conclusions of this study are summarized based on the experimental findings and observations presented in chapters 4 and 5. Subsequently, aim of the research is assessed and research question are answered. Finally, recommendations for future studies are given.

The purpose of the current study was the development of concrete mix designs with the optimal amount of fRCA and CRCA that maintain structural integrity in terms of fresh and mechanical properties. The optimal amount of fRCA was determined upon the basis that cement content should be equal or not substantially increased compared to conventional concrete mix designs. Replacement of river sand by 25% fRCA was selected and afterwards, additional concrete mixtures were designed with the maximum, allowed by regulations, CRCA percentage (30%). With respect to mortars of Series 1, optimization of the designs was attempted treating them individually, according to water demand of solid constituents and packing of aggregates.

This study has found that quality of fRCA is a major driving factor for concrete

mixtures incorporating fRCA. Agglomeration of fRCA, presence of impurities and high content of 0-0.25 mm fraction emerged as potential reliable predictors of the mechanical performance of concrete mixtures. The following conclusion are drawn according to principal research findings:

1. fRCA incorporation ratio by 25% does not require cement content increase.

On the contrary, it was highlighted that full replacement of river sand by fRCA in Series 1 mortars inevitably demanded considerably high cement content.

2. Incorporation of RCA results in higher air content of fresh concrete mixtures.

This observation may be explained by higher content of 0-0.25 mm fraction, additional porosity of old adhered cement paste and agglomerated particles.

3. Storage of fRCA has a detrimental effect on air content and consequently, on the performance of concrete mixtures.

Outdoor weather conditions create agglomerated fRCA particles that allow entrapment of air in empty spaces.

4. Content of 0-0.25 mm fraction may help workability of mixtures, but has a negative influence on mechanical properties.

fRCA C and D were produced with higher crushing steps than fRCA B. Reduced content of fines can contribute to increase compressive strength and elastic modulus.

5. Addition of 30% CRCA increased air content of concrete mixtures.

That may be again attributed to extra porosity present in the attached mortar/cement paste on surface of CRCA. As a result, mixtures with 25% fRCA and 30% CRCA demonstrated lower compressive strengths.

6. Tailor-made SP containing defoaming agents is used in relatively low dosages for the desirable consistency class F4.

The specially designed polycarboxylate SP used in this study had not only been beneficial for workability of mixtures, but also air content reduction.

7. fRCA can be used as received, but there is high probability of presence of impurities.

Impurities on the surface of fRCA might interfere with SP and reduce effectiveness of defoaming agents. In order to avoid this effect, the modified mixing sequence should be used.

8. Unanticipated results were obtained for shrinkage deformation of mixtures with 25% fRCA

It was expected that higher water absorption capacities of fRCA would lead to evaporation of larger amounts of free water and thus, higher shrinkage deformation. This was also supported by mass loss recordings. However, this was only observed for mixtures with 25% fRCA and 30% CRCA. As explained, it is possible that fRCA function as internal water reservoirs that compensate water loss and thus, being beneficial for continuation of the formation of hydration products.

The main research question as formulated at the start can be answered, taking into account above conclusions.

- *What is the max fRCA replacement percentage that does not require cement increase and can reach the target strength class of compressive strength?*

Replacement of river sand by 25% fRCA does not require cement increase and reached the target strength class under certain circumstances.

- *Which modifications are necessary when incorporating fRCA and upscaling mortars to concrete?*

Using as received fRCA requires that a modified mixing sequence should be used. This means that fRCA should be added at the end of mixing after all other constituents are mixed together with SP. Upscaling mortars to concrete resulted in no significant modifications except for adjustment of SP dosage.

- *What is the effect of using both fRCA and CRCA in structural concrete?*

Addition of 30% CRCA in concrete mixtures with 25% fRCA had negative impact on all properties. Air content was increased and compressive strengths showed considerable reduction.

- *What are the fRCA quality indicators for good performance of structural concrete?*

In this study, since source of fRCA is unknown, nothing can be said about the quality of parent concrete, which would be a major driving factor of qualitative assessment of fRCA. Nevertheless, reduced content of 0-0.25 mm fraction and absence of agglomerated particles implies that better interaction with SP is achieved and higher mechanical performance is reached.

Future recommendations for treatment of fRCA in order to produce high quality concrete mixtures can be summarized in the following key aspects:

1. **Storage of material may be avoided.**

As it was emphasized, storage of fRCA after production causes agglomeration

of particles. A significant improvement in performance of concrete mixtures was observed, when fRCA was delivered fresh.

2. Crushing steps may be limited to a single step.

This is, undoubtedly, dependent on the available equipment of the recycling plant. However, multiple crushing steps resulted in higher content of 0-0.25 mm fraction, which strongly influences workability and mechanical properties.

3. Treatment of fRCA might help in producing high quality concrete.

Surface pretreatment of fRCA may increase surface homogeneity, improve ITZ microstructure, and reduce porosity. Other treatment methods, such as carbonation, removal of adhered paste, may be considered.

4. Modified mixing sequence may be applied, when as received fRCA are used.

Water and SP should be mixed with natural aggregates and cement in advance. Presence of impurities in as received fRCA may decrease effectiveness of SP.

The most important limitation in this study lies in the fact that durability aspects of concrete mixtures with RCA were not evaluated. It is expected that additional porosity of the attached mortar/paste of RCA will introduce new paths inside the concrete matrix and therefore, permeability will be considerably affected. Even if the principal fresh and mechanical properties of mixtures with RCA were found to be promising, issues related to carbonation, chloride ingress or freeze-thaw attack might occur. These aspects are recommended by the author for future research.

In spite of its limitations, the study certainly adds to our understanding of fRCA incorporation in concrete. Findings from this study make several contributions to the current literature and industry practices. Based on the comprehensive assessment of the effect of 25% fRCA, batching effect and addition of CRCA, industry can acquire valuable insight on the key aspects of fRCA and concrete production with RCA. This understanding should help to improve predictions of the impact of fRCA on concrete performance and encourage industry to adopt production of concrete with fRCA. In this way, further steps will be taken towards preservation of natural resources and reduction of landfilling in the context of a sustainable building economy.

7

Bibliography

References

- [1] Leonora Charlotte Malabi Eberhardt , Morten Birkved & Harpa Birgisdottir(2020): Building design and construction strategies for a circular economy, Architectural Engineering and Design Management
- [2] <https://www.europarl.europa.eu/news/en/headlines/economy/20151201STO05603/circular-economy-definition-importance-and-benefits>
- [3] <https://sites.google.com/site/section2team4/cradle-to-cradle-design>
- [4] P. Villoria Sáez and M. Osmani, "A diagnosis of construction and demolition waste generation and recovery practice in the European Union," J. Clean. Prod., vol. 241, 2019, doi: 10.1016/j.jclepro.2019.118400
- [5] European Environmental Agency, "No Title," [Online]. Available: <https://www.eea.europa.eu/themes/waste/waste-management/construction-and-demolition-waste-challenges>.
- [6] R. Pour et al., "Specifications for concrete with recycled aggregates," Mater. Struct., vol. 27, no. 9, pp. 557–559, 1994, doi: 10.1007/BF02473217.
- [7] L. Evangelista and J. De Brito, "Concrete with fine recycled aggregates: A review," Eur. J. Environ. Civ. Eng., vol. 18, no. 2, pp. 129–172, 2014, doi: 10.1080/19648189.2013.851038
- [8] M. Velay-Lizancos, I. Martinez-Lage, M. Azenha, J. Granja, and P. Vazquez-Burgo, "Concrete with fine and coarse recycled aggregates: E-modulus evolution, compressive strength and non-destructive testing at

- early ages," *Constr. Build. Mater.*, vol. 193, pp. 323–331, 2018, doi: 10.1016/j.conbuildmat.2018.10.209
- [9] Architecture2030.org, "New buildings - Embodied carbon," [Online]. Available: <https://architecture2030.org/new-buildings-embodied/>.
- [10] W. G. B. Council, "The net zero carbon buildings commitment," [Online]. Available: <https://www.worldgbc.org/thecommitment>.
- [11] NASA, "Sand mining at Poyang lake," [Online]. Available: <https://earthobservatory.nasa.gov/images/87663/sand-mining-at-poyang-lake>.
- [12] B. A. G. Bossink and H. J. H. Brouwers, "Construction Waste: Quantification and Source Evaluation," *J. Constr. Eng. Manag.*, vol. 122, no. 1, pp. 55–60, 1996, doi: 10.1061/(asce)0733-9364(1996)122:1(55).
- [13] N. Tošić, S. Marinković, T. Dašić, and M. Stanić, "Multicriteria optimization of natural and recycled aggregate concrete for structural use," *J. Clean. Prod.*, vol. 87, no. 1, pp. 766–776, 2015, doi: 10.1016/j.jclepro.2014.10.070.
- [14] A. Braga, "Impacte ambiental comparado do ciclo de vida de betão com agregados grossos reciclados e naturais," 2015.
- [15] M. Nedeljković, J. Visser, T. G. Nijland, S. Valcke, and E. Schlangen, "Physical, chemical and mineralogical characterization of Dutch fine recycled concrete aggregates: A comparative study," *Constr. Build. Mater.*, vol. 270, 2021, doi: 10.1016/j.conbuildmat.2020.121475.
- [16] M. J. Martinez-Echevarria et al., "Crushing treatment on recycled aggregates to improve their mechanical behaviour for use in unbound road layers," *Constr. Build. Mater.*, vol. 263, p. 120517, 2020, doi: 10.1016/j.conbuildmat.2020.120517.
- [17] S. Ismail, M. A. A. Hamid, and Z. Yaacob, "Mechanical properties of high-strength mortars with fine recycled concrete aggregates," *AIP Conf. Proc.*, vol. 2284, no. September 2018, 2020, doi: 10.1063/5.0027237.
- [18] F. Cartuxo, J. De Brito, L. Evangelista, J. R. Jiménez, and E. F. Ledesma, "Rheological behaviour of concrete made with fine recycled concrete aggregates - Influence of the superplasticizer," *Constr. Build. Mater.*, vol. 89, pp. 36–47, 2015, doi: 10.1016/j.conbuildmat.2015.03.119.
- [19] J. A. Bogas, J. De Brito, and D. Ramos, "Freeze-thaw resistance of concrete produced with fine recycled concrete aggregates," *J. Clean. Prod.*, vol. 115, pp. 294–306, 2016, doi: 10.1016/j.jclepro.2015.12.065.
- [20] S. Omary, E. Ghorbel, G. Wardeh, and M. D. Nguyen, "Mix Design and Recycled Aggregates Effects on the Concrete's Properties," *Int. J. Civ. Eng.*, vol. 16, no. 8, pp. 973–992, 2018, doi: 10.1007/s40999-017-0247-y.

- [21] D. Pedro, J. de Brito, and L. Evangelista, "Structural concrete with simultaneous incorporation of fine and coarse recycled concrete aggregates: Mechanical, durability and long-term properties," *Constr. Build. Mater.*, vol. 154, pp. 294–309, 2017, doi: 10.1016/j.conbuildmat.2017.07.215.
- [22] V. Revilla-cuesta, V. Ortega-lópez, M. Skaf, and J. Manuel, "Effect of fine recycled concrete aggregate on the mechanical behavior of self-compacting concrete," vol. 263, 2020, doi: 10.1016/j.conbuildmat.2020.120671.
- [23] B. Li, S. Hou, Z. Duan, L. Li, and W. Guo, "Rheological behavior and compressive strength of concrete made with recycled fine aggregate of different size range," *Constr. Build. Mater.*, vol. 268, p. 121172, 2021, doi: 10.1016/j.conbuildmat.2020.121172.
- [24] Z. Zhao, S. Remond, D. Damidot, and W. Xu, "Influence of fine recycled concrete aggregates on the properties of mortars," *Constr. Build. Mater.*, vol. 81, pp. 179–186, 2015, doi: 10.1016/j.conbuildmat.2015.02.037.
- [25] C. S. Poon, Z. H. Shui, L. Lam, H. Fok, and S. C. Kou, "Influence of moisture states of natural and recycled aggregates on the slump and compressive strength of concrete," *Cem. Concr. Res.*, vol. 34, no. 1, pp. 31–36, 2004, doi: 10.1016/S0008-8846(03)00186-8.
- [26] A. Djerbi Tegger, "Determining the water absorption of recycled aggregates utilizing hydrostatic weighing approach," *Constr. Build. Mater.*, vol. 27, no. 1, pp. 112–116, 2012, doi: 10.1016/j.conbuildmat.2011.08.018.
- [27] P. Pereira, L. Evangelista, and J. De Brito, "The effect of superplasticisers on the workability and compressive strength of concrete made with fine recycled concrete aggregates," *Constr. Build. Mater.*, vol. 28, no. 1, pp. 722–729, 2012, doi: 10.1016/j.conbuildmat.2011.10.050.
- [28] D. Carro-López, B. González-Fonteboa, J. De Brito, F. Martínez-Abella, I. González-Taboada, and P. Silva, "Study of the rheology of self-compacting concrete with fine recycled concrete aggregates," *Constr. Build. Mater.*, vol. 96, pp. 491–501, 2015, doi: 10.1016/j.conbuildmat.2015.08.091.
- [29] T. Celik and K. Marar, "Effects of crushed stone dust on some properties of concrete," *Cem. Concr. Res.*, vol. 26, no. 7, pp. 1121–1130, 1996, doi: 10.1016/0008-8846(96)00078-6.
- [30] M. Westerholm, B. Lagerblad, J. Silfwerbrand, and E. Forssberg, "Influence of fine aggregate characteristics on the rheological properties of mortars," *Cem. Concr. Compos.*, vol. 30, no. 4, pp. 274–282, 2008, doi: 10.1016/j.cemconcomp.2007.08.008.
- [31] M. E. K. Bouarroudj, S. Remond, F. Michel, Z. Zhao, D. Bulteel, and L. Courard, "Use of a reference limestone fine aggregate to study the fresh and hard behavior of mortar made with recycled fine aggregate," *Mater. Struct. Constr.*, vol. 52, no. 1, 2019, doi: 10.1617/s11527-019-1325-1.

- [32] G. Chinzorigt, M. K. Lim, M. Yu, H. Lee, O. Enkbold, and D. Choi, "Strength, shrinkage and creep and durability aspects of concrete including CO₂ treated recycled fine aggregate," *Cem. Concr. Res.*, vol. 136, no. January, p. 106062, 2020, doi: 10.1016/j.cemconres.2020.106062.
- [33] V. Revilla-Cuesta, V. Ortega-López, M. Skaf, and J. M. Manso, "Effect of fine recycled concrete aggregate on the mechanical behavior of self-compacting concrete," *Constr. Build. Mater.*, vol. 263, 2020, doi: 10.1016/j.conbuildmat.2020.120671.
- [34] M. Ju, J. G. Jeong, M. Palou, and K. Park, "Mechanical behavior of fine recycled concrete aggregate concrete with the mineral admixtures," *Materials (Basel)*, vol. 13, no. 10, pp. 1–15, 2020, doi: 10.3390/ma13102264.
- [35] F. S. Khalid et al., "Effect of water to cement ratio and replacement percentage of recycled concrete aggregate on the concrete strength," *Int. J. Adv. Sci. Technol.*, vol. 29, no. 6 Special Issue, pp. 1625–1635, 2020.
- [36] A. Katz, "Properties of concrete made with recycled aggregate from partially hydrated old concrete," *Cem. Concr. Res.*, vol. 33, no. 5, pp. 703–711, 2003, doi: 10.1016/S0008-8846(02)01033-5.
- [37] L. Evangelista and J. de Brito, "Mechanical behaviour of concrete made with fine recycled concrete aggregates," *Cem. Concr. Compos.*, vol. 29, no. 5, pp. 397–401, 2007, doi: 10.1016/j.cemconcomp.2006.12.004.
- [38] K. Pandurangan, A. Dayanithy, and S. Om Prakash, "Influence of treatment methods on the bond strength of recycled aggregate concrete," *Constr. Build. Mater.*, vol. 120, pp. 212–221, 2016, doi: 10.1016/j.conbuildmat.2016.05.093.
- [39] L. Li, B. J. Zhan, J. Lu, and C. S. Poon, "Systematic evaluation of the effect of replacing river sand by different particle size ranges of fine recycled concrete aggregates (FRCA) in cement mortars," *Constr. Build. Mater.*, vol. 209, pp. 147–155, 2019, doi: 10.1016/j.conbuildmat.2019.03.044.
- [40] T. Ji, C. Y. Chen, Y. Y. Chen, Y. Z. Zhuang, J. F. Chen, and X. J. Lin, "Effect of moisture state of recycled fine aggregate on the cracking resistibility of concrete," *Constr. Build. Mater.*, vol. 44, pp. 726–733, 2013, doi: 10.1016/j.conbuildmat.2013.03.059.
- [41] Y. Wang, H. Zhang, Y. Geng, Q. Wang, and S. Zhang, "Prediction of the elastic modulus and the splitting tensile strength of concrete incorporating both fine and coarse recycled aggregate," *Constr. Build. Mater.*, vol. 215, pp. 332–346, 2019, doi: 10.1016/j.conbuildmat.2019.04.212.
- [42] L. Evangelista and J. de Brito, "Flexural behaviour of reinforced concrete beams made with fine recycled concrete aggregates," *KSCE J. Civ. Eng.*, vol. 21, no. 1, pp. 353–363, 2017, doi: 10.1007/s12205-016-0653-8.

- [43] C. J. Zega and Á. A. Di Maio, "Use of recycled fine aggregate in concretes with durable requirements," *Waste Manag.*, vol. 31, no. 11, pp. 2336–2340, 2011, doi: 10.1016/j.wasman.2011.06.011.
- [44] S. C. Kou and C. S. Poon, "Properties of self-compacting concrete prepared with coarse and fine recycled concrete aggregates," *Cem. Concr. Compos.*, vol. 31, no. 9, pp. 622–627, 2009, doi: 10.1016/j.cemconcomp.2009.06.005.
- [45] C. C. Fan, R. Huang, H. Hwang, and S. J. Chao, "Properties of concrete incorporating fine recycled aggregates from crushed concrete wastes," *Constr. Build. Mater.*, vol. 112, pp. 708–715, 2016, doi: 10.1016/j.conbuildmat.2016.02.154.
- [46] S. Medjigbodo, A. Z. Bendimerad, E. Rozière, and A. Loukili, "How do recycled concrete aggregates modify the shrinkage and self-healing properties?," *Cem. Concr. Compos.*, vol. 86, pp. 72–86, 2018, doi: 10.1016/j.cemconcomp.2017.11.003.
- [47] A. Z. Bendimerad, B. Delsaute, E. Rozière, S. Staquet, and A. Loukili, "Advanced techniques for the study of shrinkage-induced cracking of concrete with recycled aggregates at early age," *Constr. Build. Mater.*, vol. 233, p. 117340, 2020, doi: 10.1016/j.conbuildmat.2019.117340.
- [48] V. W. Y. Tam, D. Kotrayothar, and J. Xiao, "Long-term deformation behaviour of recycled aggregate concrete," *Constr. Build. Mater.*, vol. 100, pp. 262–272, 2015, doi: 10.1016/j.conbuildmat.2015.10.013.
- [49] K. K. Sagoe-Crentsil, T. Brown, and A. H. Taylor, "Performance of concrete made with commercially produced coarse recycled concrete aggregate," *Cem. Concr. Res.*, vol. 31, no. 5, pp. 707–712, 2001, doi: 10.1016/S0008-8846(00)00476-2.
- [50] A. Ajdukiewicz and A. Kliszczewicz, "Influence of recycled aggregates on mechanical properties of HS/HPC," *Cem. Concr. Compos.*, vol. 24, no. 2, pp. 269–279, 2002, doi: 10.1016/S0958-9465(01)00012-9.
- [51] M. Bravo, J. de Brito, L. Evangelista, and J. Pacheco, "Durability and shrinkage of concrete with CDW as recycled aggregates: Benefits from superplasticizer's incorporation and influence of CDW composition," *Constr. Build. Mater.*, vol. 168, pp. 818–830, 2018, doi: 10.1016/j.conbuildmat.2018.02.176.
- [52] M. Gesoglu, E. Güneysi, H. Ö. Öz, M. T. Yasemin, and I. Taha, "Durability and Shrinkage Characteristics of Self-Compacting Concretes Containing Recycled Coarse and/or Fine Aggregates," *Adv. Mater. Sci. Eng.*, vol. 2015, 2015, doi: 10.1155/2015/278296.
- [53] G. Puente de Andrade, G. de Castro Polisseni, M. Pepe, and R. D. Toledo Filho, "Design of structural concrete mixtures containing fine recycled concrete aggregate using packing model," *Constr. Build. Mater.*, vol. 252, p. 119091, 2020, doi: 10.1016/j.conbuildmat.2020.119091.

- [54] S. Manzi, C. Mazzotti, and M. C. Bignozzi, "Short and long-term behavior of structural concrete with recycled concrete aggregate," *Cem. Concr. Compos.*, vol. 37, no. 1, pp. 312–318, 2013.
- [55] K. K. Sagoe-Crentsil, T. Brown, and A. H. Taylor, "Performance of concrete made with commercially produced coarse recycled concrete aggregate," *Cem. Concr. Res.*, vol. 31, no. 5, pp. 707–712, 2001.
- [56] M. Salau, "Shrinkage Deformation of Concrete Containing Recycled Coarse Aggregate," *Br. J. Appl. Sci. Technol.*, vol. 4, no. 12, pp. 1791–1807, 2014.
- [57] A. Gonzalez-Corominas and M. Etxeberria, "Effects of using recycled concrete aggregates on the shrinkage of high performance concrete," *Constr. Build. Mater.*, vol. 115, pp. 32–41, 2016.
- [58] Nedeljkovic, Mylonas, (2021) Influence of sand drying and mixing sequence on the performance of mortars with fine recycled concrete aggregates, under preparation.
- [59] BS EN 1097-5:2008, Tests for mechanical and physical properties of aggregates. Determination of the water content by drying in a ventilated oven.
- [60] BS EN 1097-6:2013, Tests for mechanical and physical properties of aggregates. Determination of particle density and water absorption
- [61] BS EN 1015-3:1999 Methods of test for mortar for masonry. Determination of consistence of fresh mortar (by flow table)
- [62] BS EN 1015-7:1999 Methods of test for mortar for masonry. Determination of air content of fresh mortar
- [63] BS EN 1015-11:2019 Methods of test for mortar for masonry. Determination of flexural and compressive strength of hardened mortar
- [64] CPC 11.3 Absorption of water by concrete by immersion under vacuum, 1984
- [65] NEN-EN 206, Concrete - Specification, performance, production and conformity
- [66] NEN 8005 - Dutch supplement to NEN-EN 206: Concrete - Specification, performance, production and conformity
- [67] BS EN 12350-2:2009, Testing fresh concrete. Slump-test
- [68] ASTM C231 / C231M - 10, Standard Test Method for Air Content of Freshly Mixed Concrete by the Pressure Method
- [69] BS EN 12390-13:2013, Testing hardened concrete. Determination of secant modulus of elasticity in compression
- [70] ISO 1920-8:2009, Testing of concrete — Part 8: Determination of drying shrinkage of concrete for samples prepared in the field or in the laboratory
- [71] BS EN 12620:2013, Aggregates for concrete

8

Appendix

8.1. Mortar mix designs of Series 1

NB							
Mortar mix design	Volume	Density	Dry mass	Moisture	Water demands	Water absorption	Mass for AsReceived sands
Materials							
CEM I 42.5 N	183.2	3.15	577.0	-	24.5%	-	577.0
CUGLA SPL (polycarboxilate)	0.0	1.1	0.0	-	-	-	0.0
Water from SPL	0.0	1	0.0	-	-	-	0.0
Effective water	216.8	1	216.8	-	-	-	216.8
Mixing water	207.1	1	207.1	-	-	-	207.1
Air	20.0	-	-	-	-	-	-
Total (cement+water+SPL)	420.0	-	-	-	-	-	-
Total (sand + gravel)	580.0	-	-	-	-	-	-
Recycled sand 0-4 mm	580.0	2.392	1387.4	9.26%	14.0%	8.56%	1515.8
Total	1000.0						

Figure 8.1: Mortar mix design NB

NC							
Mortar mix design	Volume	Density	Dry mass	Moisture	Water demands	Water absorption	Mass for AsReceived sands
Materials							
CEM I 42.5 N	164.6	3.15	518.5	-	24.5%	-	518.5
CUGLA SPL (polycarboxilate)	0.0	1.1	0.0	-	-	-	0.0
Water from SPL	0.0	1	0.0	-	-	-	0.0
Effective water	237.4	1	237.4	-	-	-	237.4
Mixing water	251.4	1	251.4	-	-	-	251.4
Air	20.0	-	-	-	-	-	-
Total (cement+water+SPL)	422.0	-	-	-	-	-	-
Total (sand + gravel)	578.0	-	-	-	-	-	-
Recycled sand 0-4 mm	578.0	2.543	1469.9	5.7%	14.2%	6.7%	1554.2
Total	1000						

Figure 8.2: Mortar mix design NC

ND							
Mortar mix design	Volume	Density	Dry mass	Moisture	Water demands	Water absorption	Mass for AsReceived sands
Materials							
CEM I 42.5 N	193.0	3.2	608.0	-	24.5%	-	608.0
CUGLA SPL (polycarboxilate)	0.0	1.1	0.0	-	-	-	0.0
Water from SPL	0.0	1.0	0.0	-	-	-	0.0
Effective water	203.0	1.0	203.0	-	-	-	203.0
Mixing water	207.0	1.0	207.0	-	-	-	207.0
Air	20.0	-	-	-	-	-	-
Total (cement+water+SPL)	416.0	-	-	-	-	-	-
Total (sand + gravel)	584.0	-	-	-	-	-	-
Recycled sand 0-4 mm	584.0	2.4	1372.4	10.5%	14.7%	10.8%	1516.1
Total	1000						

Figure 8.3: Mortar mix design ND

NF							
Mortar mix design	Volume	Density	Dry mass	Moisture	Water demands	Water absorption	Mass for AsReceived sands
Materials							
CEM I 42.5 N	132.7	3.15	418.0	-	24.5%	-	418.0
CUGLA SPL (polycarboxilate)	0.0	1.10	0.0	-	-	-	0.0
Water from SPL	0.0	1.00	0.0	-	-	-	0.0
Effective water	167.4	1.00	167.4	-	-	-	167.4
Mixing water	228.0	1.00	228.0	-	-	-	228.0
Air	20.0	-	-	-	-	-	-
Total (cement+water+SPL)	320.0	-	-	-	-	-	-
Total (sand + gravel)	680.0	-	-	-	-	-	-
Recycled sand 0-4 mm	680.0	2.37	1608.2	7.0%	14.8%	10.8%	1720.6
Total	1000						

Figure 8.4: Mortar mix design NF

NB-FA							
Mortar mix design	Volume	Density	Dry mass	Moisture	Water demands	Water absorption	Mass for AsReceived sands
Materials							
CEM I 42.5 N	125.4	3.15	395.0	-	24.5%	-	395.0
Fly Ash	53.7	2.25	120.8	-	32.5%	-	120.8
CUGLA SPL (polycarboxilate)	0.0	1.1	0.0	-	-	-	0.0
Water from SPL	0.0	1	0.0	-	-	-	0.0
Effective water	230.3	1	230.3	-	-	-	230.3
Mixing water	220.7	1	220.7	-	-	-	220.7
Air	20.0	-	-	-	-	-	-
Total (cement+water+SPL)	429.0	-	-	-	-	-	-
Total (sand + gravel)	571.0	-	-	-	-	-	-
Recycled sand 0-4 mm	571.0	2.392	1365.8	9.26%	14.0%	8.56%	1492.3
Total	1000						

Figure 8.5: Mortar mix design NBFA

NC-FA							
Mortar mix design	Volume	Density	Dry mass	Moisture	Water demands	Water absorption	Mass for AsReceived sands
Materials							
CEM I 42.5 N	112.6	3.15	354.7	-	24.5%	-	354.7
Fly Ash	48.2	2.25	108.5	-	32.5%	-	108.5
CUGLA SPL (polycarboxilate)	0.0	1.1	0.0	-	-	-	0.0
Water from SPL	0.0	1	0.0	-	-	-	0.0
Effective water	249.0	1	249.0	-	-	-	249.0
Mixing water	262.8	1	262.8	-	-	-	262.8
Air	20.0	-	-	-	-	-	-
Total (cement+water+SPL)	429.4	-	-	-	-	-	-
Total (sand + gravel)	570.6	-	-	-	-	-	-
Recycled sand 0-4 mm	570.6	2.543	1451.0	5.7%	14.2%	6.7%	1534.3
Total	1000						

Figure 8.6: Mortar mix design NCFa

8.2. Grading curves for aggregates 0-16 mm used in concrete mixtures¹⁰⁹

ND-FA							
Mortar mix design	Volume	Density	Dry mass	Moisture	Water demands	Water absorption	Mass for AsReceived sands
Materials							
CEM I 42.5 N	129.6	3.15	408.2	-	24.5%	-	408.2
Fly Ash	54.5	2.25	122.6	-	32.5%	-	122.6
CUGLA SPL (polycarboxilate)	0.0	1.1	0.0	-	-	-	0.0
Water from SPL	0.0	1.0	0.0	-	-	-	0.0
Effective water	221.5	1.0	221.5	-	-	-	221.5
Mixing water	225.4	1.0	225.4	-	-	-	225.4
Air	20.0	-	-	-	-	-	-
Total (cement+water+SPL)	425.2	-	-	-	-	-	-
Total (sand + gravel)	574.8	-	-	-	-	-	-
Recycled sand 0-4 mm	574.8	2.350	1350.8	10.5%	14.7%	10.8%	1492.2
Total	1000						

Figure 8.7: Mortar mix design NDFA

NF-FA							
Mortar mix design	Volume	Density	Dry mass	Moisture	Water demands	Water absorption	Mass for AsReceived sands
Materials							
CEM I 42.5 N	86.5	3.15	272.5	-	24.5%	-	272.5
Fly Ash	37.0	2.25	83.3	-	32.5%	-	83.3
CUGLA SPL (polycarboxilate)	0.0	1.10	0.0	-	-	-	0.0
Water from SPL	0.0	1.00	0.0	-	-	-	0.0
Effective water	175.9	1.00	175.9	-	-	-	175.9
Mixing water	236.6	1.00	236.6	-	-	-	236.6
Air	20.0	-	-	-	-	-	-
Total (cement+water+SPL)	319.0	-	-	-	-	-	-
Total (sand + gravel)	681.0	-	-	-	-	-	-
Recycled sand 0-4 mm	681.0	2.365	1610.6	7.0%	14.8%	10.8%	1723.1
Total	1000						

Figure 8.8: Mortar mix design NFFA

8.2. Grading curves for aggregates 0-16 mm used in concrete mixtures

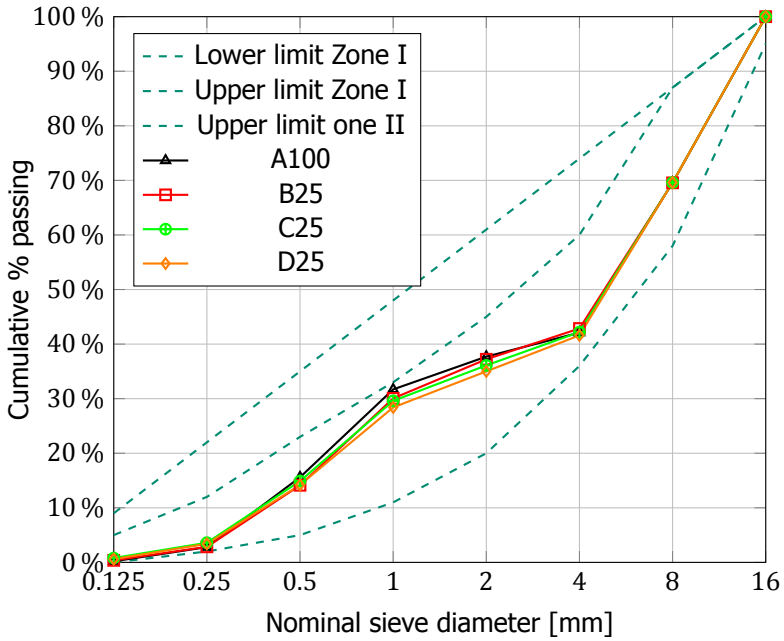


Figure 8.9: Final grading curves of A100, B25, C25 and D25

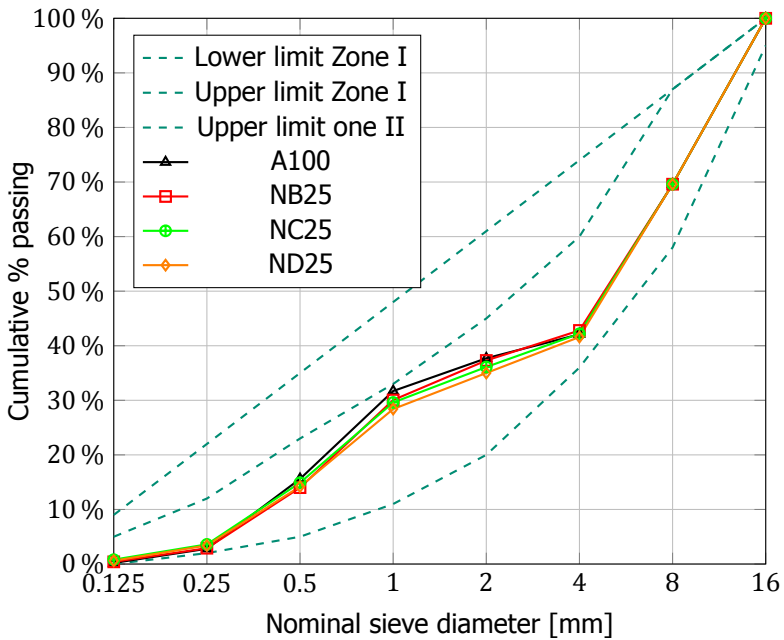


Figure 8.10: Final grading curves of A100, NB25, NC25 and ND25

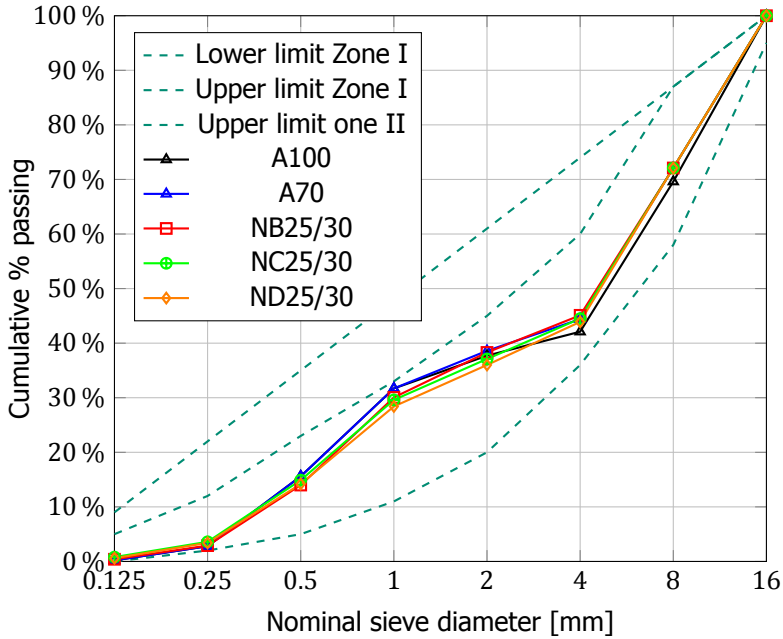


Figure 8.11: Final grading curves of A100, A70, NB25/30, NC25/30 and ND25/30

8.3. Concrete mix designs

Concrete mix design with as-received sand	Volume	Density	Dry mass	Moisture	Water absorption	Mass
	[l]	[kg/m ³]	[kg]	[%]	[%]	[kg]
Materials						
CEM I 42.5 N	117	3	350.0			350.0
CUGLA SPL (polycarboxilate)	1	1.1	0.7			0.7
Water from SPL	0.56	1	0.6			
Effective water	175	1	175.0			
Mixing water	159	1	158.9			158.9
Air	20					
Total (cement+water+SPL)	312					
Total (sand + gravel)	688					
River gravel 4-16	378	2.65	1002.3	0	0.5	1002.3
River sand 0-4 mm	309	2.65	820.1	2.8	0.3	843.0
Recycled sand 0-4 mm	0	0	0.0	0	0	0.0
Total	1000					2355.0

Figure 8.12: Concrete mix design A100

Concrete mix design with as-received sand	Volume	Density	Dry mass	Moisture	Water absorption	Mass
Materials	[L]	[kg/m ³]	[kg]	[%]	[%]	[kg]
CEM I 42.5 N	116.7	3.0	350.0			350.0
CUGLA SPL (polycarboxilate)	1.3	1.1	1.4			1.4
Water from SPL	1.1	1.0	1.1			
Effective water	175.0	1.0	175.0			
Mixing water	152.3	1.0	152.3			152.3
Air	20.0					
Total (cement+water+SPL)	312.9					
Total (sand + gravel)	687.1					
River gravel 4-16	264.5	2.65	701.0	0.0	0.5	701.0
Recycled gravel 4-16 mm	113.4	2.14	242.6	6.3	4.4	257.9
River sand 0-4 mm	309.2	2.65	819.3	2.8	0.3	842.3
Recycled sand 0-4 mm	0.0	0.0	0.0	0.0	0.0	0.0
Total	1000.0					2304.8

Figure 8.13: Concrete mix design A70

8

Concrete mix design with as-received sand	Volume	Density	Dry mass	Moisture	Water absorption	Mass
Materials	[L]	[kg/m ³]	[kg]	[%]	[%]	[kg]
CEM I 42.5 N	116.7	3.0	350.0			350.0
CUGLA SPL (polycarboxilate)	1.0	1.1	1.1			1.1
Water from SPL	0.8	1.0	0.8			
Effective water	175.0	1.0	175.0			
Mixing water	156.3	1.0	156.3			156.3
Air	20.0					
Total (cement+water+SPL)	312.6					
Total (sand + gravel)	687.4					
River gravel 4-16	378.1	2.65	1001.9	0.0	0.5	1001.9
River sand 0-4 mm	232.0	2.65	614.8	2.8	0.3	632.0
Recycled sand 0-4 mm	77.3	2.54	196.7	10.8	7.0	217.9
Total	1000.0					2359.1

Figure 8.14: Concrete mix design B25

Concrete mix design with as-received sand	Volume	Density	Dry mass	Moisture	Water absorption	Mass
Materials	[l]	[kg/m3]	[kg]	[%]	[%]	[kg]
CEM I 42.5 N	116.7	3.0	350.0			350.0
CUGLA SPL (polycarboxilate)	1.0	1.1	1.1			1.1
Water from SPL	0.8	1.0	0.8			
Effective water	175.0	1.0	175.0			
Mixing water	162.5	1.0	162.5			162.5
Air	20.0					
Total (cement+water+SPL)	312.6					
Total (sand + gravel)	687.4					
River gravel 4-16	378.1	2.65	1001.9	0.0	0.5	1001.9
River sand 0-4 mm	232.0	2.65	614.8	2.8	0.3	632.0
Recycled sand 0-4 mm	77.3	2.39	184.8	9.3	8.6	202.0
Total	1000.0					2349.4

Figure 8.15: Concrete mix design NB25

Concrete mix design with as-received sand	Volume	Density	Dry mass	Moisture	Water absorption	Mass
Materials	[l]	[kg/m3]	[kg]	[%]	[%]	[kg]
CEM I 42.5 N	116.7	3.0	350.0			350.0
CUGLA SPL (polycarboxilate)	1.6	1.1	1.8			1.8
Water from SPL	1.4	1.0	1.4			
Effective water	175.0	1.0	175.0			
Mixing water	155.8	1.0	155.8			155.8
Air	20.0					
Total (cement+water+SPL)	313.3					
Total (sand + gravel)	686.7					
River gravel 4-16	264.4	2.65	700.6	0.0	0.5	700.6
Recycled gravel 4-16 mm	113.3	2.14	242.5	6.3	4.4	257.8
River sand 0-4 mm	231.8	2.65	614.2	2.8	0.3	631.4
Recycled sand 0-4 mm	77.3	2.39	184.6	9.3	8.6	201.8
Total	1000.0					2299.2

Figure 8.16: Concrete mix design NB25/30

Concrete mix design with as-received sand	Volume	Density	Dry mass	Moisture	Water absorption	Mass
Materials	[L]	[kg/m ³]	[kg]	[%]	[%]	[kg]
CEM I 42.5 N	116.7	3.0	350.0			350.0
CUGLA SPL (polycarboxilate)	1.0	1.1	1.1			1.1
Water from SPL	0.8	1.0	0.8			
Effective water	175.0	1.0	175.0			
Mixing water	159.1	1.0	159.1			159.1
Air	20.0					
Total (cement+water+SPL)	312.6					
Total (sand + gravel)	687.4					
River gravel 4-16	378.1	2.65	1001.9	0.0	0.5	1001.9
River sand 0-4 mm	232.0	2.65	614.8	2.8	0.3	632.0
Recycled sand 0-4 mm	77.3	2.53	195.9	9.4	7.0	214.3
Total	1000.0					2358.3

Figure 8.17: Concrete mix design C25

8

Concrete mix design with as-received sand	Volume	Density	Dry mass	Moisture	Water absorption	Mass
Materials	[L]	[kg/m ³]	[kg]	[%]	[%]	[kg]
CEM I 42.5 N	116.7	3.0	350.0			350.0
CUGLA SPL (polycarboxilate)	1.0	1.1	1.1			1.1
Water from SPL	0.8	1.0	0.8			
Effective water	175.0	1.0	175.0			
Mixing water	165.8	1.0	165.8			165.8
Air	20.0					
Total (cement+water+SPL)	312.6					
Total (sand + gravel)	687.4					
River gravel 4-16	378.1	2.65	1001.9	0.0	0.5	1001.9
River sand 0-4 mm	232.0	2.65	614.8	2.8	0.3	632.0
Recycled sand 0-4 mm	77.3	2.54	196.4	5.7	6.7	207.6
Total	1000.0					2358.3

Figure 8.18: Concrete mix design NC25

Concrete mix design with as-received sand	Volume	Density	Dry mass	Moisture	Water absorption	Mass
Materials	[l]	[kg/m ³]	[kg]	[%]	[%]	[kg]
CEM I 42.5 N	116.7	3.0	350.0			350.0
CUGLA SPL (polycarboxilate)	1.6	1.1	1.8			1.8
Water from SPL	1.4	1.0	1.4			
Effective water	175.0	1.0	175.0			
Mixing water	159.1	1.0	159.1			159.1
Air	20.0					
Total (cement+water+SPL)	313.3					
Total (sand + gravel)	686.7					
River gravel 4-16	264.4	2.65	700.6	0.0	0.5	700.6
Recycled gravel 4-16 mm	113.3	2.14	242.5	6.3	4.4	257.8
River sand 0-4 mm	231.8	2.65	614.2	2.8	0.3	631.4
Recycled sand 0-4 mm	77.3	2.54	196.2	5.7	6.7	207.4
Total	1000.0					2308.1

Figure 8.19: Concrete mix design NC25/30

Concrete mix design with as-received sand	Volume	Density	Dry mass	Moisture	Water absorption	Mass
Materials	[l]	[kg/m ³]	[kg]	[%]	[%]	[kg]
CEM I 42.5 N	116.7	3.0	350.0			350.0
CUGLA SPL (polycarboxilate)	1.0	1.1	1.1			1.1
Water from SPL	0.8	1.0	0.8			
Effective water	175.0	1.0	175.0			
Mixing water	160.4	1.0	160.4			160.4
Air	20.0					
Total (cement+water+SPL)	312.6					
Total (sand + gravel)	687.4					
River gravel 4-16	378.1	2.65	1001.9	0.0	0.5	1001.9
River sand 0-4 mm	232.0	2.65	614.8	2.8	0.3	632.0
Recycled sand 0-4 mm	77.3	2.51	194.3	8.2	6.4	210.1
Total	1000.0					2355.4

Figure 8.20: Concrete mix design D25

Concrete mix design with as-received sand	Volume	Density	Dry mass	Moisture	Water absorption	Mass
Materials	[L]	[kg/m ³]	[kg]	[%]	[%]	[kg]
CEM I 42.5 N	116.7	3.0	350.0			350.0
CUGLA SPL (polycarboxilate)	1.0	1.1	1.1			1.1
Water from SPL	0.8	1.0	0.8			
Effective water	175.0	1.0	175.0			
Mixing water	164.3	1.0	164.3			164.3
Air	20.0					
Total (cement+water+SPL)	312.6					
Total (sand + gravel)	687.4					
River gravel 4-16	378.1	2.65	1001.9	0.0	0.5	1001.9
River sand 0-4 mm	232.0	2.65	614.8	2.8	0.3	632.0
Recycled sand 0-4 mm	77.3	2.35	181.7	10.5	10.8	200.8
Total	1000					2350.0

Figure 8.21: Concrete mix design ND25

8

Concrete mix design with as-received sand	Volume	Density	Dry mass	Moisture	Water absorption	Mass
Materials	[L]	[kg/m ³]	[kg]	[%]	[%]	[kg]
CEM I 42.5 N	116.7	3.0	350.0			350.0
CUGLA SPL (polycarboxilate)	1.6	1.1	1.8			1.8
Water from SPL	1.4	1.0	1.4			
Effective water	175.0	1.0	175.0			
Mixing water	157.7	1.0	157.7			157.7
Air	20.0					
Total (cement+water+SPL)	313.3					
Total (sand + gravel)	686.7					
River gravel 4-16	264.4	2.65	700.6	0.0	0.5	700.6
Recycled gravel 4-16 mm	113.3	2.14	242.5	6.3	4.4	257.8
River sand 0-4 mm	231.8	2.65	614.2	2.8	0.3	631.4
Recycled sand 0-4 mm	77.3	2.35	181.6	10.5	10.8	200.6
Total	1000.0					2299.9

Figure 8.22: Concrete mix design ND25/30